Molecular Analysis
of Mammalian Adenylyl Cyclases
and Bacterial Adenylyl Cyclase Toxins

Dissertation

zur Erlangung des Doktorgrades der Naturwissenschaften (Dr. rer. nat.)

der Naturwissenschaftlichen Fakultät IV – Chemie und Pharmazie –

der Universität Regensburg

vorgelegt von

Martin Göttle

aus Bisingen/Zollernalbkreis

2009

Die vorliegende Arbeit entstand in der Zeit von August 2005 bis Juni 2009 unter Leitung von Herrn Prof. Dr. R. Seifert am Institut für Pharmakologie und Toxikologie der Naturwissenschaftlichen Fakultät IV – Chemie und Pharmazie – der Universität Regensburg.

Das Promotionsgesuch wurde eingereicht im Juni 2009

Tag der mündlichen Prüfung: 17. Juli 2009

Prüfungsausschuss:

Prof. Dr. G. Schmeer (Vorsitzender)

Prof. Dr. R. Seifert (Erstgutachter)

Prof. Dr. B. König (Zweitgutachter)

Prof. Dr. A. Göpferich (Drittprüfer)

Acknowledgments

I would like to acknowledge and extend my heartfelt gratitude to the following persons who have made the completion of this thesis possible:

Imagination is more important than knowledge.

(Albert Einstein)

Abstracts and Publications

Parts of this thesis were published or presented as posters or short lectures:

Original Publications:

2007

Göttle, M., Dove, S., Steindel, P., Shen, Y., Tang, W.J., Geduhn, J., König, B., Seifert, R. (2007) Molecular analysis of the interaction of *Bordetella pertussis* adenylyl cyclase with fluorescent nucleotides. Mol Pharmacol 72: 526-35.

2008

Spangler, C.M., Spangler, C., **Göttle, M.**, Shen, Y., Tang, W.J., Seifert, R., Schäferling, M. (2008) A fluorimetric assay for real-time monitoring of adenylyl cyclase activity based on terbium norfloxacin. Anal Biochem 381: 86-93.

2009

Göttle, M., Geduhn, J., König, B., Gille, A., Höcherl, K., Seifert, R. (2009) Characterization of mouse heart adenylyl cyclase. J Pharmacol Exp Ther 329: 1156-65.

Taha, H.M., Schmidt, J., **Göttle, M.**, Suryanarayana, S., Shen, Y., Tang, W.J., Gille, A., Geduhn, J., König, B., Dove, S., Seifert, R. (2009) Molecular analysis of the interaction of anthrax adenylyl cyclase toxin, edema factor, with 2´(3´)-*O*-(*N*-(methyl)anthraniloyl)-substituted purine and pyrimidine nucleotides. Mol Pharmacol 75: 693-703.

Suryanarayana, S., **Göttle, M.**, Hübner, M., Gille, A., Mou, T.C., Sprang, S.R., Richter, M., Seifert, R. (2009) Differential inhibition of various adenylyl cyclase isoforms and soluble guanylyl cyclase by 2´,3´-*O*-(2,4,6-trinitrophenyl)-substituted nucleoside 5´-triphosphates. J Pharmacol Exp Ther, *published online: http://jpet.aspetjournals.org/cgi/reprint/jpet.109.155432v1.*

In preparation:

Göttle, M., Dove, S., Shen, Y., Tang, W.J., Geduhn, J., König, B., Kaever, V., Seifert, R. (2009) Nucleotidyl cyclase activity of *Bacillus anthracis* exotoxin, edema factor, and *Bordetella pertussis* exotoxin, CyaA.

Poster presentations:

2006

Fluorimetric determination of adenylyl cyclase and calmodulin activity
Göttle, M., Schäferling, M., Wolfbeis, O., Tang, W.J., Seifert, R.
47. Jahrestagung der Deutschen Gesellschaft für Experimentelle und Klinische Pharmakologie und Toxikologie (DGPT), Mainz (Germany), March 2006

Molecular investigation of cardiac adenylyl cyclase
Göttle, M., Seifert, R.
3rd International Summer School „Medicinal Chemistry", Regensburg (Germany), September 2006

2007

Interaction of fluorescent nucleotides with *Bordetella pertussis* adenylyl cyclase
Göttle, M., Shen, Y., Tang, W.J., König, B., Seifert, R.
48. Jahrestagung der Deutschen Gesellschaft für Experimentelle und Klinische Pharmakologie und Toxikologie (DGPT), Mainz (Germany), March 2007

2008

Cytidylyl cyclase activity of bacterial adenylyl cyclase toxins
Göttle, M., Kees, F., Tang, W.J., Seifert, R.
49. Jahrestagung der Deutschen Gesellschaft für Experimentelle und Klinische Pharmakologie und Toxikologie (DGPT), Mainz (Germany), March 2008

Cytidylyl cyclase activity of bacterial adenylyl cyclase toxins
Göttle, M., Kees, F., Geduhn, J., König, B., Seifert, R.
Symposium aus Anlass der Verabschiedung von Prof. Dr. med. K. Resch und des Dienstantritts von Prof. Dr. med. R. Seifert als Direktor des Instituts für Pharmakologie an der Medizinischen Hochschule Hannover, Hannover (Germany), November 2008

2009

Nucleotidyl cyclase activity of adenylyl cyclase toxins from *Bacillus anthracis* and *Bordetella pertussis*
Göttle, M., Dove, S., Kees, F., Geduhn, J., Shen, Y., Tang, W.J., König, B., Kaever, V., Seifert, R.
4th International Conference on cGMP
cGMP: Generators, Effectors and Therapeutic implications, Regensburg (Germany), June 2009

Short Lectures:

2009

Bakterielle Adenylylcyclase-Toxine mit Cytidylyl- und Uridylylcyclase-Aktivität
50. Jahrestagung der Deutschen Gesellschaft für Experimentelle und Klinische Pharmakologie und Toxikologie (DGPT), Mainz (Germany), March 2009

Contents

Abbreviations

AC	adenylyl cyclase
ANT	anthraniloyl-
6A7DA-FS	6-acetyl-7-deacetyl-forskolin
BODIPY-FS	boron-dipyrromethene-forskolin
CaM	calmodulin
CC	cytidylyl cyclase
CMG2	capillary morphogenesis protein-2
cNMP	cyclic nucleoside 3´:5´-monophosphate
CyaA	*Bordetella pertussis* adenylyl cyclase toxin
7DA-FS	7-deacetyl-forskolin
DMB-FS	7-deacetyl-7-(*N*-methyl)piperazino-γ-butyryloxy)-forskolin
1d-FS	1-deoxy-forskolin
9d-FS	9-deoxy-forskolin
EF	edema factor, *Bacillus anthracis* adenylyl cyclase toxin
ESI	electrospray ionization
FRET	fluorescence resonance energy transfer
FS	forskolin
GPCR	G protein-coupled receptor
GTPγS	guanosine 5´-[γ-thio]triphosphate
HF	heart failure
IBMX	3-isobutyl-1-methylxanthine
IS	internal standard
LC	liquid chromatography
LF	lethal factor, *Bacillus anthracis* exotoxin
mAC	mammalian AC
MANT-NTP	2´(3´)-*O*-(*N*-methylanthraniloyl)-nucleoside 5´-triphosphate
MANT- NTPγS	2´(3´)-*O*-(*N*-methylanthraniloyl)-nucleoside 5´-[γ-thio]triphosphate
MAPKK	mitogen-activated protein kinase kinase
NC	nucleotidyl cyclase
NDP	nucleoside 5´-diphosphate
NTP	nucleoside 5´-triphosphate
PA	protective antigen, *Bacillus anthracis* exotoxin
PMEApp	9-[2-(phosphonomethoxy)ethyl]adenine diphosphate
RT	retention time
SPE	solid phase extraction
SRM	selective reaction monitoring
TEM8	tumor endothelial marker-8
TNP	2,4,6-trinitrophenyl-
UC	uridylyl cyclase

Chapter 1

General Introduction

1.1   Mammalian Adenylyl Cyclases

1.1.1   Cyclic Nucleoside 3´:5´-Monophosphates as Second Messengers

The role of a cyclic nucleotide in signal transduction was first demonstrated in 1957 by Sutherland and Rall, who found cyclic adenosine 3´:5´-monophosphate (cAMP) to be a "second messenger" inducing hepatic glycogenolysis upon glucagon and epinephrine stimulation (Berthet *et al.*, 1957a, b). Since then, the role of cAMP (Fig. **1**) as a second messenger was found to comprise mediation of the biological effects of many hormones (Sutherland, 1972), non-endocrine regulation, e.g. control of immune (Parker *et al.*, 1974) and visual (Bitensky *et al.*, 1971) responses, blood coagulation (Steer and Salzman, 1980), neural functions (Kebabian, 1977a-c) and malignant transformation (DeRubertis and Craven, 1980). Therefore, cAMP is a key messenger in essential processes like function of the brain and the central nervous system, regulation of smooth muscle and vascular tone, skeletal muscle control and contraction of the heart, as well as regulation of gene transcription, cellular differentiation and ontogenic development.

In the 1970s, a second cyclic nucleotide, cyclic guanosine 3´:5´-monophosphate (cGMP), was discovered as an intracellular regulator in both endocrine and non-endocrine mechanisms (Goldberg *et al.*, 1973, 1975; Murad *et al.*, 1979). Since 1974, the potential occurrence and possible physiological relevance of a third cyclic nucleotide, cyclic cytidine 3´:5´-monophosphate (cCMP) is discussed controversially (Bloch *et al.*, 1974; Gaion and Krishna, 1979).
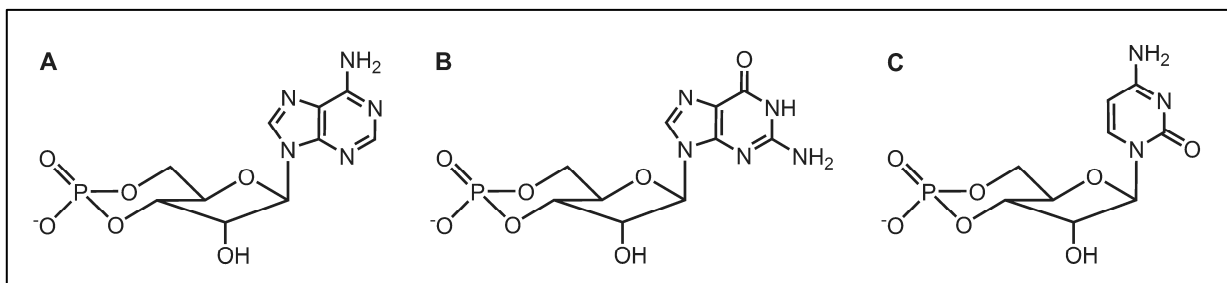
Fig. 1: Structures of cyclic nucleoside 3´:5´-monophosphates. A: Cyclic adenosine 3´:5´-monophosphate (cAMP); **B:** Cyclic guanosine 3´:5´-monophosphate (cGMP); **C:** Cyclic cytidine 3´:5´-monophosphate (cCMP).

1.1.2 The cAMP Signaling Pathway

The formation of cAMP by adenylyl cyclase (AC) is part of a signal transduction cascade including stimulation of integral membrane receptors by hormones, activation of heterotrimeric G proteins and subsequent activation of AC (Fig. **2**). G protein-coupled receptors (GPCRs) are cell membrane proteins consisting of seven hydrophobic transmembrane segments, with an extracellular amino terminus and an intracellular carboxyl terminus (Kolakowski, 1994; Palczewski *et al.*, 2000).
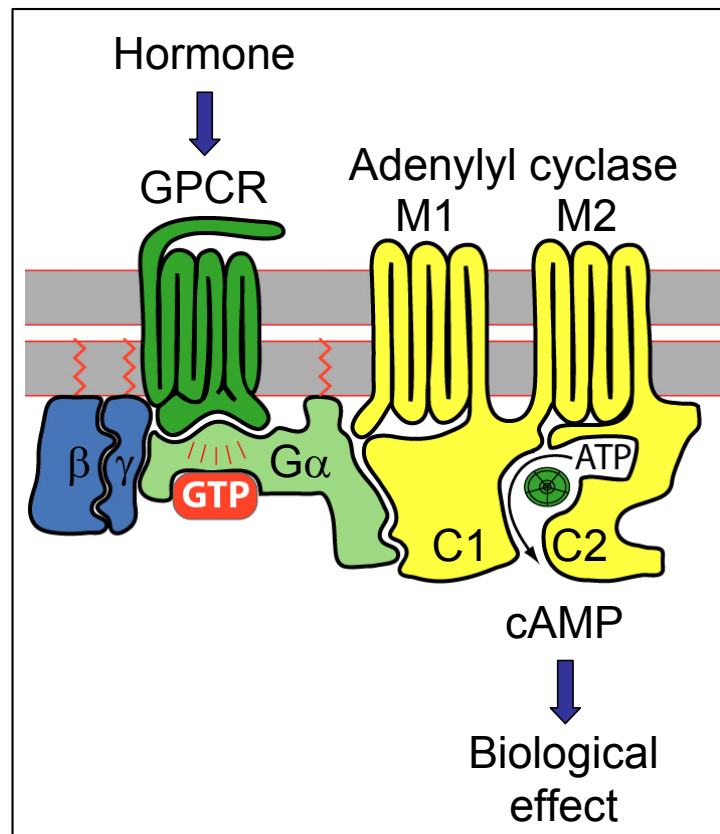
Fig. 2: The cAMP signaling pathway. Extracellular binding of hormones to G protein-coupled receptors (GPCRs) activates heterotrimeric G protein complexes consisting of Gα and Gβγ. Subsequently, adenylyl cyclase (AC) is activated to form the second messenger cAMP.

GPCRs represent the largest family of membrane proteins in the human genome and the most important source of targets for pharmacologic therapy (Venter *et al.*, 2001; Nambi and Aiyar, 2003; Kobilka, 2007). Binding of intracellular signaling molecules like epinephrine, dopamine, histamine or serotonin to GPCRs induces changes in receptor conformation, leading to an increased affinity for intracellular G protein complexes. Heterotrimeric G proteins consist of a guanine nucleotide binding $G\alpha$ subunit and a $G\beta\gamma$ heterodimer. In the inactive state, GDP is bound to the $G\alpha$ subunit. Upon interaction with the activated receptor, GDP is released and replaced by GTP. This exchange reduces the affinity of the $G\alpha$ subunit to the $G\beta\gamma$ heterodimer and leads to a disruption of the ternary complex. GTP-bound $G\alpha$ dissociates from $G\beta\gamma$ and interacts with AC either in a stimulatory ($G\alpha_s$ family), or inhibitory ($G\alpha_i$ family) manner (Gilman, 1987; Kristiansen, 2004). $G\alpha$ returns to the inactive state by its GTPase activity, hydrolyzing GTP to GDP and inorganic phosphate followed by reassociation with $G\beta\gamma$. The $\beta\gamma$-subunits also regulate AC, but in an AC subtype-specific manner (Sunahara *et al.*, 1996; Smit and Iyengar, 1998; Patel *et al.*, 2001). Depending on G protein stimulus, AC converts the substrate ATP to cAMP and pyrophosphate. cAMP exerts biological effects by activation of further signaling proteins, e.g. cyclic nucleotide-gated ion channels or protein kinase A (with subsequent protein phosphorylation steps). As one example demonstrating the importance of the cAMP signaling pathway, binding of hormones to β-adrenoceptors in the heart results in $G\alpha_s$-mediated AC stimulation and hence, elevated cAMP levels increasing cardiac contractility.

1.1.3 Structure and Catalytic Mechanism of Mammalian Adenylyl Cyclases

Mammalian AC consists of two hydrophobic regions with six transmembrane-spanning domains each (M1 and M2) and of two cytoplasmic domains (C1 and C2), yielding a pseudo-symmetrical protein (Fig. **3**). The C1 and C2 regions are further subclassified into $C1_a$ and $C1_b$, $C2_a$ and $C2_b$, respectively. $C1_a$ and $C2_a$ are highly conserved among all AC isoforms and contact each other forming the cytosolic, catalytically active core of AC where binding of the substrate ATP and cyclization to cAMP and PP_i occur (Tesmer *et al.*, 1997, 1999; Zhang *et al.*, 1997a, b; Tang and Hurley, 1998).
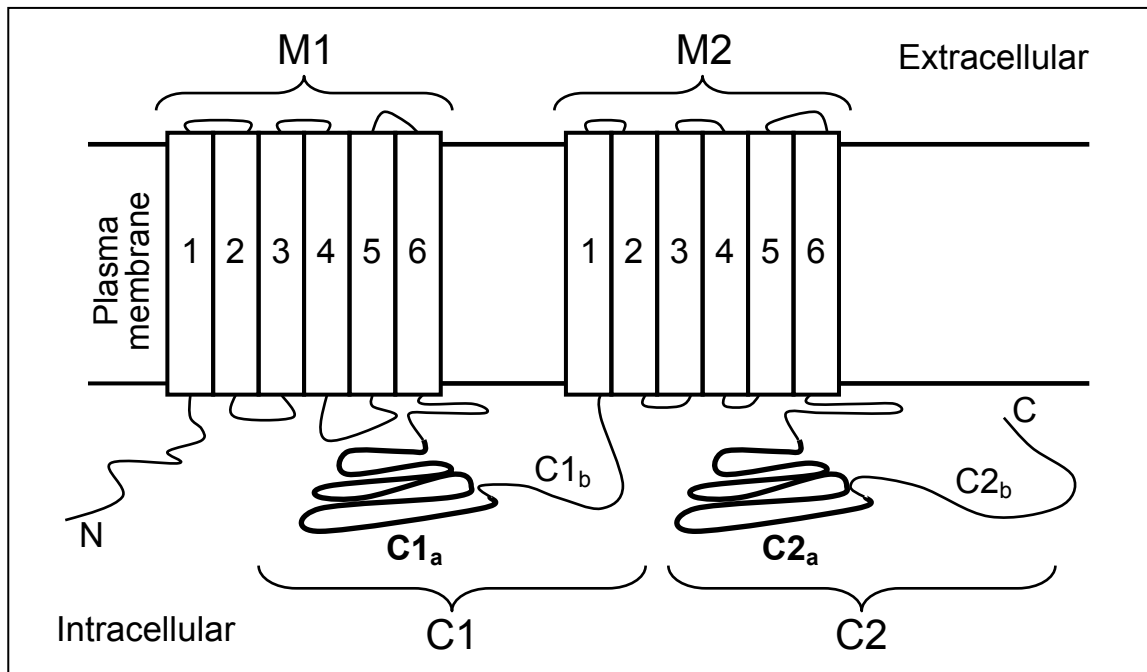
Fig. 3: Schematic model of the proposed structure of membrane-bound mammalian AC (Tang and Gilman, 1992; Hanoune *et al.*, 1997; Hurley, 1998). AC consists of the *N*-terminus (N), two hydrophobic domains (M1 and M2) with six transmembrane spans each, two cytosolic domains (C1 and C2) and the *C*-terminus (C). The intracellular domains are further divided into $C1_a/C1_b$ and $C2_a/C2_b$. The catalytical core is formed by $C1_a$ and $C2_a$.

The AC reaction proceeds by inversion of the configuration at the α-phosphorous atom, resulting from in-line displacement of pyrophosphate by nucleophilic attack of the 3´-OH group on the α-phosphate group (Eckstein *et al.*, 1981; Liu *et al.*, 1997; Tang and Hurley, 1998). This mechanism is also observed in the action of bacterial AC toxins and is described in detail in chapter 1.2.1. In

mammalian AC, a hydrophobic pocket accommodates the adenine base. Hydrogen bonds between the adenine N^1 and K938 as well as between N^6 and D1018 (AC2) confer specificity for adenine in advantage over guanine (Tang and Hurley, 1998). Therefore, in contrast to guanylyl cyclases, ACs bind ATP and lack the conversion of GTP to cGMP. The negatively charged phosphate tail formed by the α-, β- and γ-phosphates of the nucleotide interacts with the positive residues R484, R1029 and K1065 (AC2) as well as R398 and R1011 (AC1). Most importantly, N1025 and the guanidino group of R1029 bind the α-phosphate and are essential for catalysis. D396 and D440 (AC5) coordinate two Mg^{2+} cations. The first Mg^{2+} ion activates the 3′-OH group for nucleophilic attack while the second ion interacts with the β- and γ-phosphates.

1.1.4 Tissue-Specific Distribution and Pathophysiological Importance of Mammalian Adenylyl Cyclase Isoforms

Adenylyl cyclase type 1 (AC1) was the first AC to be cloned in 1989 (Krupinski *et al.*, 1989). Today, nine closely related AC isoforms, AC1-AC9, as well as two splice variants of AC8 (Cali *et al.*, 1996) have been cloned and characterized in mammals (Iyengar, 1993; Hanoune *et al.*, 1997; Simonds, 1999), all of them sharing large sequence homology in the primary structure of their catalytic site and the same predicted three-dimensional structure. Additionally, a tenth gene encoding a soluble AC isoform was found (Buck *et al.*, 1999). For the assessment of the role of AC for physiological processes and pathological disease states, two approaches were considered: Firstly, overexpression studies using cell transfection or transgenic animals expressing certain AC isoforms in increased amounts, and secondly, gene disruption studies utilizing genetic knockouts resulting in a loss of the corresponding AC isoform (Patel *et al.*, 2001; Sadana and Dessauer, 2009).

The tissue-specific distribution of distinct AC isoforms was investigated using mRNA studies (Tab. **1**). AC2, AC4 and AC6 are widely expressed, whereas other isoforms are more specifically expressed. In particular, AC1 is abundant in certain domains of the brain (hippocampus, cerebral cortex and the pineal gland) pointing to a very important role in learning and memory (Xia *et al.*, 1991). Studies with AC1-deficient mice showed decreased long-term potentiation in the hippocampus and synaptic plasticity, including deficiencies in learning and memory storage (Storm *et*

al., 1998; Villacres *et al.*, 1998). Additionally, AC1$^{(-/-)}$ mice showed significantly reduced behavorial nociceptive responses and altered pain transmission (Vadakkan *et al.*, 2006), altered behavior (Wu *et al.*, 1995) as well as enhanced sensitivity to the sedative effect of ethanol (Defer *et al.*, 2000; Maas *et al.*, 2005). Excessive activation of neuronal receptors results in damage and dying of nerve cells. As AC1$^{(-/-)}$ attenuated neuronal cell death induced by excessive injections of the agonist *N*-methyl-D-aspartate, AC1 may serve as a novel target in stroke and neurodegenerative diseases (Wang *et al.*, 2007; Sadana and Dessauer, 2009).

Tab. 1: Tissue-specific expression of AC isoforms and potential associated functions (Reiach *et al.*, 1999; Hanoune and Defer, 2001; Abdel-Majid *et al.*, 2002; Sunahara and Taussig, 2002; Tantisira *et al.*, 2005; Hines *et al.*, 2006; Dwivedi and Pandey, 2008).

AC isoform	Tissue distribution	Potential associated functions and pathophysiological relevance
AC1	Brain, adrenal gland	Circadian rhythm, synaptic plasticity, learning, memory, long-term potentiation, drug dependency
AC2	Brain, lung, skeletal muscle	Arrest of cell proliferation, synaptic plasticity
AC3	Brain, olfactory epithelium, male germ cells, pancreas	Olfaction, sperm function
AC4	Brain, kidney, liver, lung	Mood disorders, depression, photoreception
AC5	Heart, brain	Cardiac contraction, drug dependence, pain responses, motor coordination
AC6	Widespread, heart	Cardiac contraction, cell proliferation
AC7	Brain, platelets, widespread	Ethanol dependency, depression
AC8	Brain, lung	Synaptic plasticity, learning, memory, long-term potentiation, drug dependency
AC9	Brain, skeletal muscle, widespread	Polymorphism relevant in asthma treatment, learning, memory
sAC	Testis	Sperm capacitation, fertilization

Both AC1 and AC8 form the neuronal group of AC mainly expressed in the brain. Genetic disruption of both isoforms resulted in loss of long-term memory and long-term potentiation (Wong *et al.*, 1999; Wang *et al.*, 2003). Additionally, as a result from AC1 and AC8 deletion, a reduction in withdrawal behavior and altered morphine responses were observed, pointing to a potential role of the neuronal AC isoforms in the therapy of drug addiction (Li *et al.*, 2006). As AC activity in hippocampus and cerebellum from patients with Alzheimer´s disease is significantly reduced, the neural AC isoforms may be promising targets for future therapies of Alzheimer´s disease (Schnecko *et al.*, 1994; Yamamoto *et al.*, 1997). AC2 was found in brain and lung tissue pointing to importance in synaptic plasticity and in regulation of growth pathways in pulmonary artery myocytes (Furuyama *et al.*, 1993; Jourdan *et al.*, 2001).

The highest expression of AC3 is found in olfactory neuroepithelium (Xia *et al.*, 1992). AC3 deficient mice fail several olfaction-based behavorial tests implicating anosmia and a critical role for AC3 in olfaction (Wong *et al.*, 2000). Additionally, AC3 accounts for spermatozoa function and male fertility (Livera *et al.*, 2005). Immunolabeling of AC4 and investigation of AC activity in post-mortem brain of depressed suicide victims revealed decreased cAMP signaling indicating a correlation between AC activity and mood disorders (Reiach *et al.*, 1999; Dwivedi and Pandey, 2008).

AC5 and AC6 are highly expressed in the heart and striatal neurons. However, AC6 is also highly expressed in many other tissues. In cardiac myocytes, AC5 and AC6 are the major AC isoforms. Studies on transgenic mice overexpressing AC5 or AC6 demonstrate important differences between these two isoforms in cardiac tissue. In murine models of heart failure (HF) induced by $G\alpha_q$ overexpression, cardioprotective effects, improved cardiac function and increased responsiveness to β-adrenoceptor stimulation are attributed to AC6, but not to AC5 (Roth *et al.*, 1999, 2000; Tepe *et al.*, 1999). Overexpression of AC6 resulted in increased left ventricular function, reduced apoptosis and attenuated deleterious left ventricular remodeling suggesting a cardioprotective role in heart failure (Lai *et al.*, 2004, 2008; Timofeyev *et al.*, 2006). Additionally, gene transfer of AC6 reduced mortality in HF (Hammond, 2006; Phan *et al.*, 2007). In acute myocardial infarction, increased cardiac AC6 content preserved left ventricular contractile function and increased survival rates (Takahashi *et al.*, 2006). Deletion of AC6 decreased left ventricular function *via*

impaired calcium handling (Tang *et al.*, 2008). Taken together, these data suggest that increased AC6 activity might be beneficial in HF which may be accomplished by stimulating agents selective for AC6, e.g. forskolin analogs.

In contrast, disruption of AC5 preserved cardiac function against pressure overload (Okumura *et al.*, 2003) and prevented myocardial apoptosis (Iwatsubo *et al.*, 2004). Most interestingly, mice lacking cardiac AC5 had considerably increased lifespans and were protected against age-induced cardiac myopathy (Chester and Watts, 2007; Yan *et al.*, 2007; Vatner *et al.*, 2009). AC5$^{(-/-)}$ also effectively prevented apoptosis induced by isoproterenol stimulation (Ishikawa *et al.*, 2005). As chronic activation of cAMP signaling results in cardiomyopathy and heart failure, limiting AC activity by β-adrenergic blockade therapy is the standard treatment in HF (Iwase *et al.*, 1997; Engelhardt *et al.*, 1999; Antos *et al.*, 2001). However, the use of β-adrenoceptor antagonists is limited in the case of decreased receptor number (desensitization), in non-responders due to receptor polymorphisms and in case of impaired respiratory function due to pulmonary diseases as β-adrenoceptors of the respiratory system might also be blocked as a side-effect. Therefore, inhibiting AC5 instead of β-adrenergic receptors is an attractive alternative in future pharmacotherapy of HF.

Besides its importance in the heart, AC5 may also play a role in dopaminergic signaling in the striatum (Lee *et al.*, 2002) as AC5$^{(-/-)}$ mice showed Parkinson-like motor dysfunction and abnormal coordination (Iwamoto *et al.*, 2003). Additionally, attenuation of all major behavorial effects of morphine including analgesia and physiological dependence as well as loss of opioid-induced AC inhibition in the striatum was observed in AC5$^{(-/-)}$ mice, pointing to a major role of AC5 in the mediation of morphine action (Kim *et al.*, 2006; Sadana and Dessauer, 2009). Therefore, AC5 inhibitors might be used in the treatment of drug dependency (Kreek, 1997). Furthermore, AC5$^{(-/-)}$ mice had attenuated pain responses in several mechanical pain tests pointing to a role of AC5 in acute and chronic pain transmission (Kim *et al.*, 2007). AC5 inhibitors may also be used in the treatment of depression and anxiety (Kim *et al.*, 2008; Krishnan *et al.*, 2008).

In AC7 transgenic mice, acute responsiveness and tolerance to morphine was enhanced (Yoshimura *et al.*, 2000). Additionally, AC7 was found to be sensitive to ethanol (Yoshimura *et al.*, 2006) and seems to play a sex-specific role in depression (Hines *et al.*, 2006). AC8 is the only Ca^{2+}/calmodulin-stimulated isoform expressed in

the hypothalamus (Matsuoka *et al.*, 1992; Cali *et al.*, 1994; Mons and Cooper, 1994) suggesting importance in neuroendocrine function and drug dependence (Matsuoka *et al.*, 1994; Lane-Ladd *et al.*, 1997). AC8 deficient mice showed altered anxiety behavior, allowing to deduce an involvement of AC8 in the generation of stress-induced anxiety (Schaefer *et al.*, 2000). A polymorphism in AC9 was found to impact responsiveness to asthma treatment with β-adrenoceptor agonists and corticosteroids, showing relevance of AC9 in the respiratory system (Tantisira *et al.*, 2005). Moreover, AC9 contributes to learning and memory (Antoni *et al.*, 1998).

Soluble AC (sAC) is predominantly expressed in the testis and associated with sperm development suggesting the possibility of the development of sAC inhibitors as male contraceptives (Sunahara and Taussig, 2002; Geng *et al.*, 2005; Marquez and Suarez, 2008). sAC splice variants have been identified displaying a broader distribution pattern. sAC activity diverges significantly from the membrane-bound isoforms as it is unresponsive to hormones, G proteins and forskolin (Yanagimachi, 1994; Buck *et al.*, 1999; Jaiswal and Conti, 2001).

Cells or tissues chronically treated with ethanol exhibit reduced responsiveness of AC to agents that usually enhance AC activity, e.g. cerebral cortical membranes of chronically ethanol-treated mice show a decrease in AC activity stimulated by β-adrenoceptors (Tabakoff *et al.*, 1995; Yoshimura *et al.*, 2000). These data suggest that ethanol dependence greatly relies on the cAMP signaling pathway possibly offering new therapeutic points of action (Moore *et al.*, 1998; Yang *et al.*, 1998). Finally, polycystic kidney disease is also linked to the cAMP system as increased cytosolic cAMP levels correlate with increased cellular proliferation being a key factor in the enlargement of renal cysts (Yamaguchi *et al.*, 2000).

1.1.5 Isoform-Specific Regulation of Adenylyl Cyclase

Only the cytoplasmic domains C1 and C2 of AC, which form the catalytic domain, are subject to intracellular regulations specific for each AC isoform. $G\alpha_s$ contacts both domains, with most of the binding surface contributed to the C2 domain (Sunahara *et al.*, 1997; Tesmer *et al.*, 1997). $G\alpha_s$ increases the affinity between C1 and C2 and facilitates closure of the active site around ATP. Thereby, key residues in the active site reach closer to the 3´-hydroxyl group of ATP, creating a conformation more favorable for catalysis. As shown in Tab. **2**, stimulation by $G\alpha_s$ is the major mechanism by which all membranous AC isoforms are activated and the intracellular cAMP level is elevated (Tang *et al.*, 1992). Different ACs display different affinities for $G\alpha_s$, possibly providing an explanation for the various responses of different cell types to hormones and neurotransmitters that elevate cAMP levels (Harry *et al.*, 1997).

Tab. 2: Regulations of mammalian AC (Defer *et al.*, 2000; Hanoune and Defer, 2001; Sunahara and Taussig, 2002; Iwatsubo *et al.*, 2003; Sadana and Dessauer, 2009).

	AC1	AC2	AC3	AC4	AC5	AC6	AC7	AC8	AC9	sAC
$G\alpha_s$	↑	↑	↑	↑	↑	↑	↑	↑	↑	-
$G\alpha_i$	↓	-	↓		↓	↓		↓	↓	-
$G\beta\gamma$	↓	↑	-	↑	↓	↓	↑	↑	-	-
Forskolin	↑	↑	↑	↑	↑	↑	↑	↑	-	-
Protein kinase A					↓	↓				
Protein kinase C	↑	↑	↑	↓	↑	↓	↑		↓	
Ca^{2+}/Calmodulin	↑		↑					↑		
Calmodulin kinase	↓		↓							

By binding to the C1 domain, $G\alpha_i$ decreases the affinity of the C1 and C2 domains for one another and stabilizes a more open inactive conformation. Thereby, $G\alpha_s$-stimulated AC5 and AC6 activities are inhibited, whereas $G\alpha_i$ has no effect on AC2 and AC8, showing isoenzyme specific actions of $G\alpha_i$-coupled receptors (Chen and Iyengar, 1993; Taussig *et al.*, 1993, 1994; Kozasa and Gilman, 1995; Rodbell,

1995; Scholich *et al.*, 1997; Dessauer *et al.*, 1998). This inhibitory action of GPCRs on AC activity can be blocked by *pertussis* toxin, causing ADP-ribosylation of the G_i protein.

Besides $G\alpha$, $G\beta\gamma$ subunits are effective modulators of AC activity inhibiting AC1, AC5, AC6 and AC8, and activating AC2, AC4 and AC7, which explains many aspects of cross-talk between different receptors (Gao and Gilman, 1991; Tang and Gilman, 1991; Federman *et al.*, 1992; Bygrave and Roberts, 1995; Taussig and Gilman, 1995; Yung *et al.*, 1995; Bayewitch *et al.*, 1998). For example, stimulation of G_q-coupled receptors can lead to an increase of intracellular calcium concentrations mediated by $G\alpha_q$ and additionally, to an increase in cAMP due to the stimulation of AC by $G\beta\gamma$. $G\beta\gamma$ is specifically relevant in brain physiology, because the $G\alpha_i$ family and their accompanying $\beta\gamma$ subunits are, together with AC1 and AC8, highly expressed in brain tissue (Sternweis and Robishaw, 1984).

With the exceptions of AC9 and sAC, all AC isoforms are strongly activated by the diterpene forskolin, a natural plant extract from *Coleus forskolii* used in traditional medicine in India (Seamon and Daly, 1981a, b; Seamon *et al.*, 1981). Elucidating the structure of AC and particularly the interface of $C1_a$/$C2_a$, a hydrophobic pocket was discovered, implicating binding of forskolin (Fig. **4**). By interacting with residues in $C1_a$ and $C2_a$, forskolin stabilizes the interactions between the two cytoplasmic domains and increases the affinity of the two domains for each other, resulting in assembly of the catalytically active core of AC and stimulated enzymatic activity (Sunahara *et al.*, 1997; Tesmer *et al.*, 1997; Zhang *et al.*, 1997b). In AC9, one single mutation (Y1082L) confers binding of forskolin and therefore, AC activation (Yan *et al.*, 1998). Forskolin analogs selectively activating distinct AC isoforms could be used in pharmacotherapy of diseases related to decreased AC activity, e.g. Alzheimer´s disease (Pinto *et al.*, 2008).
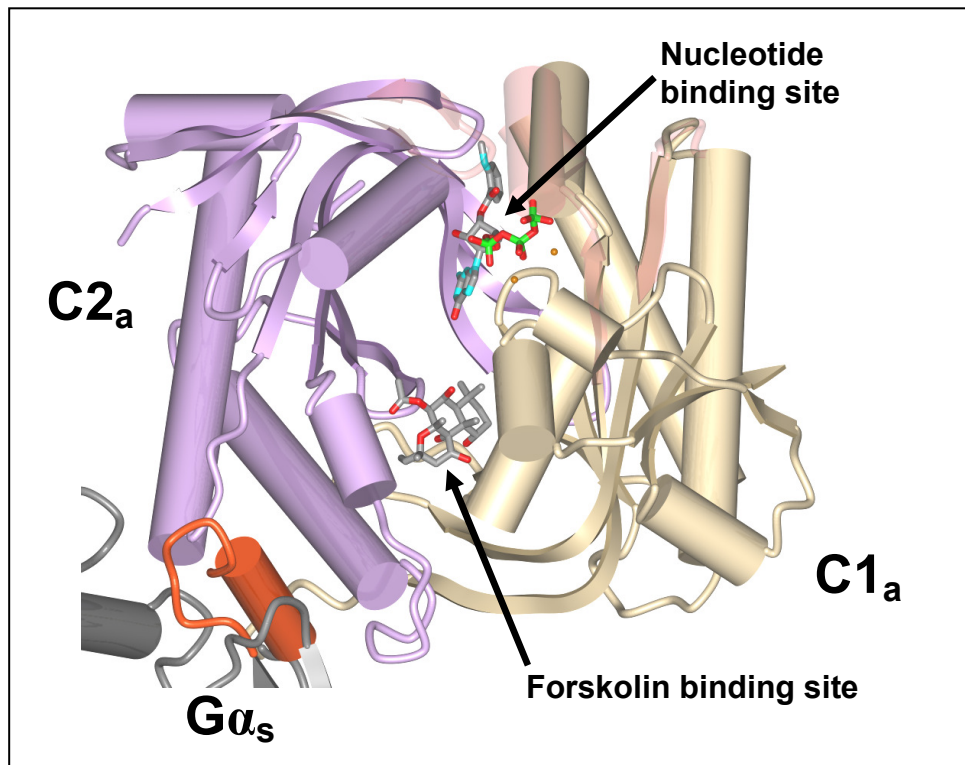
Fig. 4: Crystal structure of the catalytic domain of AC formed by C1$_a$ and C2$_a$ in complex with Gα_s (Mou *et al.*, 2005). The C1$_a$ and C2$_a$ domains are colored tan and mauve, respectively; Gα_s is shown as a red cylinder. Forskolin and the substrate analog MANT-GTP are drawn as stick models at the forskolin binding site and the catalytic site, respectively. Two Mn^{2+} ions are shown as orange spheres.

Elevated concentrations of pyrophosphate inhibit AC, which has also been shown for the antiviral agent foscarnet, a pyrophosphate anolog (Kudlacek *et al.*, 2001). The so-called P-site inhibitors are purine-based substrate analogs, binding to the catalytic site of AC resulting in non-competitive AC inhibition (Desaubry *et al.*, 1996a, b; Desaubry and Johnson, 1998; Dessauer *et al.*, 1999). For example, 2′,5′-dideoxyadenosine 3′-tetraphosphate inhibited AC purified from bovine brain with a K$_i$ value of 23 nM.

Modulation of AC activity by phosphorylation is a common feature of downstream and feedback regulations within signal transduction cascades mediated by protein kinase A (PKA) or protein kinase C (PKC). Thus, phosphorylation of AC5 and AC6 by PKA provides a means of desensitization at the effector level (Iwami *et al.*, 1995; Chen *et al.*, 1997). Interestingly, phosphorylation by PKC enhances Gα_s-stimulated AC2 activity, inhibits Gα_s-stimulated AC4 activity, but causes both AC2 and AC4 to lose responsiveness to the stimulatory effect of G$\beta\gamma$ (Zimmermann and

Taussig, 1996). While AC1, AC2, AC3, AC5 and AC7 activities are increased by PKC (Jacobowitz and Iyengar, 1994; Kawabe et $al.$, 1994; Watson et $al.$, 1994), $G\alpha_s$-stimulated AC4 and AC6 activity is decreased in presence of PKC (Zimmermann and Taussig, 1996; Lai et $al.$, 1999).

Submillimolar concentrations of Ca^{2+} inhibit all AC isoforms, possibly by competition with magnesium, which is essential for catalysis of the cyclization reaction. While AC5 and AC6 are inhibited by lower Ca^{2+} concentrations, the endogenous Ca^{2+} sensor protein calmodulin (CaM) stimulates AC1, AC3 and AC8 in a Ca^{2+}-dependent manner (Choi et $al.$, 1992; Vorherr et $al.$, 1993; Cali et $al.$, 1994; Gu and Cooper, 1999). AC3 is stimulated by Ca^{2+}/calmodulin in $vitro$ (Choi et $al.$, 1992), but inhibited in $vivo$, presumably through phosphorylation by calmodulin kinase (Wei et $al.$, 1996), which has also been shown for AC1 (Wayman et $al.$, 1996). AC9 is not affected by Ca^{2+}/calmodulin but is inhibited by the protein phosphatase calcineurin (Antoni et $al.$, 1998).

Binding of AC5 to the PKA-scaffolding protein AKAP79 was observed, facilitating PKA-mediated inhibition of AC5 (Bauman et $al.$, 2006; Sadana and Dessauer, 2009). Finally, the hydrophobic transmembrane-spanning domains of AC, M1 and M2, are subject to isoform-specific glycosylation, which is an additional mechanism for modulation of the functional properties of AC (Wu et $al.$, 2001).

In conclusion, different AC isoforms have different regulatory properties and the same effector can exert positive or negative regulating effects. In different cell types displaying different protein expression patterns, the same AC isoform may be regulated differently, and different signaling pathways can talk together in regulating cell functions. The cAMP signaling pathway is very complex, offering many therapeutic implications.

However, many unanswered questions still remain, e.g. heterodimerization of different AC isoforms has been discovered (Gu et $al.$, 2002; Cooper and Crossthwaite, 2006; Baragli et $al.$, 2008), but the detailed functional importance of this phenomenon is unknown. What is the exact role of the large transmembrane domains of AC? What is the relevance of localization of AC in lipid rafts and caveolae in combination with other signaling components? What are the effects of isoform-specific glycosylation? What is the detailed role of AC in mental disorders, addiction, pain transmission and cardiac function? And how can the different AC isoforms be targeted selectively for the multiplicity of different therapeutic indications? Detailed

characterization of AC from different tissues will contribute to the clarification of mechanisms of pathogenesis and to the development of new therapeutic approaches. In particular, pharmacological characterization of AC in the heart is required for the exploration of isoform-selective AC inhibitors and activators as a novel therapeutic strategy in heart failure.

1.1.6 MANT-Nucleotides as Fluorescent Inhibitors of AC

2´(3´)-*O*-(*N*-methylanthraniloyl)- (MANT)-substituted nucleotides form a class of fluorescent substrate analogs that are used in the investigation of a broad variety of nucleotide binding enzymes (Hiratsuka, 1983; Jameson and Eccleston, 1997). Fig. **5** shows the general structure of MANT-nucleotides, substrate analogs bearing a MANT-group which isomerizes between the 2´- and 3´-ribosyl position by acyl migration (Hiratsuka, 1982).
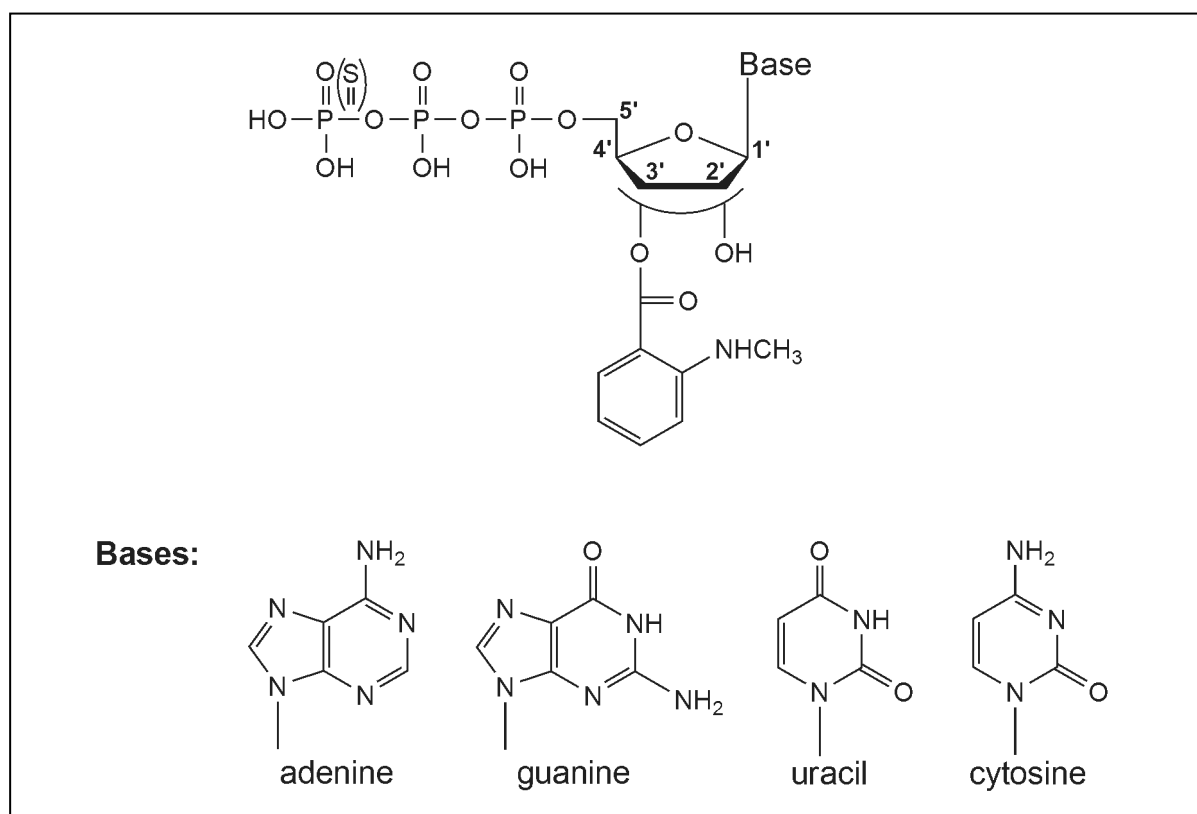
Fig. 5: Structure of 2´(3´)-*O*-(*N*-methylanthraniloyl)- (MANT)-substituted nucleotides. Besides adenine, different bases may be attached to ribose. Oxygen in the phosphate tail may be substituted by sulfur. The MANT-group isomerizes between the 2´- and 3´-ribosyl position by acyl migration.

Previously, MANT-substituted nucleoside 5´-triphosphates were found to constitute a novel class of potent and competitive AC inhibitors (Gille and Seifert, 2003a, b). The aromatic MANT-group forms hydrophobic interactions with lipophilic residues of AC, e.g. F400, W1020, V1006 in C1:C2, accounting for the increased affinity of MANT-substituted nucleotides in comparison to non-substituted nucleotides (Mou *et al.*, 2005). As shown in Fig. **4**, elucidation of the crystal structure of the

catalytic site of AC in complex with accommodated MANT-nucleotides showed the MANT-group to act as a wedge preventing closure of the catalytic site resulting in AC inhibition (Mou *et al.*, 2005). Investigating the interactions of MANT-nucleotides bearing different bases and different substitution patterns at the phosphate tail, e.g. MANT-ATP, MANT-GTP, MANT-ITPγS and MANT-ADP, the catalytic site of AC was found to be spacious and flexible, binding both purine and pyrimidine nucleotides (Gille *et al.*, 2004; Mou *et al.*, 2005, 2006). A tripartite pharmacophore model was established to describe the contributions of the ribose substituent (MANT-group), the phosphate residue and the base to nucleotide affinity to AC. Major significance was attributed to the ribose substituent and, to a smaller degree, to the triphosphate tail, while the contribution of the base to nucleotide-affinity was found to be inferior (Mou *et al.*, 2006). As different MANT-nucleotides showed differential inhibitory potency on different AC isoforms, the development of isoform-selective AC inhibitors and their application as a novel therapeutic strategy in various diseases is feasible.

1.2   Bacterial Adenylyl Cyclase Toxins

Disruption of crucial cellular processes is often a very critical event in the pathogenesis of infectious diseases of animals and humans. Several pathogenic bacteria secrete toxins to alter the intracellular cAMP concentration in mammalian host cells, resulting in a profound effect on various cellular processes. These toxins either disrupt the normal regulation of the cAMP signaling system or they themselves catalyze the synthesis of cAMP in the host cell. The latter are known as the AC toxins having a catalytic rate of 100-fold to 1000-fold higher than mammalian ACs. AC toxins are able to enter the cytosol of eukaryotic host cells and become activated by eukaryotic cofactors, like calmodulin (CaM), triggering uncontrolled synthesis of cAMP. As mammalian immune effector cells are the primary target of AC toxins, the resulting toxic cAMP accumulation poisons the immune system and thus facilitates the survival of the bacteria in the host (Ahuja *et al.*, 2004). For instance, toxin-induced elevation of cAMP levels causes loss of bactericidal functions of phagocytes and promotes apoptosis of macrophages (Boyd *et al.*, 2005; Basler *et al.*, 2006). Hence, AC toxins are a bacterial strategy to manipulate and subvert host defenses, impairing cellular antimicrobial responses.

1.2.1 Adenylyl Cyclase Toxin Edema Factor (EF) from *Bacillus anthracis*

Anthrax is primarily an infection of herbivores caused by pathogenic strains of *Bacillus anthracis,* a spore-forming, aerobic, gram-positive bacterium (Mock and Fouet, 2001; Mourez *et al.*, 2002; Oncu *et al.*, 2003). Humans are accidental hosts through the contact with infected animals, contaminated food or animal products; historical accounts on anthrax disease reach back to antiquity. Since the late 1800s, there has been impressive progress in the development of anthrax vaccines (Brey, 2005; Scorpio *et al.*, 2006, 2007). Anthrax disease is divided in three types depending on the mode of entry of the agent: Cutaneous anthrax, gastrointestinal anthrax and inhalational anthrax. Cutaneous anthrax results from entry of the agent through skin injuries and results in necrosis, edema and black eschar, see Fig. **6**. Gastrointestinal anthrax as a result from ingestion of anthrax spores causes edema and necrosis accounting for a considerably high mortality rate. Inhalation of anthrax spores results in the most lethal form of anthrax disease which is characterized by fever, cough, dyspnea, respiratory failure and finally, death within days.

Fig. 6: Cutaneous anthrax with the typical black eschar. The name anthrax is derived from Ανθρακιτις, the Greek word for anthracite (coal). The pictures are taken from the Center for Biologic Counterterrorism and Emerging Diseases (CBC-ED), MedStar Health Group, Washington, DC (http://bepast.org).

The high virulence and fatality rates of anthrax are a product of the secretion of multiple exotoxins by the agent. *Bacillus anthracis* produces a tripartite toxin comprising a receptor binding moiety termed protective antigen (PA) and two effector moieties termed edema factor (EF) and lethal factor (LF) (Brossier and Mock, 2001; Ascenzi *et al.*, 2002; Cunningham *et al.*, 2002). Secreted from the bacteria as non-toxic monomers, these proteins assemble on the cell surface of receptor-bearing eukaryotic cells to form toxic non-covalent complexes (Cunningham *et al.*, 2002; Mourez *et al.*, 2002). As shown in Fig. **7**, PA binds to certain cell membrane receptors: Firstly, tumor endothelial marker-8 (TEM8), which is expressed in a wide variety of tissues but at increased levels in colon tumor vasculature and secondly, capillary morphogenesis protein-2 (CMG2), which was initially identified in human umbilical vein endothelial cells induced to undergo capillary formation (Bradley *et al.*, 2001; Liu and Leppla, 2003; Scobie *et al.*, 2003; Santelli *et al.*, 2004; Hong *et al.*, 2005). Upon receptor binding, PA is cleaved into two fragments by cell-associated proteases (Klimpel *et al.*, 1992). The smaller 20 kDa fragment PA_{20} dissociates allowing the larger 63 kDa *C*-terminal receptor-bound fragment PA_{63} to self-associate into ring-shaped heptamers (Milne *et al.*, 1994; Petosa *et al.*, 1997; Cunningham *et al.*, 2002). The heptamer binds three molecules of EF and/or LF and is endocytosed and trafficked to an acidic intracellular compartment (Gordon *et al.*, 1988; Cunningham *et al.*, 2002; Mogridge *et al.*, 2002; Abrami *et al.*, 2003; Christensen *et*

al., 2006). There, the low pH induces conformational changes in the heptameric PA_{63} moiety allowing it to form a membrane-spanning pore and translocate bound EF and/or LF across the membrane into the cytosol (Friedlander, 1986; Benson *et al.*, 1998; Cunningham *et al.*, 2002).
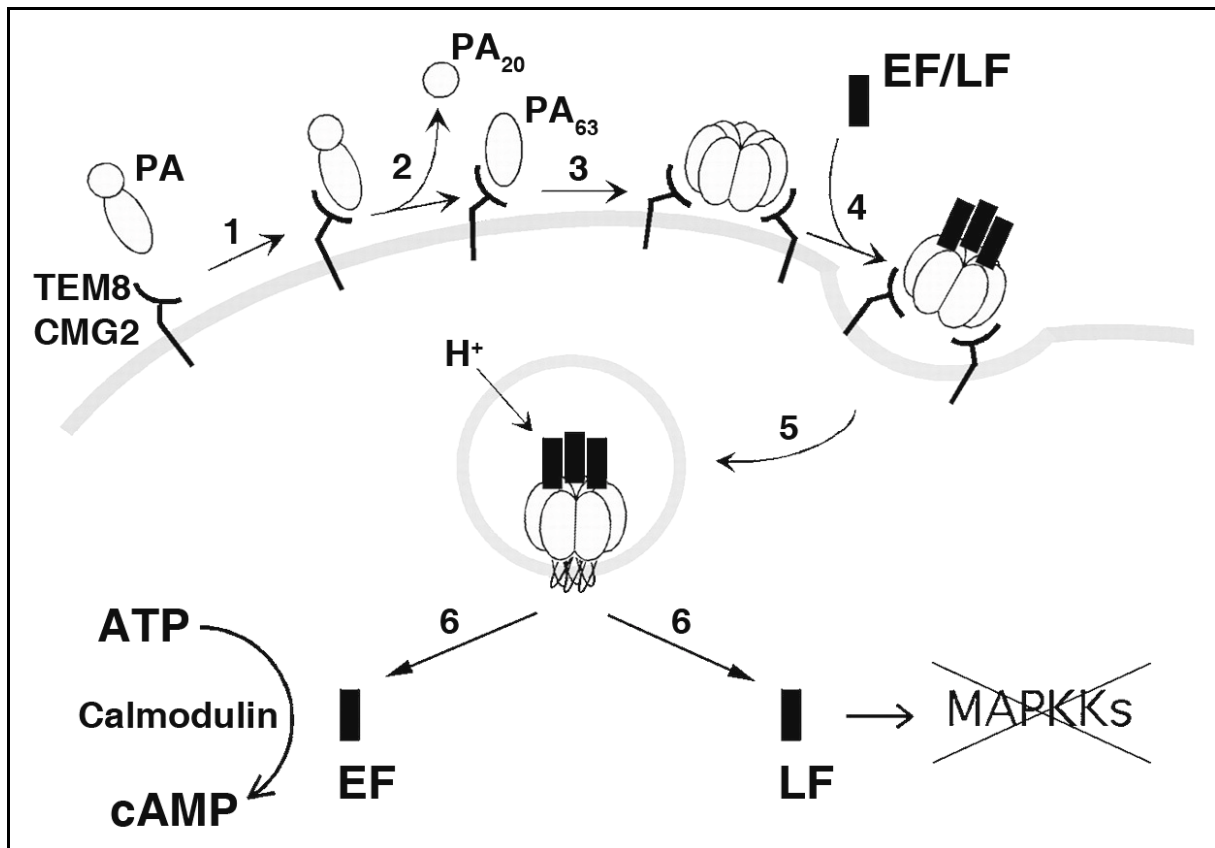
Fig. 7: Mechanism of PA-mediated delivery of EF and LF to the cytosol of host cells. 1: Binding of PA to the host cell receptors TEM8 or CMG2; 2: Cleavage of PA into PA_{20} and PA_{63}; 3: Formation of heptameric complexes of PA_{63}; 4: Binding of 3 molecules of EF and/or LF; 5: Endocytosis to the complex; 6: Release of EF and LF to the cytosol by PA induced by low pH. EF is activated by calmodulin and effects cAMP accumulation, LF disrupts MAPKK signaling. The figure is adapted from literature (Krantz *et al.*, 2004, 2006; Wigelsworth *et al.*, 2004) and http://mcb.berkeley.edu/labs/krantz/research/anthrax.html.

LF is a Zn^{2+}-dependent protease cleaving members of the mitogen-activated protein kinase kinase family (Duesbery *et al.*, 1998; Vitale *et al.*, 1998; Hong *et al.*, 2005). LF can induce apoptosis of macrophages and endothelial cells and impair the function of dendritic cells (Park *et al.*, 2002; Agrawal *et al.*, 2003; Kirby, 2004). Edema factor (EF) is an AC toxin that is inactive outside the host cell. However,

within the cell, EF binds calmodulin resulting in assembly of the active catalytic site and toxin activation (Fig. **8**).
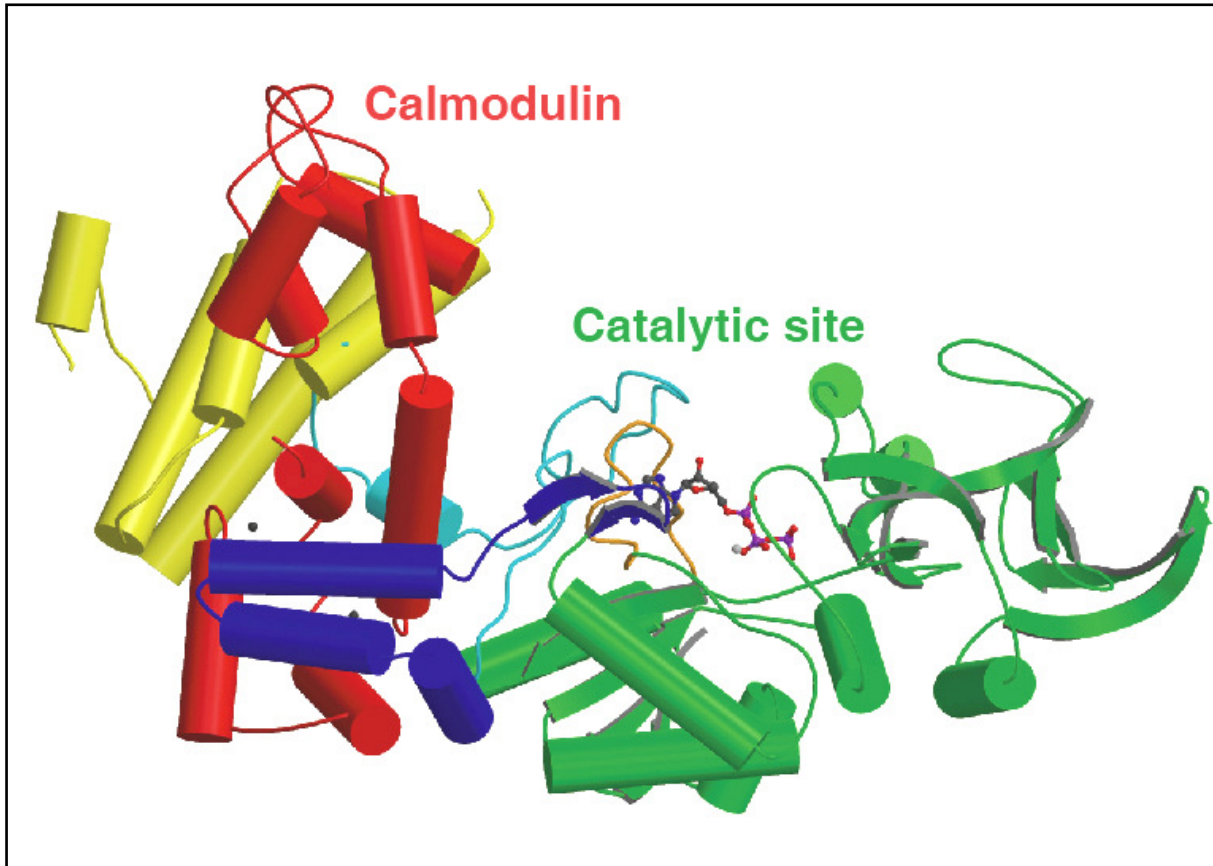
Fig. 8: Crystal structure of EF with bound calmodulin (Drum *et al.*, 2002; Guo *et al.*, 2005). The catalytic region of EF coordinating 3´d-ATP is shown in green, calmodulin is shown in red. The subunits of EF binding and embracing calmodulin are colored blue, yellow and cyan.

By effecting excessive cAMP accumulation, EF activity protects the bacteria from phagocytic destruction (Confer and Eaton, 1982; Leppla, 1982) and causes a broad range of tissue damage (Hong *et al.*, 2005). EF can block the phagocytic abilities of monocytes (O´Brien *et al.*, 1985), compromise the function of dendritic cells (Tournier *et al.*, 2005), impair activation and proliferation of T-cells (Paccani *et al.*, 2005) and manipulate cytokine secretion (Tournier *et al.*, 2005). Additionally, inhibition of human neutrophil NADPH oxidase activity was observed (Crawford *et al.*, 2006). EF is lethal to mice, causing multiple tissue damage and cardiovascular malfunction (Stanley and Smith, 1961; Pezard *et al.*, 1991). EF and LF synergize in their action against host immunity (Paccani *et al.*, 2005; Tournier *et al.*, 2005; Firoved

et al., 2007) and deletion of the EF or LF gene leads to reduced virulence of anthrax bacteria (Pezard *et al.*, 1991; Brossier *et al.*, 2000). A strain of anthrax with a defective EF gene caused 100-fold reduced lethality in mice (Brossier *et al.*, 2000) pointing to major importance of EF in the pathogenesis of anthrax. Peptide inhibitors can prevent binding of LF and EF to PA neutralizing anthrax toxin *in vivo* (Pini *et al.*, 2006).

As shown in Fig. **9**, the catalytic mechanism of EF is assumed to proceed in two-metal-ion catalysis, involving two divalent metal ions in nucleotide cyclization and a nucleophilic attack of the 3´-oxygen atom of ribose on the α-phosphate group (Guo *et al.*, 2004; Shen *et al.*, 2005; Gupta *et al.*, 2006). The adenine moiety of ATP is recognised by a main chain carbonyl group. Two divalent metal ions are coordinated by D491, D493 and H577. The negatively charged triphosphate tail is coordinated by the positive residues K346, K353, K372 and R329. N583 interacts with the ribose oxygen atom, decreasing the rotational freedom of ribose and holding the 3´-OH group of ribose in position for its nucleophilic attack. H351 serves as a catalytic base to activate a surrounding water molecule by deprotonation. The protonated H351 stabilizes an OH^- ion near the 3´-OH of ATP, which facilitates the deprotonation of 3´-OH. Mutation of H351 results in dramatically reduced catalytic activity, confirming the important role of H351 (Shen *et al.*, 2005; Gupta *et al.*, 2006). The first divalent metal ion also facilitates the deprotonation of 3´-OH by stabilizing the negative charge of the resulting 3´-oxyanion. Thus, the action of the first divalent metal ion and H351 is additive with respect to deprotonation of 3´-OH. The second metal ion facilitates the bond breakage between α- and β-phosphates by stabilizing the developing negative charges. The positive residues K346, K353, K372 and R329 coordinating the triphosphate tail also stabilize the negative charges developing during catalysis.
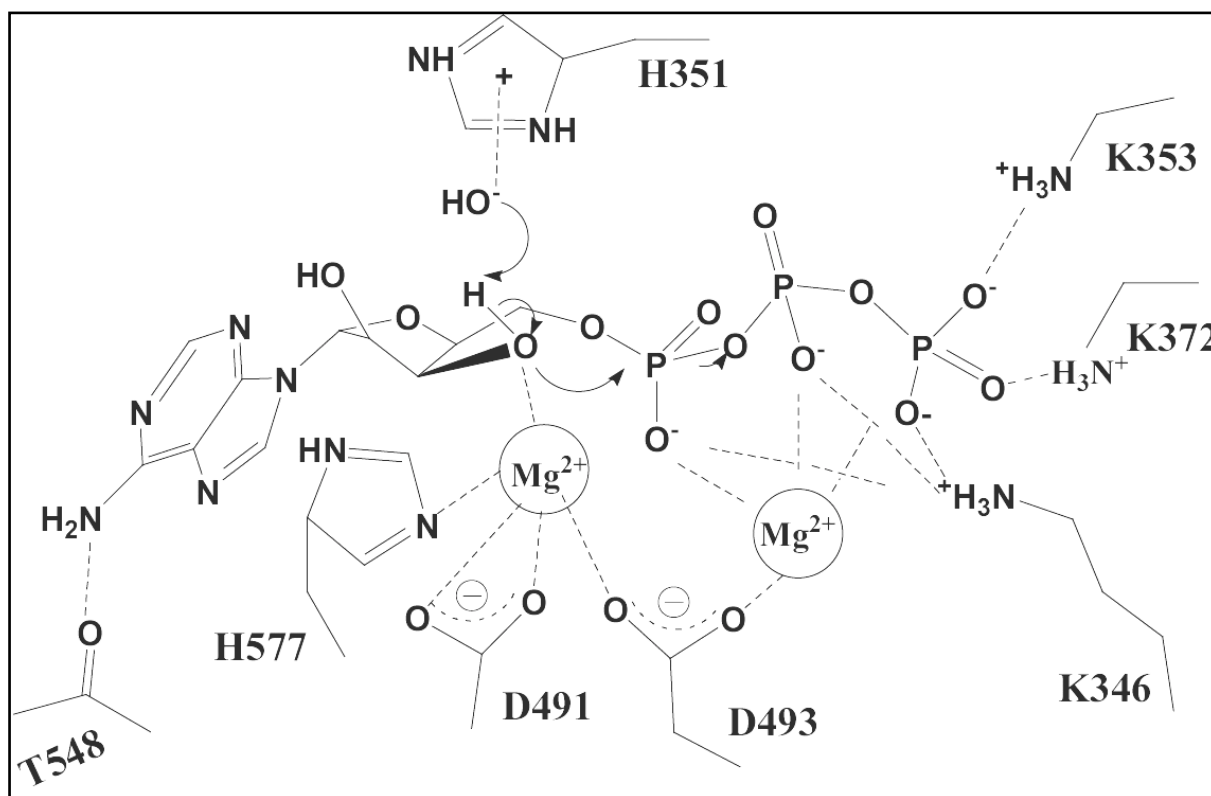
Fig. 9: Catalytic mechanism of EF (Shen *et al.*, 2005). The cyclization of ATP to cAMP and PP$_i$ occurs by nucleophilic attack of the 3′-oxygen atom of ribose on the α-phosphate group. Two divalent metal ions are coordinated by D491, D493 and H577. H351 serves as a catalytic base. The first divalent metal ion stabilizes the negative charge of the resulting 3′-oxyanion. The second metal ion facilitates the bond breakage between α- and β-phosphates by stabilizing the developing negative charges. The negatively charged triphosphate tail is coordinated by positive amino acid residues (K346, K353, K372 and R329).

In 2001, *Bacillus anthracis* was unleashed upon the US public by bioterrorists. Of the eleven infected people who had inhaled the agent, five died within a few days after infection. Thus, antibiotic treatment used for the victims resulted in a survival rate of only about 50% (Stubbs, 2002; Shen *et al.*, 2004). Anthrax kills because the agent overwhelms the patient before innate host defense systems have the chance to eradicate the invaders. Generally, when the bacteria are inhaled, sepsis and toxaemia occur, resulting in death 2 to 5 days after infection (Little and Ivins, 1999). This restricted time frame, limited efficacy of antibiotic treatment, and additionally, the possibility that the anthrax strain had been made resistant to known antibiotics make anthrax an ideal offensive weapon for bioterrorists (Trull *et al.*, 2007; Wallin *et al.*, 2007). Additionally, anthrax still is a civilian medical problem in several developing countries (Vijaikumar *et al.*, 2001; Rao *et al.*, 2007). Further investigations are

needed for the elucidation of agent-host interactions, and particularly, the function of EF has to be clarified in detail. This is the prerequisite for the development of EF inhibitors that could be administered in combination with antibiotics to improve cellular antimicrobial responses and survival rates.

1.2.2 Adenylyl Cyclase Toxin CyaA from *Bordetella pertussis*

With about 50 million yearly cases of whooping cough and with up to 400,000 deaths worldwide, mostly young infants in developing countries, the circulation of the disease throughout the world continues (Mattoo and Cherry, 2005; Tan *et al.*, 2005; Yeh and Mink, 2006). *Bordetella pertussis* (Fig. **10**), the etiologic agent of whooping cough, is a Gram-negative bacterial pathogen secreting numerous toxins, including *pertussis* toxin (PTX) and AC toxin CyaA (Hewlett *et al.*, 1989; Gentile *et al.*, 1990;

Antoine *et al.*, 2000). PTX ADP-ribosylates the α-subunit of heterotrimeric G_i proteins in mammalian cells manipulating a wide range of effects of signaling pathways (Munoz *et al.*, 1981; Moss *et al.*, 1983; Reisine, 1990; Carbonetti *et al.*, 2003, 2005).

The AC toxin CyaA is one of the major virulence factors of *Bordetella pertussis* facilitating respiratory tract colonization by the agent (Carbonetti *et al.*, 2005; Mattoo and Cherry, 2005; Bauche *et al.*, 2006). Deletion of the structural gene encoding for this toxin dramatically decreases the pathological effects of the infection as shown by reduced bacteria numbers found in the lung, almost abolished lung lesions,

Fig. 10: Colonization of ciliated epithelium of the respiratory tract by the agent of whooping cough, *Bordetella pertussis*.

as well as loss of haemolysis and inflammatory cell recruitment (Guermonprez *et al.*, 2001; Hewlett *et al.*, 2006). CyaA is able to invade eukaryotic cells by a unique mechanism comprising direct translocation of the CyaA catalytic domain across the plasma membrane of the target cells without the need for endocytosis (Ladant and Ullmann, 1999; Basler *et al.*, 2006; Bauche *et al.*, 2006). As shown in Fig. **11**, CyaA consists of an *N*-terminal AC enzyme domain, a pore-forming region with four

hydrophobic segments, a region where CyaA possesses a palmitoyl chain as well as a glycine- and aspartate-rich nonapeptide repeat. The latter mediates binding to the cell and is able to undergo conformational changes translocating the AC domain to the cytosol, where it is activated by CaM and consequently, effects uncontrolled conversion of cellular ATP to cAMP (Ladant and Ullmann, 1999; Basler *et al.*, 2006).
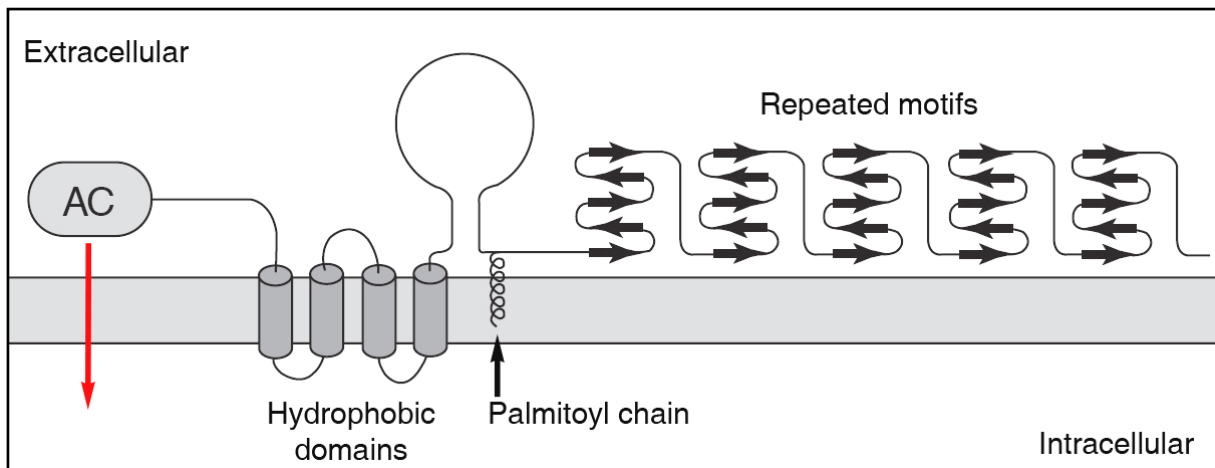
Fig. 11: Hypothetical mechanism for the translocation of *Bordetella pertussis* AC toxin across the target cell membrane. The four hydrophobic domains and the palmitoyl chain insert into the cell membrane. The repeated motifs bind divalent cations and mediate translocation of the AC domain across the membrane (Ladant and Ullmann, 1999).

By its hydrophobic residues, CyaA is able to form small cation-selective pores in target cell membranes, accounting for its haemolytic activity on erythrocytes (Basler *et al.*, 2006). CyaA specifically targets immune effector cells like neutrophils, macrophages or dendritic cells expressing the $\alpha_M\beta_2$ membrane receptor (Guermonprez *et al.*, 2001). CyaA inhibits neutrophil functions, including chemotaxis, phagocytic abilities, superoxide generation (Confer and Eaton, 1982; Friedman *et al.*, 1987; Weingart and Weiss, 2000) and induces apoptosis in macrophages (Khelef *et al.*, 1993; Gueirard *et al.*, 1998; Carbonetti *et al.*, 2005).

Several crystal structures of CyaA have been resolved, revealing the interactions of the substrate ATP with amino acid residues of the catalytic site and the domain interacting with the activator protein CaM (Guo *et al.*, 2005). Cyclization of ATP to cAMP and pyrophosphate by CyaA is assumed to occur by two-metal-ion catalysis which is described in more detail for the catalysis by *Bacillus anthracis* AC

toxin edema factor (EF). Amino acid residues crucial for catalysis by CyaA are well aligned with the corresponding residues of EF. At the catalytic site of CyaA, divalent metal ions are coordinated by D188, D190 and H298 (Glaser *et al.*, 1991; Guo *et al.*, 2005). The metal ions interact with the negatively charged triphosphate residue of ATP, which is also accommodated by the positive residues R37, K58, K65 and K84. N304 interacts with the ribose oxygen atom and holds the ribose in position. H63 serves as a catalytic base to deprotonate the 3′-OH group allowing the nucleophilic attack of the 3′-oxyanion on the α-phosphate group.

It has been reported that under certain circumstances, standard antibiotic treatment of whooping cough may not be sufficient to ensure complete eradication of the bacteria, e.g. a low-weight neonate relapsed after antibiotic treatments (Bonacorsi *et al.*, 2006). Therefore, further research is necessary to identify host/organism factors associated with severe disease and death. A combination of vaccines, antibiotics and - in particular - potent and selective CyaA inhibitors may be used to reduce morbidity and mortality and to control the ongoing circulation of *Bordetella pertussis*. As the CyaA enzyme contains the tryptophan residues W69 and W242, enzyme-tryptophan fluorescence approaches may be developed for the search for inhibitor molecules possessing affinity to CyaA.

1.2.3 Fluorescence Methods in the Investigation of Bacterial AC Toxins

Aromatic tryptophan residues in proteins can be excited by ultraviolet light to yield fluorescence emission. Additionally, tryptophan fluorescence is subject to environmental properties like polarity of the solvent or of interacting amino acid residues. Therefore, enzyme-tryptophan fluorescence approaches can be applied to study essential processes like conformational changes within the protein structure upon ligand binding or protein-protein interactions.

Fluorescence resonance energy transfer (FRET) has become widely used in many applications of fluorescence. FRET is an electrodynamic phenomenon between a donor molecule in the excited state and an acceptor molecule in the ground state (Lakowicz, 1999). Based on the concept of a fluorophore as an oscillating dipole, which can exchange energy with another dipole with a similar resonance frequency, excitation energy of the donor is transferred to the acceptor *via* a long-range dipole-dipole coupling mechanism resulting in an increase of fluorescence intensity of the acceptor molecule. The extent of FRET is predictable from the spectral properties of the fluorophores and is not significantly affected by the biomolecules in the sample. As a function of the extent of spectral overlap of the emission spectrum of the donor with the absorption spectrum of the acceptor, FRET depends on the quantum yield of the donor and the relative orientation of donor and acceptor. Moreover, the rate of energy transfer E strongly depends on the distance r between the donor and the acceptor molecule and is proportional to r^{-6}:

$$E = \frac{R_0^6}{R_0^6 + r^6} \qquad\qquad \textbf{Eq. 1.1}$$

R_0 is called the Förster radius and is the distance at which FRET is 50% efficient, typically being in the range of 20 to 60 Å. Therefore, FRET is convenient for studies of biological macromolecules. With κ being a factor describing the relative spacial orientation of donor and acceptor, the refractive index of the medium n, the quantum yield of the donor Q_D and the overlap integral expressing the degree of spectral overlap between the donor emission and the acceptor absorption $J(\lambda)$, the Förster radius is given by Eq. **1.2**. The greater the overlap of the emission spectrum of the donor with the absorption spectrum of the acceptor, the higher the value of R_0.

$$R_0 = 9.78 \cdot 10^3 (\kappa^2 \cdot n^{-4} \cdot Q_D \cdot J(\lambda))^{1/6} \qquad [\text{Å}] \qquad \textbf{Eq. 1.2}$$

Tryptophan residues can be excited at a wavelength of 280 nm, fluorescence emission occurs at 350 nm. The MANT-group in MANT-substituted nucleoside triphosphates is fluorescent; light is absorbed at a wavelength of 350 nm yielding fluorescence emission at 430 nm. Thus, the tryptophan emission spectrum and the MANT excitation spectrum overlap. Consequently, when tryptophan residues in AC are excited with MANT-nucleotides being in spacial proximity, e.g. due to binding at the catalytic site, FRET occurs, increasing fluorescence emission of the MANT-group at 430 nm (Fig. **12**).
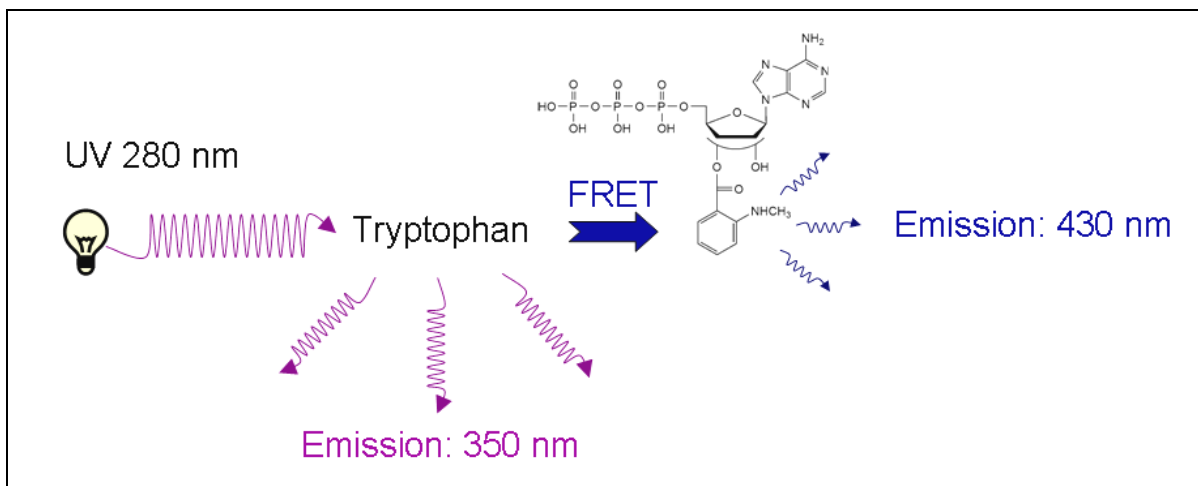
Fig. 12: Principle of FRET experiments with AC and MANT-nucleotides. Tryptophan residues in AC are excited at a wavelength of 280 nm, effecting fluorescence at 350 nm. Binding of MANT-nucleotides to the catalytic site of AC causes FRET, yielding emission at a wavelength of 430 nm.

As shown in Fig. **13**, two tryptophan residues are contained within the *Bordetella pertussis* CyaA protein, one close to the catalytic site (W69) and one being part of the domain interacting with CaM (W242). Therefore, binding of MANT-substituted nucleotides to the catalytic site of CyaA can be monitored by the occurrence of FRET due to excitation of tryptophan residues. Additionally, when the MANT-nucleotide binds to the protein, the MANT-group resides in an environment different from the solvent as it interacts with certain, mainly hydrophobic amino acid residues, e.g. phenylalanine. Therefore, fluorescence intensity and emission wavelength of MANT fluorescence change upon binding of the substituted nucleotide to the protein. Thus, MANT-nucleotide binding to CyaA can also be monitored by directly exciting the MANT-group at 350 nm and recording the resulting changes in direct fluorescence.
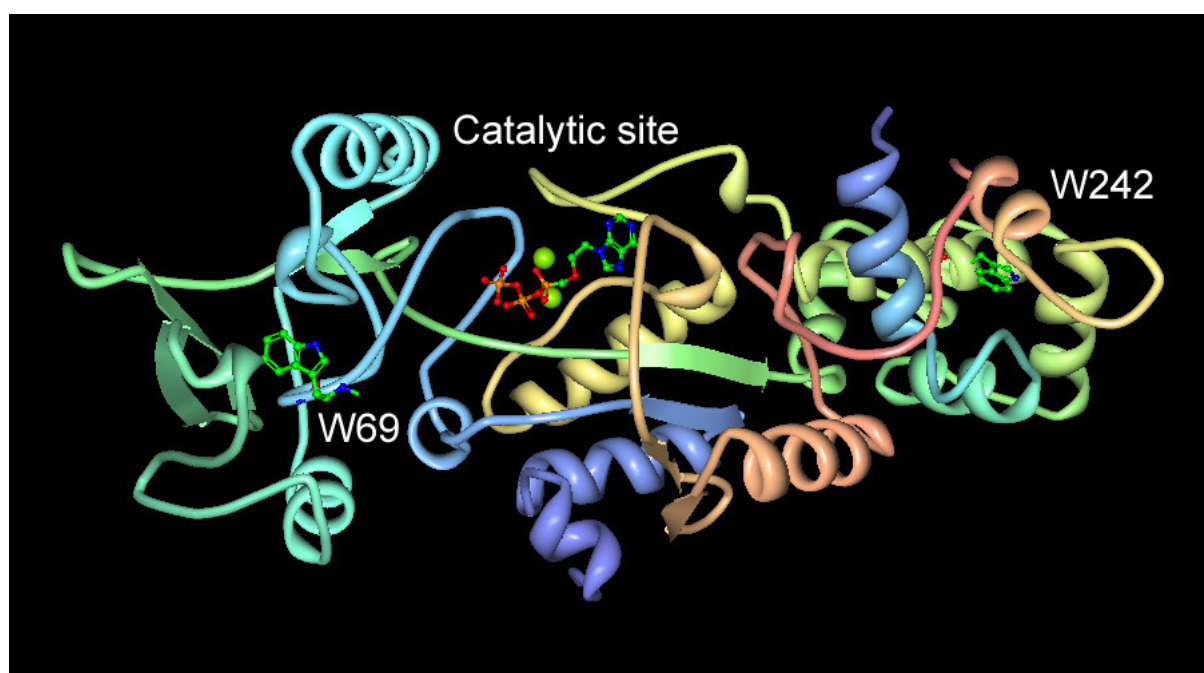
Fig. 13: Crystal structure of CyaA in complex with the substrate analog PMEApp bound at the catalytic site. Two metal ions coordinating the triphosphate chain of PMEApp are indicated as green spheres. W69 and W242 are located in close proximity of the catalytic site and the CaM binding site, respectively. Carbon atoms are colored green, nitrogen blue, phosphorous orange and oxygen red. PMEApp is the active metabolite of adefovir, a drug for the treatment of chronic hepatitis B virus infection, and a potent inhibitor of EF and CyaA. The figure was generated according to the structure reported previously (Guo *et al.*, 2005) using the PDB Protein Workshop 3.3 (Moreland *et al.*, 2005).

1.2.4 cCMP as a Third Cyclic Nucleotide Serving as Second Messenger

Besides the well-known key second messengers cAMP and cGMP, cyclic cytidine 3′:5′-monophosphate (cCMP) could be a third important cyclic nucleotide serving as a second messenger. Since the initial reports in 1974 by Bloch *et al.*, the natural occurrence of cCMP in various mammalian organs was confirmed unambiguously by mass spectrometry methods (Bloch *et al.*, 1974; Newton *et al.*, 1984). The kinetic parameters of the cytidylyl cyclase (CC) reaction were revealed and CC activities were characterized in nine organs of rat (Newton *et al.*, 1990, 1997). The discovery of phosphodiesterase activity accounting for the selective degradation of cCMP accentuates the potential importance of cCMP as a regulator of cell function (Newton *et al.*, 1986, 1999). Additionally, cCMP has been shown to stimulate protein kinase activity (Newton *et al.*, 1992) and ten proteins underwent cCMP-stimulated phosphorylation in brain tissue (Bond *et al.*, 2007; Ding *et al.*, 2008).

Most importantly, cCMP was shown to impair immune system functions. The cell-permeant cCMP-analog dibutyryl-cCMP inhibited the formation of thromboxanes and leukotrienes in macrophages, two important mediators of inflammation. Hence, dibutyryl-cCMP modulates macrophage eicosanoid synthesis (Elliott *et al.*, 1991). Dibutyryl-cCMP also inhibited the superoxide (O_2^-) formation in human neutrophils and effected neutrophil inactivation (Ervens and Seifert, 1991). Therefore, these findings point to cCMP being a potential novel second messenger with a negative regulatory function on immune responses. The question arises if bacterial adenylyl cyclase toxins might also possess cytidylyl cyclase activity forming cCMP to cause collateral impairment of host immune responses.

1.3   Scope and Objectives of the Work

The cAMP signaling pathway is crucial for many physiological processes and many disease states like neurodegenerative diseases, mood disorders, pain, drug dependency or heart failure. The use of drugs targeting GPCRs to exert influence on the cAMP signaling pathway is limited, e.g. due to receptor desensitization, receptor polymorphisms or additional receptors not targeted by the specific drug. As mammalian AC isoforms are expressed in a tissue-specific manner, isoform-selective AC activation or inhibition may be a promising novel therapeutic strategy. Therefore, the aim of this doctoral thesis is to develop analytical methods for the investigation and characterization of AC enzyme activity in specific mammalian tissues, e.g. in the heart. It is intended to develop a procedure for preparing cell membrane-bound AC from mammalian tissues exhibiting enzymatic activity. It is planned to clarify the expression patterns of the different AC isoforms in the considered tissues by using molecular biological approaches and immunoblotting methods. The biochemical parameters required for AC activity will be determined. With these prerequisites fulfilled, biochemical assays will be developed to pharmacologically characterize AC activity and to screen for molecules stimulating or inhibiting AC. The structure-activity relationships for AC inhibitors and activators shall be explored; highly potent and isoform-selective inhibitors and activators will be developed. As the cAMP signaling pathway is essential for cardiac contractility, and as heart failure is one of the most important causes for morbidity and mortality in elderly patients, the heart - hence AC from cardiac tissue - will be considered primarily. Thus, this work will provide the basis for exploring AC as target for the treatment of heart failure.

Anthrax disease and whooping cough, caused by *Bacillus anthracis* and *Bordetella pertussis*, respectively, are characterized by high morbidity rates and by severe courses of disease, causing death in many cases. Bacterial AC toxins are key virulence factors contributing to impairment of host immune responses and worsening of the infections. Therefore, the aim of this doctoral thesis is to provide the basis for the development of inhibitors of the AC toxins EF and CyaA from *B. anthracis* and *B. pertussis*, respectively. Biochemical methods will be developed allowing fluorescence-based screening for AC toxin inhibitors. Moreover, the detailed modes of action of EF and CyaA will be clarified. The question will be answered, if

cAMP formation is the only enzymatic activity of the AC toxins, or if the agents possess other hitherto unknown activities.

1.4   References

Abdel-Majid RM, Tremblay F and Baldridge WH (2002) Localization of adenylyl cyclase proteins in the rodent retina. *Brain Res Mol Brain Res* **101**:62-70.

Abrami L, Liu S, Cosson P, Leppla SH and van der Goot FG (2003) Anthrax toxin triggers endocytosis of its receptor *via* a lipid raft-mediated clathrin-dependent process. *J Cell Biol* **160**:321-328.

Agrawal A, Lingappa J, Leppla SH, Agrawal S, Jabbar A, Quinn C and Pulendran B (2003) Impairment of dendritic cells and adaptive immunity by anthrax lethal toxin. *Nature* **424**:329-334.

Ahuja N, Kumar P and Bhatnagar R (2004) The adenylate cyclase toxins. *Crit Rev Microbiol* **30**:187-196.

Antoine R, Raze D and Locht C (2000) Genomics of *Bordetella pertussis* toxins. *Int J Med Microbiol* **290**:301-305.

Antoni FA, Palkovits M, Simpson J, Smith SM, Leitch AL, Rosie R, Fink G and Paterson JM (1998) Ca^{2+}/calcineurin-inhibited adenylyl cyclase, highly abundant in forebrain regions, is important for learning and memory. *J Neurosci* **18**:9650-9661.

Antos CL, Frey N, Marx SO, Reiken S, Gaburjakova M, Richardson JA, Marks AR and Olson EN (2001) Dilated cardiomyopathy and sudden death resulting from constitutive activation of protein kinase A. *Circ Res* **89**:997-1004.

Ascenzi P, Visca P, Ippolito G, Spallarossa A, Bolognesi M and Montecucco C (2002) Anthrax toxin: A tripartite lethal combination. *FEBS Lett* **531**:384-388.

Baragli A, Grieco ML, Trieu P, Villeneuve LR and Hebert TE (2008) Heterodimers of adenylyl cyclases 2 and 5 show enhanced functional responses in the presence of Gα_s. *Cell Signal* **20**:480-492.

Basler M, Masin J, Osicka R and Sebo P (2006) Pore-forming and enzymatic activities of *Bordetella pertussis* adenylate cyclase toxin synergize in promoting lysis of monocytes. *Infect Immun* **74**:2207-2214.

Bauche C, Chenal A, Knapp O, Bodenreider C, Benz R, Chaffotte A and Ladant D (2006) Structural and functional characterization of an essential RTX subdomain of *Bordetella pertussis* adenylate cyclase toxin. *J Biol Chem* **281**:16914-16926.

Bauman AL, Soughayer J, Nguyen BT, Willoughby D, Carnegie GK, Wong W, Hoshi N, Langeberg LK, Cooper DM, Dessauer CW and Scott JD (2006) Dynamic regulation of cAMP synthesis through anchored PKA-adenylyl cyclase 5/6 complexes. *Mol Cell* **23**:925-931.

Bayewitch ML, Avidor-Reiss T, Levy R, Pfeuffer T, Nevo I, Simonds WF and Vogel Z (1998) Inhibition of adenylyl cyclase isoforms 5 and 6 by various Gβγ subunits. *FASEB J* **12**:1019-1025.

Benson EL, Huynh PD, Finkelstein A and Collier RJ (1998) Identification of residues lining the anthrax protective antigen channel. *Biochemistry* **37**:3941-3948.

Berthet J, Rall TW and Sutherland EW (1957a) The relationship of epinephrine and glucagon to liver phosphorylase. IV. Effect of epinephrine and glucagon on the reactivation of phosphorylase in liver homogenates. *J Biol Chem* **224**:463-475.

Berthet J, Sutherland EW and Rall TW (1957b) The assay of glucagon and epinephrine with use of liver homogenates. *J Biol Chem* **229**:351-361.

Bitensky MW, Gorman RE and Miller WH (1971) Adenyl cyclase as a link between photon capture and changes in membrane permeability of frog photoreceptors. *Proc Natl Acad Sci USA* **68**:561-562.

Bloch A (1974) Cytidine 3′,5′-monophosphate (cyclic CMP). I. Isolation from extracts of leukemia L-1210 Cells. *Biochem Biophys Res Commun* **58**:652-659.

Bloch A, Dutschman G and Maue R (1974) Cytidine 3′,5′-monophosphate (cyclic CMP). II. Initiation of leukemia L-1210 cell growth *in vitro*. *Biochem Biophys Res Commun* **59**:955-959.

Bonacorsi S, Farnoux C, Bidet P, Caro V, Aizenfisz S, Benhayoun M, Aujard Y, Guiso N and Bingen E (2006) Treatment failure of nosocomial *pertussis* infection in a very-low-birth-weight neonate. *J Clin Microbiol* **44**:3830-3832.

Bond AE, Dudley E, Tuytten R, Lemiere F, Smith CJ, Esmans EL and Newton RP (2007) Mass spectrometric identification of Rab23 phosphorylation as a response to challenge by cytidine 3′,5′-cyclic monophosphate in mouse brain. *Rapid Commun Mass Spectrom* **21**:2685-2692.

Boyd AP, Ross PJ, Conroy H, Mahon N, Lavelle EC and Mills KH (2005) *Bordetella pertussis* adenylate cyclase toxin modulates innate and adaptive immune responses: Distinct roles for acylation and enzymatic activity in immunomodulation and cell death. *J Immunol* **175**:730-738.

Bradley KA, Mogridge J, Mourez M, Collier RJ and Young JA (2001) Identification of the cellular receptor for anthrax toxin. *Nature* **414**:225-229.

Brey RN (2005) Molecular basis for improved anthrax vaccines. *Adv Drug Deliv Rev* **57**:1266-1292.

Brossier F and Mock M (2001) Toxins of *Bacillus anthracis*. *Toxicon* **39**:1747-1755.

Brossier F, Weber-Levy M, Mock M and Sirard JC (2000) Role of toxin functional domains in anthrax pathogenesis. *Infect Immun* **68**:1781-1786.

Buck J, Sinclair ML, Schapal L, Cann MJ and Levin LR (1999) Cytosolic adenylyl cyclase defines a unique signaling molecule in mammals. *Proc Natl Acad Sci USA* **96**:79-84.

Bygrave FL and Roberts HR (1995) Regulation of cellular calcium through signaling cross-talk involves an intricate interplay between the actions of receptors, G proteins, and second messengers. *FASEB J* **9**:1297-1303.

Cali JJ, Parekh RS and Krupinski J (1996) Splice variants of type 8 adenylyl cyclase. Differences in glycosylation and regulation by Ca^{2+}/calmodulin. *J Biol Chem* **271**:1089-1095.

Cali JJ, Zwaagstra JC, Mons N, Cooper DM and Krupinski J (1994) Type 8 adenylyl cyclase. A Ca^{2+}/calmodulin-stimulated enzyme expressed in discrete regions of rat brain. *J Biol Chem* **269**:12190-12195.

Carbonetti NH, Artamonova GV, Andreasen C and Bushar N (2005) *Pertussis* toxin and adenylate cyclase toxin provide a one-two punch for establishment of *Bordetella pertussis* infection of the respiratory tract. *Infect Immun* **73**:2698-2703.

Carbonetti NH, Artamonova GV, Mays RM and Worthington ZE (2003) *Pertussis* toxin plays an early role in respiratory tract colonization by *Bordetella pertussis*. *Infect Immun* **71**:6358-6366.

Chen J and Iyengar R (1993) Inhibition of cloned adenylyl cyclases by mutant-activated $G\alpha_i$ and specific suppression of type 2 adenylyl cyclase inhibition by phorbol ester treatment. *J Biol Chem* **268**:12253-12256.

Chen Y, Harry A, Li J, Smit MJ, Bai X, Magnusson R, Pieroni JP, Weng G and Iyengar R (1997) Adenylyl cyclase 6 is selectively regulated by protein kinase A phosphorylation in a region involved in $G\alpha_s$ stimulation. *Proc Natl Acad Sci USA* **94**:14100-14104.

Chester JA and Watts VJ (2007) Adenylyl cyclase 5: A new clue in the search for the "fountain of youth"? *Sci STKE* **2007**:pe64.

Choi EJ, Xia Z and Storm DR (1992) Stimulation of the type 3 olfactory adenylyl cyclase by calcium and calmodulin. *Biochemistry* **31**:6492-6498.

Christensen KA, Krantz BA and Collier RJ (2006) Assembly and disassembly kinetics of anthrax toxin complexes. *Biochemistry* **45**:2380-2386.

Confer DL and Eaton JW (1982) Phagocyte impotence caused by an invasive bacterial adenylate cyclase. *Science* **217**:948-950.

Cooper DM and Crossthwaite AJ (2006) Higher-order organization and regulation of adenylyl cyclases. *Trends Pharmacol Sci* **27**:426-431.

Crawford MA, Aylott CV, Bourdeau RW and Bokoch GM (2006) *Bacillus anthracis* toxins inhibit human neutrophil NADPH oxidase activity. *J Immunol* **176**:7557-7565.

Cunningham K, Lacy DB, Mogridge J and Collier RJ (2002) Mapping the lethal factor and edema factor binding sites on oligomeric anthrax protective antigen. *Proc Natl Acad Sci USA* **99**:7049-7053.

Defer N, Best-Belpomme M and Hanoune J (2000) Tissue specificity and physiological relevance of various isoforms of adenylyl cyclase. *Am J Physiol Renal Physiol* **279**:F400-416.

DeRubertis FR and Craven PA (1980) Cyclic nucleotides in carcinogenesis: Activation of the guanylate cyclase-cyclic GMP system by chemical carcinogens. *Adv Cyclic Nucleotide Res* **12**:97-109.

Desaubry L and Johnson RA (1998) Adenine nucleoside 3´-tetraphosphates are novel and potent inhibitors of adenylyl cyclases. *J Biol Chem* **273**:24972-24977.

Desaubry L, Shoshani I and Johnson RA (1996a) 2´,5´-Dideoxyadenosine 3´-polyphosphates are potent inhibitors of adenylyl cyclases. *J Biol Chem* **271**:2380-2382.

Desaubry L, Shoshani I and Johnson RA (1996b) Inhibition of adenylyl cyclase by a family of newly synthesized adenine nucleoside 3´-polyphosphates. *J Biol Chem* **271**:14028-14034.

Dessauer CW, Tesmer JJ, Sprang SR and Gilman AG (1998) Identification of a $G\alpha_i$ binding site on type 5 adenylyl cyclase. *J Biol Chem* **273**:25831-25839.

Dessauer CW, Tesmer JJ, Sprang SR and Gilman AG (1999) The interactions of adenylate cyclases with P-site inhibitors. *Trends Pharmacol Sci* **20**:205-210.

Ding S, Bond AE, Lemiere F, Tuytten R, Esmans EL, Brenton AG, Dudley E and Newton RP (2008) Online immobilized metal affinity chromatography/mass spectrometric analysis of changes elicited by cCMP in the murine brain phosphoproteome. *Rapid Commun Mass Spectrom* **22**:4129-4138.

Drum CL, Yan SZ, Bard J, Shen YQ, Lu D, Soelaiman S, Grabarek Z, Bohm A and Tang WJ (2002) Structural basis for the activation of anthrax adenylyl cyclase exotoxin by calmodulin. *Nature* **415**:396-402.

Duesbery NS, Webb CP, Leppla SH, Gordon VM, Klimpel KR, Copeland TD, Ahn NG, Oskarsson MK, Fukasawa K, Paull KD and Vande Woude GF (1998) Proteolytic inactivation of MAP-kinase-kinase by anthrax lethal factor. *Science* **280**:734-737.

Dwivedi Y and Pandey GN (2008) Adenylyl cyclase-cyclicAMP signaling in mood disorders: Role of the crucial phosphorylating enzyme protein kinase A. *Neuropsychiatr Dis Treat* **4**:161-176.

Eckstein F, Romaniuk PJ, Heideman W and Storm DR (1981) Stereochemistry of the mammalian adenylate cyclase reaction. *J Biol Chem* **256**:9118-9120.

Elliott GR, Lauwen AP and Bonta IL (1991) Dibutyryl cytidine 3´:5´-cyclic monophosphate; an inhibitor of A23187-stimulated macrophage leukotriene B$_4$ synthesis. *Agents Actions* **32**:90-91.

Engelhardt S, Hein L, Wiesmann F and Lohse MJ (1999) Progressive hypertrophy and heart failure in β_1-adrenergic receptor transgenic mice. *Proc Natl Acad Sci USA* **96**:7059-7064.

Ervens J and Seifert R (1991) Differential modulation by N^4, 2´-*O*-dibutyryl cytidine 3´:5´-cyclic monophosphate of neutrophil activation. *Biochem Biophys Res Commun* **174**:258-267.

Federman AD, Conklin BR, Schrader KA, Reed RR and Bourne HR (1992) Hormonal stimulation of adenylyl cyclase through G$_i$ protein $\beta\gamma$-subunits. *Nature* **356**:159-161.

Firoved AM, Moayeri M, Wiggins JF, Shen Y, Tang WJ and Leppla SH (2007) Anthrax edema toxin sensitizes DBA/2J mice to lethal toxin. *Infect Immun* **75**:2120-2125.

Friedlander AM (1986) Macrophages are sensitive to anthrax lethal toxin through an acid-dependent process. *J Biol Chem* **261**:7123-7126.

Friedman RL, Fiederlein RL, Glasser L and Galgiani JN (1987) *Bordetella pertussis* adenylate cyclase: Effects of affinity-purified adenylate cyclase on human polymorphonuclear leukocyte functions. *Infect Immun* **55**:135-140.

Furuyama T, Inagaki S and Takagi H (1993) Distribution of type 2 adenylyl cyclase mRNA in the rat brain. *Brain Res Mol Brain Res* **19**:165-170.

Gaion RM and Krishna G (1979) Cytidylate cyclase: The product isolated by the method of Cech and Ignarro is not cytidine 3´,5´-monophosphate. *Biochem Biophys Res Commun* **86**:105-111.

Gao BN and Gilman AG (1991) Cloning and expression of a widely distributed (type 4) adenylyl cyclase. *Proc Natl Acad Sci USA* **88**:10178-10182.

Geng W, Wang Z, Zhang J, Reed BY, Pak CY and Moe OW (2005) Cloning and characterization of the human soluble adenylyl cyclase. *Am J Physiol Cell Physiol* **288**:C1305-1316.

Gentile F, Knipling LG, Sackett DL and Wolff J (1990) Invasive adenylyl cyclase of *Bordetella pertussis*. Physical, catalytic, and toxic properties. *J Biol Chem* **265**:10686-10692.

Gille A, Lushington GH, Mou TC, Doughty MB, Johnson RA and Seifert R (2004) Differential inhibition of adenylyl cyclase isoforms and soluble guanylyl cyclase by purine and pyrimidine nucleotides. *J Biol Chem* **279**:19955-19969.

Gille A and Seifert R (2003a) 2´(3´)-*O*-(*N*-methylanthraniloyl)-substituted GTP analogs: A novel class of potent competitive adenylyl cyclase inhibitors. *J Biol Chem* **278**:12672-12679.

Gille A and Seifert R (2003b) MANT-substituted guanine nucleotides: A novel class of potent adenylyl cyclase inhibitors. *Life Sci* **74**:271-279.

Gilman AG (1987) G proteins: Transducers of receptor-generated signals. *Annu Rev Biochem* **56**:615-649.

Glaser P, Munier H, Gilles AM, Krin E, Porumb T, Barzu O, Sarfati R, Pellecuer C and Danchin A (1991) Functional consequences of single amino acid substitutions in calmodulin-activated adenylate cyclase of *Bordetella pertussis*. *EMBO J* **10**:1683-1688.

Goldberg ND, Haddox MK, Nicol SE, Glass DB, Sanford CH, Kuehl FA, Jr. and Estensen R (1975) Biologic regulation through opposing influences of cyclic

GMP and cyclic AMP: The Yin Yang hypothesis. *Adv Cyclic Nucleotide Res* **5**:307-330.

Goldberg ND, O´Dea RF and Haddox MK (1973) Cyclic GMP. *Adv Cyclic Nucleotide Res* **3**:155-223.

Gordon VM, Leppla SH and Hewlett EL (1988) Inhibitors of receptor-mediated endocytosis block the entry of *Bacillus anthracis* adenylate cyclase toxin but not that of *Bordetella pertussis* adenylate cyclase toxin. *Infect Immun* **56**:1066-1069.

Gu C, Cali JJ and Cooper DM (2002) Dimerization of mammalian adenylate cyclases. *Eur J Biochem* **269**:413-421.

Gu C and Cooper DM (1999) Calmodulin-binding sites on adenylyl cyclase type 8. *J Biol Chem* **274**:8012-8021.

Gueirard P, Druilhe A, Pretolani M and Guiso N (1998) Role of adenylate cyclase-hemolysin in alveolar macrophage apoptosis during *Bordetella pertussis* infection *in vivo*. *Infect Immun* **66**:1718-1725.

Guermonprez P, Khelef N, Blouin E, Rieu P, Ricciardi-Castagnoli P, Guiso N, Ladant D and Leclerc C (2001) The adenylate cyclase toxin of *Bordetella pertussis* binds to target cells *via* the $\alpha_M\beta_2$ integrin (CD11b/CD18). *J Exp Med* **193**:1035-1044.

Guo Q, Shen Y, Lee YS, Gibbs CS, Mrksich M and Tang WJ (2005) Structural basis for the interaction of *Bordetella pertussis* adenylyl cyclase toxin with calmodulin. *EMBO J* **24**:3190-3201.

Guo Q, Shen Y, Zhukovskaya NL, Florian J and Tang WJ (2004) Structural and kinetic analyses of the interaction of anthrax adenylyl cyclase toxin with reaction products cAMP and pyrophosphate. *J Biol Chem* **279**:29427-29435.

Gupta M, Alam S and Bhatnagar R (2006) Kinetic characterization and ligand binding studies of H351 mutants of *Bacillus anthracis* adenylate cyclase. *Arch Biochem Biophys* **446**:28-34.

Hammond HK (2006) Adenylyl cyclase gene transfer in heart failure. *Ann N Y Acad Sci* **1080**:426-436.

Hanoune J and Defer N (2001) Regulation and role of adenylyl cyclase isoforms. *Annu Rev Pharmacol Toxicol* **41**:145-174.

Hanoune J, Pouille Y, Tzavara E, Shen T, Lipskaya L, Miyamoto N, Suzuki Y and Defer N (1997) Adenylyl cyclases: Structure, regulation and function in an enzyme superfamily. *Mol Cell Endocrinol* **128**:179-194.

Harry A, Chen Y, Magnusson R, Iyengar R and Weng G (1997) Differential regulation of adenylyl cyclases by $G\alpha_s$. *J Biol Chem* **272**:19017-19021.

Hewlett EL, Donato GM and Gray MC (2006) Macrophage cytotoxicity produced by adenylate cyclase toxin from *Bordetella pertussis*: More than just making cyclic AMP! *Mol Microbiol* **59**:447-459.

Hewlett EL, Gordon VM, McCaffery JD, Sutherland WM and Gray MC (1989) Adenylate cyclase toxin from *Bordetella pertussis*. Identification and purification of the holotoxin molecule. *J Biol Chem* **264**:19379-19384.

Hines LM, Hoffman PL, Bhave S, Saba L, Kaiser A, Snell L, Goncharov I, LeGault L, Dongier M, Grant B, Pronko S, Martinez L, Yoshimura M and Tabakoff B (2006) A sex-specific role of type 7 adenylyl cyclase in depression. *J Neurosci* **26**:12609-12619.

Hiratsuka T (1982) New fluorescent analogs of cAMP and cGMP available as substrates for cyclic nucleotide phosphodiesterase. *J Biol Chem* **257**:13354-13358.

Hiratsuka T (1983) New ribose-modified fluorescent analogs of adenine and guanine nucleotides available as substrates for various enzymes. *Biochim Biophys Acta* **742**:496-508.

Hong J, Beeler J, Zhukovskaya NL, He W, Tang WJ and Rosner MR (2005) Anthrax edema factor potency depends on mode of cell entry. *Biochem Biophys Res Commun* **335**:850-857.

Hurley JH (1998) The adenylyl and guanylyl cyclase superfamily. *Curr Opin Struct Biol* **8**:770-777.

Ishikawa Y, Iwatsubo K, Tsunematsu T and Okumura S (2005) Genetic manipulation and functional analysis of cAMP signalling in cardiac muscle: Implications for a new target of pharmacotherapy. *Biochem Soc Trans* **33**:1337-1340.

Iwami G, Kawabe J, Ebina T, Cannon PJ, Homcy CJ and Ishikawa Y (1995) Regulation of adenylyl cyclase by protein kinase A. *J Biol Chem* **270**:12481-12484.

Iwamoto T, Okumura S, Iwatsubo K, Kawabe J, Ohtsu K, Sakai I, Hashimoto Y, Izumitani A, Sango K, Ajiki K, Toya Y, Umemura S, Goshima Y, Arai N, Vatner

SF and Ishikawa Y (2003) Motor dysfunction in type 5 adenylyl cyclase-null mice. *J Biol Chem* **278**:16936-16940.

Iwase M, Uechi M, Vatner DE, Asai K, Shannon RP, Kudej RK, Wagner TE, Wight DC, Patrick TA, Ishikawa Y, Homcy CJ and Vatner SF (1997) Cardiomyopathy induced by cardiac Gα_s overexpression. *Am J Physiol* **272**:H585-589.

Iwatsubo K, Minamisawa S, Tsunematsu T, Nakagome M, Toya Y, Tomlinson JE, Umemura S, Scarborough RM, Levy DE and Ishikawa Y (2004) Direct inhibition of type 5 adenylyl cyclase prevents myocardial apoptosis without functional deterioration. *J Biol Chem* **279**:40938-40945.

Iwatsubo K, Tsunematsu T and Ishikawa Y (2003) Isoform-specific regulation of adenylyl cyclase: A potential target in future pharmacotherapy. *Expert Opin Ther Targets* **7**:441-451.

Iyengar R (1993) Molecular and functional diversity of mammalian G$_s$-stimulated adenylyl cyclases. *FASEB J* **7**:768-775.

Jacobowitz O and Iyengar R (1994) Phorbol ester-induced stimulation and phosphorylation of adenylyl cyclase 2. *Proc Natl Acad Sci USA* **91**:10630-10634.

Jaiswal BS and Conti M (2001) Identification and functional analysis of splice variants of the germ cell soluble adenylyl cyclase. *J Biol Chem* **276**:31698-31708.

Jameson DM and Eccleston JF (1997) Fluorescent nucleotide analogs: Synthesis and applications. *Methods Enzymol* **278**:363-390.

Jourdan KB, Mason NA, Long L, Philips PG, Wilkins MR and Morrell NW (2001) Characterization of adenylyl cyclase isoforms in rat peripheral pulmonary arteries. *Am J Physiol Lung Cell Mol Physiol* **280**:L1359-1369.

Kawabe J, Ebina T, Ismail S, Kitchen DB, Homcy CJ and Ishikawa Y (1994) A novel peptide inhibitor of adenylyl cyclase (AC). A peptide from type 5 AC directly inhibits AC catalytic activity. *J Biol Chem* **269**:24906-24911.

Kebabian JW (1977a) Biochemical regulation and physiological significance of cyclic nucleotides in the nervous system. *Adv Cyclic Nucleotide Res* **8**:421-508.

Kebabian JW (1977b) Brain Biochemistry. *Science* **198**:599-600.

Kebabian JW (1977c) Cyclic nucleotides and synaptic transmission in sympathetic ganglia. *Adv Biochem Psychopharmacol* **16**:533-539.

Khelef N, Zychlinsky A and Guiso N (1993) *Bordetella pertussis* induces apoptosis in macrophages: Role of adenylate cyclase-hemolysin. *Infect Immun* **61**:4064-4071.

Kim KS, Kim J, Back SK, Im JY, Na HS and Han PL (2007) Markedly attenuated acute and chronic pain responses in mice lacking adenylyl cyclase 5. *Genes Brain Behav* **6**:120-127.

Kim KS, Lee KW, Baek IS, Lim CM, Krishnan V, Lee JK, Nestler EJ and Han PL (2008) Adenylyl cyclase 5 activity in the nucleus accumbens regulates anxiety-related behavior. *J Neurochem* **107**:105-115.

Kim KS, Lee KW, Lee KW, Im JY, Yoo JY, Kim SW, Lee JK, Nestler EJ and Han PL (2006) Adenylyl cyclase type 5 (AC5) is an essential mediator of morphine action. *Proc Natl Acad Sci USA* **103**:3908-3913.

Kirby JE (2004) Anthrax lethal toxin induces human endothelial cell apoptosis. *Infect Immun* **72**:430-439.

Klimpel KR, Molloy SS, Thomas G and Leppla SH (1992) Anthrax toxin protective antigen is activated by a cell surface protease with the sequence specificity and catalytic properties of furin. *Proc Natl Acad Sci USA* **89**:10277-10281.

Kobilka BK (2007) G protein-coupled receptor structure and activation. *Biochim Biophys Acta* **1768**:794-807.

Kolakowski LF, Jr. (1994) GCRDb: A G protein-coupled receptor database. *Receptors Channels* **2**:1-7.

Kozasa T and Gilman AG (1995) Purification of recombinant G proteins from Sf9 cells by hexahistidine tagging of associated subunits. Characterization of α_{12} and inhibition of adenylyl cyclase by α_z. *J Biol Chem* **270**:1734-1741.

Krantz BA, Finkelstein A and Collier RJ (2006) Protein translocation through the anthrax toxin transmembrane pore is driven by a proton gradient. *J Mol Biol* **355**:968-979.

Krantz BA, Trivedi AD, Cunningham K, Christensen KA and Collier RJ (2004) Acid-induced unfolding of the amino-terminal domains of the lethal and edema factors of anthrax toxin. *J Mol Biol* **344**:739-756.

Kreek MJ (1997) Opiate and cocaine addictions: Challenge for pharmacotherapies. *Pharmacol Biochem Behav* **57**:551-569.

Krishnan V, Graham A, Mazei-Robison MS, Lagace DC, Kim KS, Birnbaum S, Eisch AJ, Han PL, Storm DR, Zachariou V and Nestler EJ (2008) Calcium-sensitive

adenylyl cyclases in depression and anxiety: Behavioral and biochemical consequences of isoform targeting. *Biol Psychiatry* **64**:336-343.

Kristiansen K (2004) Molecular mechanisms of ligand binding, signaling, and regulation within the superfamily of G protein-coupled receptors: Molecular modeling and mutagenesis approaches to receptor structure and function. *Pharmacol Ther* **103**:21-80.

Krupinski J, Coussen F, Bakalyar HA, Tang WJ, Feinstein PG, Orth K, Slaughter C, Reed RR and Gilman AG (1989) Adenylyl cyclase amino acid sequence: Possible channel- or transporter-like structure. *Science* **244**:1558-1564.

Kudlacek O, Mitterauer T, Nanoff C, Hohenegger M, Tang WJ, Freissmuth M and Kleuss C (2001) Inhibition of adenylyl and guanylyl cyclase isoforms by the antiviral drug foscarnet. *J Biol Chem* **276**:3010-3016.

Ladant D and Ullmann A (1999) *Bordetella pertussis* adenylate cyclase: A toxin with multiple talents. *Trends Microbiol* **7**:172-176.

Lai HL, Lin TH, Kao YY, Lin WJ, Hwang MJ and Chern Y (1999) The *N* terminus domain of type 6 adenylyl cyclase mediates its inhibition by protein kinase C. *Mol Pharmacol* **56**:644-650.

Lai NC, Roth DM, Gao MH, Tang T, Dalton N, Lai YY, Spellman M, Clopton P and Hammond HK (2004) Intracoronary adenovirus encoding adenylyl cyclase 6 increases left ventricular function in heart failure. *Circulation* **110**:330-336.

Lai NC, Tang T, Gao MH, Saito M, Takahashi T, Roth DM and Hammond HK (2008) Activation of cardiac adenylyl cyclase expression increases function of the failing ischemic heart in mice. *J Am Coll Cardiol* **51**:1490-1497.

Lakowicz JR (1999) *Principles of fluorescence spectroscopy*. Kluwer Academic/Plenum, New York.

Lane-Ladd SB, Pineda J, Boundy VA, Pfeuffer T, Krupinski J, Aghajanian GK and Nestler EJ (1997) CREB (cAMP response element-binding protein) in the locus coeruleus: Biochemical, physiological, and behavioral evidence for a role in opiate dependence. *J Neurosci* **17**:7890-7901.

Lee KW, Hong JH, Choi IY, Che Y, Lee JK, Yang SD, Song CW, Kang HS, Lee JH, Noh JS, Shin HS and Han PL (2002) Impaired D_2 dopamine receptor function in mice lacking type 5 adenylyl cyclase. *J Neurosci* **22**:7931-7940.

Leppla SH (1982) Anthrax toxin edema factor: A bacterial adenylate cyclase that increases cyclic AMP concentrations of eukaryotic cells. *Proc Natl Acad Sci USA* **79**:3162-3166.

Li S, Lee ML, Bruchas MR, Chan GC, Storm DR and Chavkin C (2006) Calmodulin-stimulated adenylyl cyclase gene deletion affects morphine responses. *Mol Pharmacol* **70**:1742-1749.

Little SF and Ivins BE (1999) Molecular pathogenesis of *Bacillus anthracis* infection. *Microbes Infect* **1**:131-139.

Liu S and Leppla SH (2003) Cell surface tumor endothelium marker 8 cytoplasmic tail-independent anthrax toxin binding, proteolytic processing, oligomer formation, and internalization. *J Biol Chem* **278**:5227-5234.

Liu Y, Ruoho AE, Rao VD and Hurley JH (1997) Catalytic mechanism of the adenylyl and guanylyl cyclases: Modeling and mutational analysis. *Proc Natl Acad Sci USA* **94**:13414-13419.

Livera G, Xie F, Garcia MA, Jaiswal B, Chen J, Law E, Storm DR and Conti M (2005) Inactivation of the mouse adenylyl cyclase 3 gene disrupts male fertility and spermatozoon function. *Mol Endocrinol* **19**:1277-1290.

Maas JW, Jr., Vogt SK, Chan GC, Pineda VV, Storm DR and Muglia LJ (2005) Calcium-stimulated adenylyl cyclases are critical modulators of neuronal ethanol sensitivity. *J Neurosci* **25**:4118-4126.

Marquez B and Suarez SS (2008) Soluble adenylyl cyclase is required for activation of sperm but does not have a direct effect on hyperactivation. *Reprod Fertil Dev* **20**:247-252.

Matsuoka I, Giuili G, Poyard M, Stengel D, Parma J, Guellaen G and Hanoune J (1992) Localization of adenylyl and guanylyl cyclase in rat brain by *in situ* hybridization: Comparison with calmodulin mRNA distribution. *J Neurosci* **12**:3350-3360.

Matsuoka I, Maldonado R, Defer N, Noel F, Hanoune J and Roques BP (1994) Chronic morphine administration causes region-specific increase of brain type 8 adenylyl cyclase mRNA. *Eur J Pharmacol* **268**:215-221.

Mattoo S and Cherry JD (2005) Molecular pathogenesis, epidemiology, and clinical manifestations of respiratory infections due to *Bordetella pertussis* and other *Bordetella* subspecies. *Clin Microbiol Rev* **18**:326-382.

Milne JC, Furlong D, Hanna PC, Wall JS and Collier RJ (1994) Anthrax protective antigen forms oligomers during intoxication of mammalian cells. *J Biol Chem* **269**:20607-20612.

Mock M and Fouet A (2001) Anthrax. *Annu Rev Microbiol* **55**:647-671.

Mogridge J, Cunningham K, Lacy DB, Mourez M and Collier RJ (2002) The lethal and edema factors of anthrax toxin bind only to oligomeric forms of the protective antigen. *Proc Natl Acad Sci USA* **99**:7045-7048.

Mons N and Cooper DM (1994) Adenylyl cyclase mRNA expression does not reflect the predominant Ca^{2+}/calmodulin-stimulated activity in the hypothalamus. *J Neuroendocrinol* **6**:665-671.

Moore MS, DeZazzo J, Luk AY, Tully T, Singh CM and Heberlein U (1998) Ethanol intoxication in Drosophila: Genetic and pharmacological evidence for regulation by the cAMP signaling pathway. *Cell* **93**:997-1007.

Moreland JL, Gramada A, Buzko OV, Zhang Q and Bourne PE (2005) The Molecular Biology Toolkit (MBT): A modular platform for developing molecular visualization applications. *BMC Bioinformatics* **6**:21.

Moss J, Stanley SJ, Burns DL, Hsia JA, Yost DA, Myers GA and Hewlett EL (1983) Activation by thiol of the latent NAD glycohydrolase and ADP-ribosyltransferase activities of *Bordetella pertussis* toxin (islet-activating protein). *J Biol Chem* **258**:11879-11882.

Mou TC, Gille A, Fancy DA, Seifert R and Sprang SR (2005) Structural basis for the inhibition of mammalian membrane adenylyl cyclase by 2´(3´)-*O*-(*N*-Methylanthraniloyl)-guanosine 5´-triphosphate. *J Biol Chem* **280**:7253-7261.

Mou TC, Gille A, Suryanarayana S, Richter M, Seifert R and Sprang SR (2006) Broad specificity of mammalian adenylyl cyclase for interaction with 2´,3´-substituted purine- and pyrimidine nucleotide inhibitors. *Mol Pharmacol* **70**:878-886.

Mourez M, Lacy DB, Cunningham K, Legmann R, Sellman BR, Mogridge J and Collier RJ (2002) 2001: A year of major advances in anthrax toxin research. *Trends Microbiol* **10**:287-293.

Munoz JJ, Arai H, Bergman RK and Sadowski PL (1981) Biological activities of crystalline pertussigen from *Bordetella pertussis*. *Infect Immun* **33**:820-826.

Murad F, Arnold WP, Mittal CK and Braughler JM (1979) Properties and regulation of guanylate cyclase and some proposed functions for cyclic GMP. *Adv Cyclic Nucleotide Res* **11**:175-204.

Nambi P and Aiyar N (2003) G protein-coupled receptors in drug discovery. *Assay Drug Dev Technol* **1**:305-310.

Newton RP, Bayliss MA, Khan JA, Bastani A, Wilkins AC, Games DE, Walton TJ, Brenton AG and Harris FM (1999) Kinetic analysis of cyclic CMP-specific and multifunctional phosphodiesterases by quantitative positive-ion fast-atom bombardment mass spectrometry. *Rapid Commun Mass Spectrom* **13**:574-584.

Newton RP, Groot N, van Geyschem J, Diffley PE, Walton TJ, Bayliss MA, Harris FM, Games DE and Brenton AG (1997) Estimation of cytidylyl cyclase activity and monitoring of side-product formation by fast-atom bombardment mass spectrometry. *Rapid Commun Mass Spectrom* **11**:189-194.

Newton RP, Khan JA, Brenton AG, Langridge JI, Harris FM and Walton TJ (1992) Quantitation by fast-atom bombardment mass spectrometry: Assay of cytidine 3´,5´-cyclic monophosphate-responsive protein kinase. *Rapid Commun Mass Spectrom* **6**:601-607.

Newton RP and Salih SG (1986) Cyclic CMP phosphodiesterase: Isolation, specificity and kinetic properties. *Int J Biochem* **18**:743-752.

Newton RP, Salih SG, Salvage BJ and Kingston EE (1984) Extraction, purification and identification of cytidine 3´,5´-cyclic monophosphate from rat tissues. *Biochem J* **221**:665-673.

Newton RP, Salvage BJ and Hakeem NA (1990) Cytidylate cyclase: Development of assay and determination of kinetic properties of a cytidine 3´,5´-cyclic monophosphate-synthesizing enzyme. *Biochem J* **265**:581-586.

O´Brien J, Friedlander A, Dreier T, Ezzell J and Leppla S (1985) Effects of anthrax toxin components on human neutrophils. *Infect Immun* **47**:306-310.

Okumura S, Takagi G, Kawabe J, Yang G, Lee MC, Hong C, Liu J, Vatner DE, Sadoshima J, Vatner SF and Ishikawa Y (2003) Disruption of type 5 adenylyl cyclase gene preserves cardiac function against pressure overload. *Proc Natl Acad Sci USA* **100**:9986-9990.

Oncu S, Oncu S and Sakarya S (2003) Anthrax - An overview. *Med Sci Monit* **9**:RA276-283.

Paccani SR, Tonello F, Ghittoni R, Natale M, Muraro L, D´Elios MM, Tang WJ, Montecucco C and Baldari CT (2005) Anthrax toxins suppress T lymphocyte activation by disrupting antigen receptor signaling. *J Exp Med* **201**:325-331.

Palczewski K, Kumasaka T, Hori T, Behnke CA, Motoshima H, Fox BA, Le Trong I, Teller DC, Okada T, Stenkamp RE, Yamamoto M and Miyano M (2000) Crystal structure of rhodopsin: A G protein-coupled receptor. *Science* **289**:739-745.

Park JM, Greten FR, Li ZW and Karin M (2002) Macrophage apoptosis by anthrax lethal factor through p38 MAP kinase inhibition. *Science* **297**:2048-2051.

Parker CW, Sullivan TJ and Wedner HJ (1974) Cyclic AMP and the immune response. *Adv Cyclic Nucleotide Res* **4**:1-79.

Patel TB, Du Z, Pierre S, Cartin L and Scholich K (2001) Molecular biological approaches to unravel adenylyl cyclase signaling and function. *Gene* **269**:13-25.

Petosa C, Collier RJ, Klimpel KR, Leppla SH and Liddington RC (1997) Crystal structure of the anthrax toxin protective antigen. *Nature* **385**:833-838.

Pezard C, Berche P and Mock M (1991) Contribution of individual toxin components to virulence of *Bacillus anthracis*. *Infect Immun* **59**:3472-3477.

Phan HM, Gao MH, Lai NC, Tang T and Hammond HK (2007) New signaling pathways associated with increased cardiac adenylyl cyclase 6 expression: Implications for possible congestive heart failure therapy. *Trends Cardiovasc Med* **17**:215-221.

Pini A, Runci Y, Falciani C, Lelli B, Brunetti J, Pileri S, Fabbrini M, Lozzi L, Ricci C, Bernini A, Tonello F, Dal Molin F, Neri P, Niccolai N and Bracci L (2006) Stable peptide inhibitors prevent binding of lethal and edema factors to protective antigen and neutralize anthrax toxin *in vivo*. *Biochem J* **395**:157-163.

Pinto C, Papa D, Hubner M, Mou TC, Lushington GH and Seifert R (2008) Activation and inhibition of adenylyl cyclase isoforms by forskolin analogs. *J Pharmacol Exp Ther* **325**:27-36.

Rao GR, Padmaja J, Lalitha MK, Rao PV, Kumar HK, Gopal KV, Jaideep M and Mohanraj P (2007) Cutaneous anthrax in a remote tribal area - Araku Valley, Visakhapatnam district, Andhra Pradesh, southern India. *Int J Dermatol* **46**:55-58.

Reiach JS, Li PP, Warsh JJ, Kish SJ and Young LT (1999) Reduced adenylyl cyclase immunolabeling and activity in postmortem temporal cortex of depressed suicide victims. *J Affect Disord* **56**:141-151.

Reisine T (1990) *Pertussis* toxin in the analysis of receptor mechanisms. *Biochem Pharmacol* **39**:1499-1504.

Rodbell M (1995) Nobel Lecture. Signal transduction: Evolution of an idea. *Biosci Rep* **15**:117-133.

Roth DM, Bayat H, Drumm JD, Gao MH, Swaney JS, Ander A and Hammond HK (2002) Adenylyl cyclase increases survival in cardiomyopathy. *Circulation* **105**:1989-1994.

Roth DM, Gao MH, Lai NC, Drumm J, Dalton N, Zhou JY, Zhu J, Entrikin D and Hammond HK (1999) Cardiac-directed adenylyl cyclase expression improves heart function in murine cardiomyopathy. *Circulation* **99**:3099-3102.

Sadana R and Dessauer CW (2009) Physiological roles for G protein-regulated adenylyl cyclase isoforms: Insights from knockout and overexpression studies. *Neurosignals* **17**:5-22.

Santelli E, Bankston LA, Leppla SH and Liddington RC (2004) Crystal structure of a complex between anthrax toxin and its host cell receptor. *Nature* **430**:905-908.

Schaefer ML, Wong ST, Wozniak DF, Muglia LM, Liauw JA, Zhuo M, Nardi A, Hartman RE, Vogt SK, Luedke CE, Storm DR and Muglia LJ (2000) Altered stress-induced anxiety in adenylyl cyclase type 8-deficient mice. *J Neurosci* **20**:4809-4820.

Schnecko A, Witte K, Bohl J, Ohm T and Lemmer B (1994) Adenylyl cyclase activity in Alzheimer´s disease brain: Stimulatory and inhibitory signal transduction pathways are differently affected. *Brain Res* **644**:291-296.

Scholich K, Barbier AJ, Mullenix JB and Patel TB (1997) Characterization of soluble forms of nonchimeric type 5 adenylyl cyclases. *Proc Natl Acad Sci USA* **94**:2915-2920.

Scobie HM, Rainey GJ, Bradley KA and Young JA (2003) Human capillary morphogenesis protein 2 functions as an anthrax toxin receptor. *Proc Natl Acad Sci USA* **100**:5170-5174.

Scorpio A, Blank TE, Day WA and Chabot DJ (2006) Anthrax vaccines: Pasteur to the present. *Cell Mol Life Sci* **63**:2237-2248.

Scorpio A, Chabot DJ, Day WA, O´Brien D K, Vietri NJ, Itoh Y, Mohamadzadeh M and Friedlander AM (2007) Poly-γ-glutamate capsule-degrading enzyme treatment enhances phagocytosis and killing of encapsulated *Bacillus anthracis*. *Antimicrob Agents Chemother* **51**:215-222.

Seamon K and Daly JW (1981a) Activation of adenylate cyclase by the diterpene forskolin does not require the guanine nucleotide regulatory protein. *J Biol Chem* **256**:9799-9801.

Seamon KB and Daly JW (1981b) Forskolin: A unique diterpene activator of cyclic AMP-generating systems. *J Cyclic Nucleotide Res* **7**:201-224.

Seamon KB, Padgett W and Daly JW (1981) Forskolin: Unique diterpene activator of adenylate cyclase in membranes and in intact cells. *Proc Natl Acad Sci USA* **78**:3363-3367.

Shen Y, Zhukovskaya NL, Guo Q, Florian J and Tang WJ (2005) Calcium-independent calmodulin binding and two-metal-ion catalytic mechanism of anthrax edema factor. *EMBO J* **24**:929-941.

Shen Y, Zhukovskaya NL, Zimmer MI, Soelaiman S, Bergson P, Wang CR, Gibbs CS and Tang WJ (2004) Selective inhibition of anthrax edema factor by adefovir, a drug for chronic hepatitis B virus infection. *Proc Natl Acad Sci USA* **101**:3242-3247.

Simonds WF (1999) G protein regulation of adenylate cyclase. *Trends Pharmacol Sci* **20**:66-73.

Smit MJ and Iyengar R (1998) Mammalian adenylyl cyclases. *Adv Second Messenger Phosphoprotein Res* **32**:1-21.

Stanley JL and Smith H (1961) Purification of factor 1 and recognition of a third factor of the anthrax toxin. *J Gen Microbiol* **26**:49-63.

Steer ML and Salzman EW (1980) Cyclic nucleotides in hemostasis and thrombosis. *Adv Cyclic Nucleotide Res* **12**:71-92.

Sternweis PC and Robishaw JD (1984) Isolation of two proteins with high affinity for guanine nucleotides from membranes of bovine brain. *J Biol Chem* **259**:13806-13813.

Storm DR, Hansel C, Hacker B, Parent A and Linden DJ (1998) Impaired cerebellar long-term potentiation in type 1 adenylyl cyclase mutant mice. *Neuron* **20**:1199-1210.

Stubbs MT (2002) Anthrax X-rayed: New opportunities for biodefence. *Trends Pharmacol Sci* **23**:539-541.

Sunahara RK, Dessauer CW and Gilman AG (1996) Complexity and diversity of mammalian adenylyl cyclases. *Annu Rev Pharmacol Toxicol* **36**:461-480.

Sunahara RK and Taussig R (2002) Isoforms of mammalian adenylyl cyclase: Multiplicities of signaling. *Mol Interv* **2**:168-184.

Sunahara RK, Tesmer JJ, Gilman AG and Sprang SR (1997) Crystal structure of the adenylyl cyclase activator Gα_s. *Science* **278**:1943-1947.

Sutherland EW (1972) Studies on the mechanism of hormone action. *Science* **177**:401-408.

Tabakoff B, Whelan JP, Ovchinnikova L, Nhamburo P, Yoshimura M and Hoffman PL (1995) Quantitative changes in G proteins do not mediate ethanol-induced downregulation of adenylyl cyclase in mouse cerebral cortex. *Alcohol Clin Exp Res* **19**:187-194.

Takahashi T, Tang T, Lai NC, Roth DM, Rebolledo B, Saito M, Lew WY, Clopton P and Hammond HK (2006) Increased cardiac adenylyl cyclase expression is associated with increased survival after myocardial infarction. *Circulation* **114**:388-396.

Tan T, Trindade E and Skowronski D (2005) Epidemiology of *pertussis*. *Pediatr Infect Dis J* **24**:S10-18.

Tang T, Gao MH, Lai NC, Firth AL, Takahashi T, Guo T, Yuan JX, Roth DM and Hammond HK (2008) Adenylyl cyclase type 6 deletion decreases left ventricular function *via* impaired calcium handling. *Circulation* **117**:61-69.

Tang WJ and Gilman AG (1991) Type-specific regulation of adenylyl cyclase by G protein $\beta\gamma$ subunits. *Science* **254**:1500-1503.

Tang WJ and Gilman AG (1992) Adenylyl cyclases. *Cell* **70**:869-872.

Tang WJ and Hurley JH (1998) Catalytic mechanism and regulation of mammalian adenylyl cyclases. *Mol Pharmacol* **54**:231-240.

Tang WJ, Iniguez-Lluhi JA, Mumby S and Gilman AG (1992) Regulation of mammalian adenylyl cyclases by G protein α and $\beta\gamma$ subunits. *Cold Spring Harb Symp Quant Biol* **57**:135-144.

Tantisira KG, Small KM, Litonjua AA, Weiss ST and Liggett SB (2005) Molecular properties and pharmacogenetics of a polymorphism of adenylyl cyclase type

9 in asthma: Interaction between β-agonist and corticosteroid pathways. *Hum Mol Genet* **14**:1671-1677.

Taussig R and Gilman AG (1995) Mammalian membrane-bound adenylyl cyclases. *J Biol Chem* **270**:1-4.

Taussig R, Iniguez-Lluhi JA and Gilman AG (1993) Inhibition of adenylyl cyclase by Gα$_i$. *Science* **261**:218-221.

Taussig R, Tang WJ, Hepler JR and Gilman AG (1994) Distinct patterns of bidirectional regulation of mammalian adenylyl cyclases. *J Biol Chem* **269**:6093-6100.

Tepe NM, Lorenz JN, Yatani A, Dash R, Kranias EG, Dorn GW, 2nd and Liggett SB (1999) Altering the receptor-effector ratio by transgenic overexpression of type 5 adenylyl cyclase: Enhanced basal catalytic activity and function without increased cardiomyocyte β-adrenergic signalling. *Biochemistry* **38**:16706-16713.

Tesmer JJ, Sunahara RK, Gilman AG and Sprang SR (1997) Crystal structure of the catalytic domains of adenylyl cyclase in a complex with Gα$_s$·GTPγS. *Science* **278**:1907-1916.

Tesmer JJ, Sunahara RK, Johnson RA, Gosselin G, Gilman AG and Sprang SR (1999) Two-metal-ion catalysis in adenylyl cyclase. *Science* **285**:756-760.

Timofeyev V, He Y, Tuteja D, Zhang Q, Roth DM, Hammond HK and Chiamvimonvat N (2006) Cardiac-directed expression of adenylyl cyclase reverses electrical remodeling in cardiomyopathy. *J Mol Cell Cardiol* **41**:170-181.

Tournier JN, Quesnel-Hellmann A, Mathieu J, Montecucco C, Tang WJ, Mock M, Vidal DR and Goossens PL (2005) Anthrax edema toxin cooperates with lethal toxin to impair cytokine secretion during infection of dendritic cells. *J Immunol* **174**:4934-4941.

Trull MC, du Laney TV and Dibner MD (2007) Turning biodefense dollars into products. *Nat Biotechnol* **25**:179-184.

Vadakkan KI, Wang H, Ko SW, Zastepa E, Petrovic MJ, Sluka KA and Zhuo M (2006) Genetic reduction of chronic muscle pain in mice lacking calcium/calmodulin-stimulated adenylyl cyclases. *Mol Pain* **2**:7.

Vatner SF, Yan L, Ishikawa Y, Vatner DE and Sadoshima J (2009) Adenylyl cyclase type 5 disruption prolongs longevity and protects the heart against stress. *Circ J* **73**:195-200.

Venter JC, Adams MD and Myers EW (2001) The sequence of the human genome. *Science* **291**:1304-1351.

Vijaikumar M, Thappa DM and Jeevankumar B (2001) Cutaneous anthrax: Still a reality in India. *Pediatr Dermatol* **18**:456-457.

Villacres EC, Wong ST, Chavkin C and Storm DR (1998) Type 1 adenylyl cyclase mutant mice have impaired mossy fiber long-term potentiation. *J Neurosci* **18**:3186-3194.

Vitale G, Pellizzari R, Recchi C, Napolitani G, Mock M and Montecucco C (1998) Anthrax lethal factor cleaves the *N*-terminus of MAPKKs and induces tyrosine/threonine phosphorylation of MAPKs in cultured macrophages. *Biochem Biophys Res Commun* **248**:706-711.

Vorherr T, Knopfel L, Hofmann F, Mollner S, Pfeuffer T and Carafoli E (1993) The calmodulin binding domain of nitric oxide synthase and adenylyl cyclase. *Biochemistry* **32**:6081-6088.

Wallin A, Luksiene Z, Zagminas K and Surkiene G (2007) Public health and bioterrorism: Renewed threat of anthrax and smallpox. *Medicina (Kaunas)* **43**:278-284.

Wang H, Gong B, Vadakkan KI, Toyoda H, Kaang BK and Zhuo M (2007) Genetic evidence for adenylyl cyclase 1 as a target for preventing neuronal excitotoxicity mediated by *N*-methyl-D-aspartate receptors. *J Biol Chem* **282**:1507-1517.

Wang H, Pineda VV, Chan GC, Wong ST, Muglia LJ and Storm DR (2003) Type 8 adenylyl cyclase is targeted to excitatory synapses and required for mossy fiber long-term potentiation. *J Neurosci* **23**:9710-9718.

Watson PA, Krupinski J, Kempinski AM and Frankenfield CD (1994) Molecular cloning and characterization of the type 7 isoform of mammalian adenylyl cyclase expressed widely in mouse tissues and in S49 mouse lymphoma cells. *J Biol Chem* **269**:28893-28898.

Wayman GA, Wei J, Wong S and Storm DR (1996) Regulation of type 1 adenylyl cyclase by calmodulin kinase 4 *in vivo*. *Mol Cell Biol* **16**:6075-6082.

Wei J, Wayman G and Storm DR (1996) Phosphorylation and inhibition of type 3 adenylyl cyclase by calmodulin-dependent protein kinase 2 *in vivo*. *J Biol Chem* **271**:24231-24235.

Weingart CL and Weiss AA (2000) *Bordetella pertussis* virulence factors affect phagocytosis by human neutrophils. *Infect Immun* **68**:1735-1739.

Wigelsworth DJ, Krantz BA, Christensen KA, Lacy DB, Juris SJ and Collier RJ (2004) Binding stoichiometry and kinetics of the interaction of a human anthrax toxin receptor, CMG2, with protective antigen. *J Biol Chem* **279**:23349-23356.

Wong ST, Athos J, Figueroa XA, Pineda VV, Schaefer ML, Chavkin CC, Muglia LJ and Storm DR (1999) Calcium-stimulated adenylyl cyclase activity is critical for hippocampus-dependent long-term memory and late phase LTP. *Neuron* **23**:787-798.

Wong ST, Trinh K, Hacker B, Chan GC, Lowe G, Gaggar A, Xia Z, Gold GH and Storm DR (2000) Disruption of the type 3 adenylyl cyclase gene leads to peripheral and behavioral anosmia in transgenic mice. *Neuron* **27**:487-497.

Wu GC, Lai HL, Lin YW, Chu YT and Chern Y (2001) *N*-glycosylation and residues N805 and N890 are involved in the functional properties of type 6 adenylyl cyclase. *J Biol Chem* **276**:35450-35457.

Wu ZL, Thomas SA, Villacres EC, Xia Z, Simmons ML, Chavkin C, Palmiter RD and Storm DR (1995) Altered behavior and long-term potentiation in type 1 adenylyl cyclase mutant mice. *Proc Natl Acad Sci USA* **92**:220-224.

Xia Z, Choi EJ, Wang F and Storm DR (1992) The type 3 calcium/calmodulin-sensitive adenylyl cyclase is not specific to olfactory sensory neurons. *Neurosci Lett* **144**:169-173.

Xia ZG, Refsdal CD, Merchant KM, Dorsa DM and Storm DR (1991) Distribution of mRNA for the calmodulin-sensitive adenylate cyclase in rat brain: Expression in areas associated with learning and memory. *Neuron* **6**:431-443.

Yamaguchi T, Pelling JC, Ramaswamy NT, Eppler JW, Wallace DP, Nagao S, Rome LA, Sullivan LP and Grantham JJ (2000) cAMP stimulates the *in vitro* proliferation of renal cyst epithelial cells by activating the extracellular signal-regulated kinase pathway. *Kidney Int* **57**:1460-1471.

Yamamoto M, Ozawa H, Saito T, Hatta S, Riederer P and Takahata N (1997) Ca^{2+}/CaM-sensitive adenylyl cyclase activity is decreased in the Alzheimer´s brain: Possible relation to type 1 adenylyl cyclase. *J Neural Transm* **104**:721-732.

Yan L, Vatner DE, O´Connor JP, Ivessa A, Ge H, Chen W, Hirotani S, Ishikawa Y, Sadoshima J and Vatner SF (2007) Type 5 adenylyl cyclase disruption increases longevity and protects against stress. *Cell* **130**:247-258.

Yan SZ, Huang ZH, Andrews RK and Tang WJ (1998) Conversion of forskolin-insensitive to forskolin-sensitive (mouse-type 9) adenylyl cyclase. *Mol Pharmacol* **53**:182-187.

Yanagimachi R (1994) Fertility of mammalian spermatozoa: Its development and relativity. *Zygote* **2**:371-372.

Yang X, Horn K and Wand GS (1998) Chronic ethanol exposure impairs phosphorylation of CREB and CRE-binding activity in rat striatum. *Alcohol Clin Exp Res* **22**:382-390.

Yeh SH and Mink CM (2006) Shift in the epidemiology of pertussis infection: An indication for *pertussis* vaccine boosters for adults? *Drugs* **66**:731-741.

Yoshimura M, Pearson S, Kadota Y and Gonzalez CE (2006) Identification of ethanol responsive domains of adenylyl cyclase. *Alcohol Clin Exp Res* **30**:1824-1832.

Yoshimura M, Wu PH, Hoffman PL and Tabakoff B (2000) Overexpression of type 7 adenylyl cyclase in the mouse brain enhances acute and chronic actions of morphine. *Mol Pharmacol* **58**:1011-1016.

Yung LY, Tsim ST and Wong YH (1995) Stimulation of cAMP accumulation by the cloned *Xenopus* melatonin receptor through G_i and G_z proteins. *FEBS Lett* **372**:99-102.

Zhang G, Liu Y, Qin J, Vo B, Tang WJ, Ruoho AE and Hurley JH (1997a) Characterization and crystallization of a minimal catalytic core domain from mammalian type 2 adenylyl cyclase. *Protein Sci* **6**:903-908.

Zhang G, Liu Y, Ruoho AE and Hurley JH (1997b) Structure of the adenylyl cyclase catalytic core. *Nature* **386**:247-253.

Zimmermann G and Taussig R (1996) Protein kinase C alters the responsiveness of adenylyl cyclases to G protein α and $\beta\gamma$ subunits. *J Biol Chem* **271**:27161-27166.

Chapter 2

Characterization of
Mouse Heart Adenylyl Cyclase

2.1   Abstract

Chronic heart failure is one of the most frequent causes of death in humans. Knock-out of type 5 adenylyl cyclase (AC) in mice causes longevity and protection from cardiomyopathy, and an AC5 inhibitor reduces β-adrenoceptor-stimulated Ca^{2+} inward currents in isolated mouse cardiomyocytes. These data indicate that selective AC5 inhibitors may be beneficial in chronic heart failure patients. Therefore, we characterized AC in mouse heart membranes. Real-time polymerase chain reaction and immunoblot analysis suggested that AC5 is an important heart AC isoform. Enzyme kinetics of heart AC and recombinant AC5 in the presence of Mg^{2+} were similar. Moreover, the stimulatory profile of forskolin and six forskolin analogs on mouse heart AC was similar to recombinant AC5. Furthermore, the inhibitory profile of eight 2´(3´)-O-(N-methylanthraniloyl) (MANT)-nucleoside 5´-([γ-thio])triphosphates on mouse heart in the presence of Mg^{2+} was similar to AC5. MANT-ITP was the most potent inhibitor of heart AC and recombinant AC5 with K_i values in the 1-5 nM range in the presence of Mn^{2+} and in the 15-25 nM range in the presence of Mg^{2+}. However, in the presence of Mn^{2+}, we also noted differences between mouse heart AC and AC5 with respect to enzyme kinetics and forskolin analog effects. In conclusion, with respect to expression, kinetics, activation by forskolin analogs and inhibition by MANT-nucleotides in the presence of Mg^{2+}, AC5 is an important AC isoform in the heart, with MANT-ITP being an excellent starting point for the design of AC5-selective inhibitors. Unfortunately, a limitation of our study is the fact that immunologically and biochemically, AC5 and AC6 are quite similar although they play different roles in heart function. Moreover, lack of antibody specificity was a problem.

2.2   Introduction

In the human heart, the β_1-adrenoceptor-G_s-protein-AC system is the major physiological mechanism for acute modulation of contractility (Lohse *et al.*, 2003). Gene knock-out studies confirmed the major significance of the β_1-adrenoceptor for the regulation of heart function in mouse (Devic *et al.*, 2001). Nine membrane-bound AC isoforms (AC1-AC9), producing the second messenger cAMP, have been cloned in mammals. Gene expression studies showed that AC5 is the major cardiac AC isoform (Defer *et al.*, 2000; Sunahara and Taussig, 2002; Beazely and Watts, 2006). The diterpene forskolin (FS) from *Coleus forskohlii* effectively activates ACs 1-8 but not AC9 (Sunahara and Taussig, 2002). Moreover, FS and FS analogs differentially activate recombinant ACs 1, 2 and 5 expressed in Sf9 insect cells (Pinto *et al.*, 2008). This was not expected in view of the fact that the FS binding site is highly conserved among the various AC isoforms (Sunahara and Taussig, 2002).

Chronic heart failure is one of the most important causes of death in humans (Fonarow, 2008; Yu *et al.*, 2008). In chronic heart failure, desensitization of the myocardial β_1-adrenoceptor occurs, reducing the positive inotropic effects of catecholamines. An inverse correlation between survival and activation of the sympathetic system has been observed in chronic heart failure patients. Thus, β_1-adrenoceptor desensitization can be interpreted as energy-saving adaptation, protecting against the detrimental consequences of excessive adrenergic drive (El-Armouche *et al.*, 2003; Lohse *et al.*, 2003). Accordingly, the standard long-term treatment of chronic heart failure includes β_1-adrenoceptor antagonists, considerably reducing morbidity and mortality (Bristow, 2000; Lohse *et al.*, 2003).

In a pressure overload model based on thoracic aortic banding, AC5 knock-out mice show a stable left ventricular ejection fraction, whereas the cardiac performance of wild-type mice is impaired (Okumura *et al.*, 2003a, b). Most strikingly, compared to wild-type mice, AC5 knock-out mice show a considerably increased lifespan and protection from aging-induced cardiomyopathy and oxidative stress (Yan *et al.*, 2007). Additionally, the AC5 knock-out protects mice against β_1-adrenoceptor-induced cardiomyocyte apoptosis (Iwatsubo *et al.*, 2004). However, AC regulation in the heart is more complex. Specifically, the overexpression of AC6 in the heart reduces left ventricular remodeling, preserves left ventricular function and reduces

mortality in a myocardial infarction model (Takahashi *et al.*, 2006). Thus, it appears that AC5 and AC6 play opposing roles in heart function.

MANT-nucleotides inhibit AC isoforms 1, 2, 5 and 6, with ACs 1, 5 and 6 being more sensitive to inhibition than AC2 (Gille *et al.*, 2004). In mouse ventricular cardiomyocytes, the AC5 inhibitor MANT-GTPγS effectively reduces isoproterenol-stimulated L-type Ca^{2+} inward currents, while in myocytes from AC5 knock-out mice, the residual Ca^{2+} current is not further attenuated by MANT-GTPγS (Rottländer *et al.*, 2007). These data support the notion that AC5 is the major AC isoform mediating acute β-adrenergic stimulation in mouse heart.

Based on all of the above findings, AC5 inhibitors should be explored as new candidates for chronic heart failure therapy. Therefore, as a first step towards this ambitious goal, the aim of our present study was to provide a detailed characterization of mouse heart AC in comparison to recombinant AC isoforms, specifically AC5, using MANT-nucleotides and FS analogs as pharmacological tools. For the preparation of crude mouse heart membranes, we used a membrane preparation protocol that had previously shown to yield robust AC activities (Rohrer *et al.*, 1996). To the best of our knowledge, this is the first study on the pharmacological characterization of AC activity in a native membrane system.

Fig. **1** shows the structures of the MANT-nucleotides and FS analogs examined in this study. All nucleotides possess a MANT-group at the 2´(3´)-*O*-ribosyl function. The MANT-group spontaneously isomerizes between the 2´- and 3´-*O*-ribosyl function (Gille *et al.*, 2004; Taha *et al.*, 2009). We studied MANT-nucleotides with purine bases (guanine, adenine or hypoxanthine) as well as nucleotides with pyrimidine bases (uracil or cytosine). Moreover, we studied nucleotides with a triphosphate chain and nucleotides with a thiophosphate at the γ-position, with the thiophosphate introducing bulkiness into the molecule and resistance against degradation by nucleotidases (Eckstein, 1985). Concerning FS derivatives, we studied FS and FS derivatives missing an OH-function at the 1´- or 9´-position of the diterpene ring or the acetyl group at the 7´-position. We also examined the diterpene with the acetyl group at the 6´- instead at the 7´-position, also referred to as iso-FS. Finally, we examined FS analogs with bulky substituents at the 6´-position, i.e. the fluorescent FS analog BODIPY-FS, and the water-soluble FS analog DMB-FS, which is commonly used in experiments with intact cells (Pinto *et al.*, 2008).
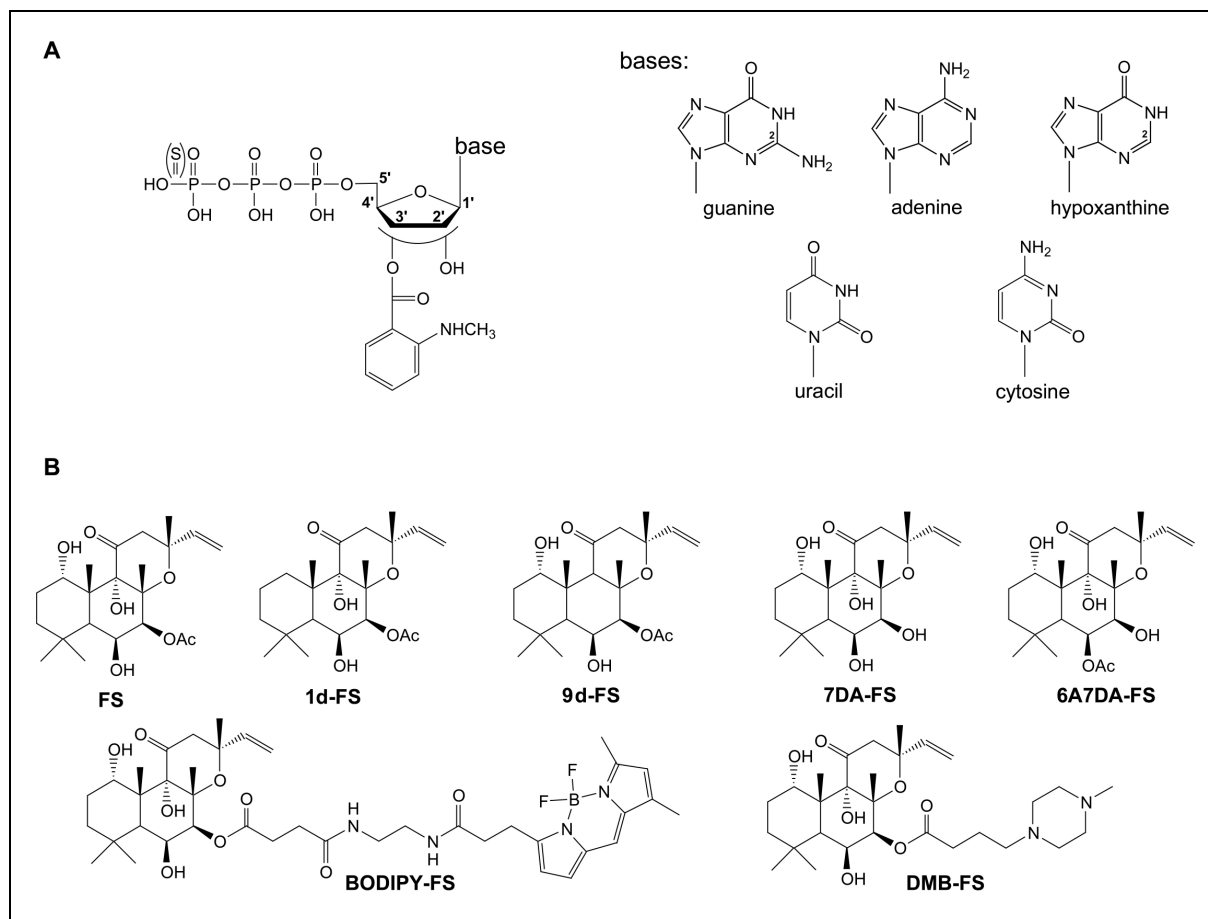
Fig. 1: Structures of compounds analyzed in this study. A: Structures of MANT-nucleotides. Note that the MANT-group spontaneously isomerizes between the 2´- and 3´-O-ribosyl group. **B:** Structures of FS and FS derivatives. In some structures, numbers highlight important carbon atoms bearing substitutions.

2.3   Materials and Methods

Materials. MANT-ITP, MANT-CTP and MANT-UTP were synthesized as described (Taha *et al.*, 2009). MANT-ATP, MANT-GTP, MANT-ATPγS, MANT-GTPγS and MANT-ITPγS were from Jena Bioscience (Jena, Germany). [α-^{32}P]ATP (800 Ci/mmol) was purchased from PerkinElmer (Wellesley, MA, USA). Neutral alumina (N Super 1) was purchased from MP Biomedicals (Eschwege, Germany). Histamine, serotonin, dopamine, (-)-isoproterenol, (-)-epinephrine, (-)-norepinephrine, 6A7DA-FS, 7DA-FS, 1d-FS, 9d-FS, cAMP, IBMX and triethanolamine were from Sigma-Aldrich (St. Louis, MO, USA). BODIPY-FS was purchased from Molecular Probes (Eugene, OR, USA). Glucagon was from American Peptide Company (Sunnyvale, CA, USA). FS was from LC Laboratories (Woburn, MA, USA). MnCl$_2$ and MgCl$_2$ (highest quality) were from Merck (Darmstadt, Germany). GTP, GTPγS, ATP and creatine kinase were purchased from Roche (Mannheim, Germany). Porcine neuropeptide Y was synthesized by solid phase synthesis at the Institute of Organic Chemistry, University of Regensburg. Antibodies for ACs 2, 3, 4 and 6 were from Abcam (Cambridge, UK). The AC1 antibody (V-20) and the AC5/6 antibody (C-17) were from Santa Cruz Biotechnology, Inc. (Santa Cruz CA, USA). DMB-FS was from Calbiochem (San Diego, CA, USA).

Real-Time PCR. Total RNA from mouse hearts was extracted and reverse-transcribed and real-time PCR was carried out as described (Matzdorf *et al.*, 2007). In brief, total RNA was extracted using TRIzol reagent (Invitrogen, Karlsruhe, Germany). cDNA was synthesized in a 20-μL reaction with 2 μg total RNA, 0.5 μg oligo(dT)$_{12-18}$, 20 U RNasin (Promega, Mannheim, Germany), 4 μL of 5x RT buffer, 0.5 mM dNTPs, and 20 U Moloney murine leukemia virus RT enzyme (Invitrogen). Real-time PCR was performed with the LightCycler System (Roche). All PCR experiments were performed using a LightCycler-FastStart DNA Master SYBR Green kit (Roche). Each reaction (20 μL) contained 2 μL of cDNA, 3.0 mM MgCl$_2$, 1 pmol of each primer, and 2 μL of Fast Starter Mix (containing buffer, dNTPs, SYBR Green, and *Taq* polymerase).

The specific primer sequences used are shown in Tab. **1**. The amplification program consisted of one cycle of 95°C with 10-min hold ("hot start") followed by 30 cycles of 15 s at 95°C, 5 s at 60°C, and 20 s at 72°C. Amplification was followed by

melting curve analysis (increasing the temperature of the reaction mixtures up to 95°C, by 0.1°C/s, starting at 50°C for 15 s) to verify the correctness of the amplicon. To verify the accuracy of amplification, PCR products were further analyzed on ethidium bromide-stained 2% (m/v) agarose gels (Fig. **2**). AC primers produced specific PCR products of the following sizes: 121 bp (AC1), 141 bp (AC2), 443 bp (AC3), 121 bp (AC4), 456 bp (AC5), 131 bp (AC6), 569 bp (AC7), 133 bp (AC8), 134 bp (AC9). Data were analyzed using the LightCycler software, version 3.5.3.

Tab. 1: Primer sequences for real-time PCR of AC isoforms in mouse heart.

AC isoform	Primer sequence
AC1	Forward: 5´-CCAGCCAAGAGGATGAAGTT-3´ Reverse: 5´-AATGCCCTCCGCTTGTC-3´
AC2	Forward: 5´-AGCATTCAAGTACTACGTGACC-3´ Reverse: 5´-ACAAAGAGGATGAAGATGAGGG-3´
AC3	Forward: 5´-CATCGAGTGTCTACGCTTC-3´ Reverse: 5´-GGATGACCTGTGTCTCTTCT-3´
AC4	Forward: 5´-TGCTGTCTTCTCTGGAGGG-3´ Reverse: 5´-GTGGACACGGGACTGTCAA-3´
AC5	Forward: 5´-ACGATTGGTAGTACAGCTCGTCATTGCGCC-3´ Reverse: 5´-TGCTCAGCCTGCTGGCCTGCTCCGTGTTCC-3´
AC6	Forward: 5´-GAGGCAAACAACGAGGGC-3´ Reverse: 5´-GCCATGTAGGTGCTACCG-3´
AC7	Forward: 5´-GCTTGCTCATCAGGGCCATGCTAA-3´ Reverse: 5´-CCAGTTATTTAGAGAGAGACCT-3´
AC8	Forward: 5´-CGCATCTACATCCATCGCTAT-3´ Reverse: 5´-GGTCGAATCTGGCAAAGAGTT-3´
AC9	Forward: 5´-ATGGGCGGCTTGAAGAAATA-3´ Reverse: 5´-GCAGGCGTGAGCTTGGA-3´

Sf9 Cell Culture and Expression of Recombinant ACs. Sf9 cell culture, expression of recombinant AC isoforms 1, 2, 4, 5 and 6 and the preparation of Sf9 membranes were performed as described (Gille *et al.*, 2004). For the AC assay, Sf9 membranes were thawed and sedimented by a 15-min centrifugation at 4°C and 15,000 x g to remove residual endogenous nucleotides and resuspended in assay buffer as described below.

SDS-Polyacrylamide Gel Electrophoresis and Immunoblot Analysis. The detection of AC proteins using isoform-specific antibodies was performed as described with minor modifications (Houston *et al.*, 2002). Mouse heart membrane-

or Sf9 membrane proteins were separated on SDS-polyacrylamide gels containing 5% (m/v) acrylamide. Proteins were transferred onto Trans-Blot nitrocellulose membranes (Bio-Rad Laboratories, Hercules, CA) and reacted with the corresponding AC antibody (1:200-1:500). Protein bands were visualized by enhanced chemiluminescence (Pierce Chemical, Rockford, IL) using peroxidase-coupled goat anti-rabbit IgG (1:1,000; Santa Cruz Biotechnology, Inc.).

Preparation of Mouse Heart Membranes. Female CD1 mice were housed in cages in a temperature- and light-controlled environment according to the German animal protection law. At the age of eight weeks, mice were sacrificed by cervical dislocation and hearts were removed, shock-frozen in liquid nitrogen and stored at -80°C. Mouse heart membranes were prepared according to a previously described protocol with minor modifications (Rohrer *et al.*, 1996). Briefly, hearts were thawed and rinsed in ice-cold homogenization buffer containing 5 mM Tris/HCl, pH 7.4, and 5 mM EDTA. All membrane preparation steps were conducted at 4°C. Homogenization was performed in a buffer volume amounting to 20-fold the heart tissue weight. Hearts were cut into small pieces and then homogenized in a glass-glass homogenizer (Braun, Melsungen, Germany) at 1,500 rpm, applying 5 series of 5 strokes each with a 1-min cooling period between each series. Organ debris was removed by an 8-min centrifugation at 500 x g. The supernatant suspension was sedimented by a 30-min centrifugation at 40,000 x g. The resultant membrane pellet was washed in a buffer volume amounting to 60-fold the heart tissue weight and sedimented by a 30-min centrifugation at 40,000 x g. In order to remove residual endogenous ligands and nucleotides, this washing procedure was performed three times before the membranes were resuspended in assay buffer consisting of 50 mM triethanolamine and 1 mM EGTA, pH 7.4. Membranes were resuspended with syringes in the sequence 21 G, 25 G, 27 G and then shock-frozen in liquid nitrogen and stored at -80°C. In order to detect robust AC activity in heart membranes, it was essential to follow the protocol described above. Specifically, the use of the above-described buffers was critical. When hearts were homogenized in the standard buffer used for Sf9 cell homogenization (Houston *et al.*, 2002; Gille *et al.*, 2005), no AC activity was recovered.

AC Activity Assay. Assay tubes contained 10 μL of FS analogs, MANT-nucleotides or receptor ligands and 20 μL of reaction mixture consisting of (final) 7 mM Mn^{2+} or Mg^{2+}, 10 μM GTP, 10 μM GTPγS, 100 μM cAMP, 0.4 mg/mL creatine kinase, 9 mM phosphocreatine, 100 μM IBMX, 10 μM isoproterenol and, unless stated otherwise, 100 μM FS. In experiments aiming at the assessment of GPCR ligand effects on AC activity, GTPγS and FS were omitted from reaction mixtures. Tubes also contained 40 μM ATP and 0.2-1.0 μCi [α-^{32}P]ATP. Tubes were preincubated for 2 min at 30°C, and reactions were initiated by the addition of 20 μL of membranes (20 μg of protein per tube), yielding 20 mM triethanolamine and 0.4 mM EGTA, pH 7.4, as assay buffer. For determination of K_m and V_{max} values, ATP/Mn^{2+} or ATP/Mg^{2+} (10 μM - 2 mM) plus 7 mM of free Mn^{2+} or Mg^{2+} were added. In experiments with FS analogs, the $MnCl_2$ concentrations were increased to 10 mM to match previous conditions (Pinto *et al.*, 2008). Moreover, in those studies, GTPγS (10 μM) was included in reaction mixtures. To ensure linear reaction progress, tubes were incubated for 10 min at 30°C. In experiments for the determination of inhibitor potencies on cardiac AC, incubation time was reduced to 1-2 min to avoid nucleotide degradation. Reactions were terminated by the addition of 20 μL of 2.2 N HCl, and denatured protein was sedimented by a 1-min centrifugation at 12,000 x g. [^{32}P]cAMP was separated from [α-^{32}P]ATP by transferring the samples to columns containing 1.4 g of neutral alumina. [^{32}P]cAMP was eluted into 20-ml scintillation vials by adding 4 mL of 0.1 M ammonium acetate, pH 7.0. Blank values were ~0.02% of the total amount of [α-^{32}P]ATP added; substrate turnover was < 3% of the total added [α-^{32}P]ATP. Scintillation vials were filled up with 10 mL double-distilled water, and Čerenkov radiation was determined.

Miscellaneous. Protein was determined using the DC protein assay kit (Bio-Rad, Hercules, CA). Data shown in Tab. **2** to **5** and Figs. **4**, **5** and **7** were obtained by non-linear regression analysis performed with the Prism 4.02 software (Graphpad, San Diego, CA). Statistical comparisons shown in Figs. **5** and **6** were performed using the *t*-test.

2.4   Results

2.4.1 Detection of AC Isoforms in Mouse Heart by Real-Time PCR and Immunoblot Analysis

To investigate the mRNA expression levels of AC isoforms in mouse heart, we reverse-transcribed mRNA and performed real-time PCR using isoform-specific primers (Tab. **1**). PCR products were detected for ACs 1, 3 to 7, and 9 (Fig. **2**). No PCR products were obtained for ACs 2 and 8. The threshold values were 22 cycles for ACs 5 and 6, 25 cycles for ACs 1, 3, and 4, 26 cycles for AC7, and 27 cycles for AC 9.
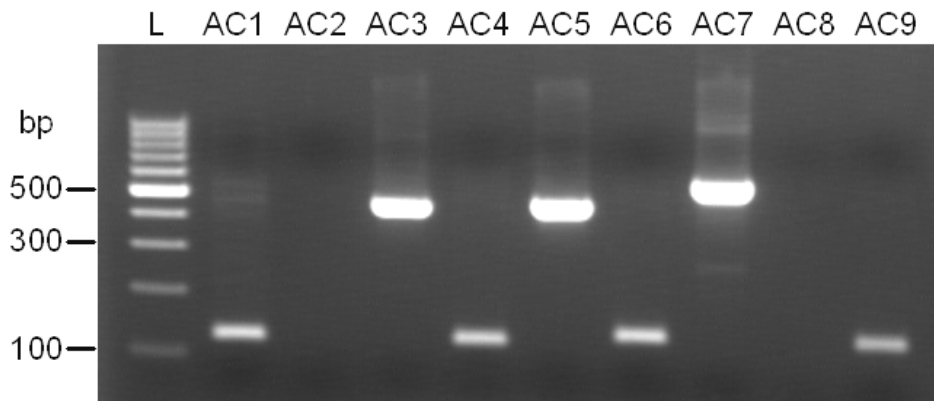
Fig. 2: Detection of AC isoforms in mouse heart by real-time PCR. Total RNA extraction from mouse hearts, reverse transcription and real-time PCR were carried out as described under "Materials and Methods". PCR products were analyzed on ethidium bromide-stained 2% (m/v) agarose gels after completion of the PCR. Mouse heart cDNA fragments produced specific PCR products of the following sizes: 121 bp (AC1), 141 bp (AC2), 443 bp (AC3), 121 bp (AC4), 456 bp (AC5), 131 bp (AC6), 569 bp (AC7), 133 bp (AC8), 134 bp (AC9). Data analysis was performed using the LightCycler software, version 3.5.3, and LightCycler Relative Quantification (RelQuant) Software. Data shown are representative of experiments with 5 different mice.

Next, we examined AC expression at the protein level. The AC5/6 antibody yielded bands at ~120 to 140 kDa in mouse heart membranes using recombinant AC5 as positive control (Fig. **3A**). Immunologically detected bands were diffuse, compatible with ACs being glycosylated (Beazely and Watts, 2006). Sf9 membranes expressing AC3 were used as negative control and did not show an immunoreactive

band. The difference in migration between recombinant AC5 and native cardiac AC5/6 may be due to differences in AC5 glycosylation between Sf9 insect cells and mouse heart. It is also possible that the antibody primarily detected AC6 in heart membranes.
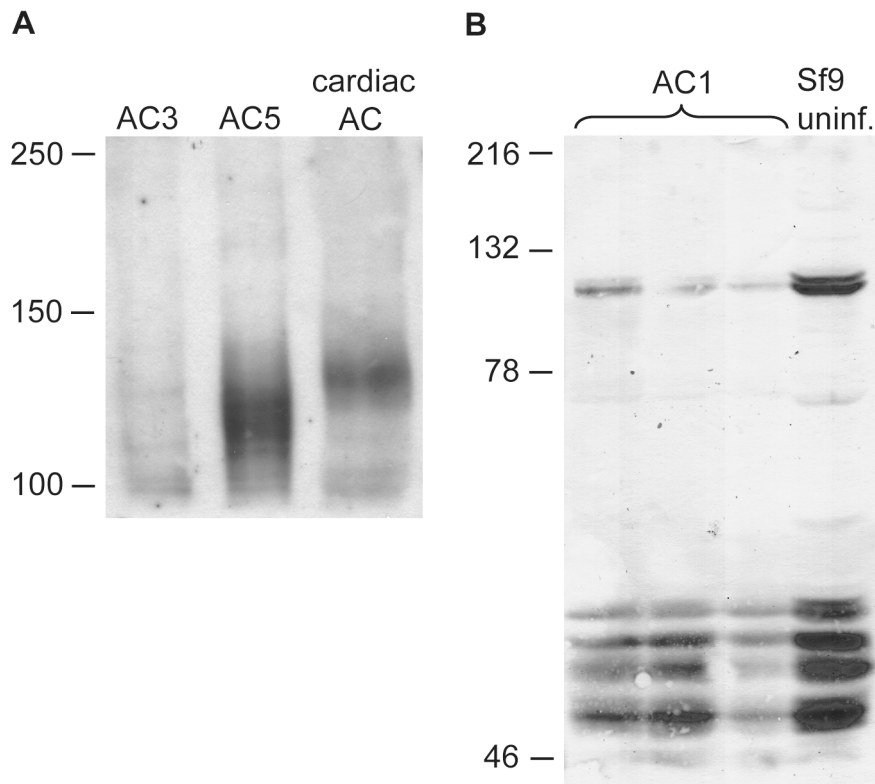
Fig. 3: Detection of AC isoforms in mouse heart and Sf9 insect cell membranes by immunoblot analysis. A: Immunoblot with the AC5/6 antibody C-17 from Santa Cruz Biotechnology, Inc. (1:500) with membranes from Sf9 cells expressing AC3 (negative control, 25 μg of protein per lane), AC5 (positive control, 25 μg of protein per lane), and mouse heart membranes (100 μg of protein per lane). **B:** Immunoblot with the AC1 antibody V-20 from Santa Cruz Biotechnology, Inc. (1:200), with three different membrane preparations expressing AC1 ("positive" control, 75 μg of protein per lane) and membranes from uninfected (uninf.) Sf9 cells ("negative" control, 75 μg of protein per lane). Immunoblot analysis was performed as described under "Materials and Methods". Data shown are representative of three independent experiments.

Unfortunately, our substantial efforts to conduct a comprehensive analysis of AC isoform expression in heart membranes were not successful. First, except for the AC5/6 antibody, in our hands, the other antibodies examined did not display sufficient sensitivity and/or selectivity to obtain reliable information about AC isoform expression in heart membranes, using Sf9 membranes expressing the corresponding

AC isoform as standard. *In pars pro toto*, Fig. **3B** illustrates this problem for AC1. In Sf9 cell membranes, AC1 is expressed very well as assessed by enzyme activity (Gille *et al.*, 2004; Pinto *et al.*, 2008). Thus, we expected to obtain clear immunoreactive bands with the AC1 antibody. However, both in membranes from uninfected Sf9 cells and AC1-expressing Sf9 cells, bands in the 120-kDa region and in the 50-kDa region were detected, but we failed to reveal a unique band in the AC1-expressing membranes. The immunologically recognized bands in membranes from uninfected Sf9 cells were actually more intense than in AC1 virus-infected cells, probably reflecting that the expression of certain proteins in Sf9 cells is decreased as a result of virus infection (Pinto *et al.*, 2008). Real-time PCR experiments and stimulation experiments with Ca^{2+}/calmodulin confirmed that the AC expressed in Sf9 cells infected with AC1 virus was actually AC1 (data not shown). In heart membranes, the AC1 antibody failed to detect a specific band as well (data not shown). Similar problems concerning the specificity of AC antibodies are already described to some extent in the literature (Defer *et al.*, 2000; Liu *et al.*, 2007). Moreover, we do not yet have in hand all recombinant AC isoforms in functionally active form, resulting in a lack of positive and negative controls. Collectively, these data indicate that the presently available AC isoform antibodies must be used with great caution and very critically, both in native systems and in membranes expressing recombinant ACs. This unsatisfying situation also emphasizes the importance of real-time PCR studies to assess AC isoform expression in native tissues.

2.4.2 Stimulation of Mouse Heart AC by FS and FS Analogs: Comparison with Recombinant AC Isoforms

FS and FS analogs differentially activate AC isoforms (Pinto *et al.*, 2008). FS robustly increased AC activity in mouse heart membranes (Fig. **4A**). In the presence of Mn^{2+} or Mg^{2+}, the EC_{50} values for FS and the relative maximum stimulatory effects of FS were similar (Tab. **2**). FS activated ACs in the order of potency AC1 > AC5 ~ mouse heart AC > AC2 (Fig. **4B**; Tab. **2**).
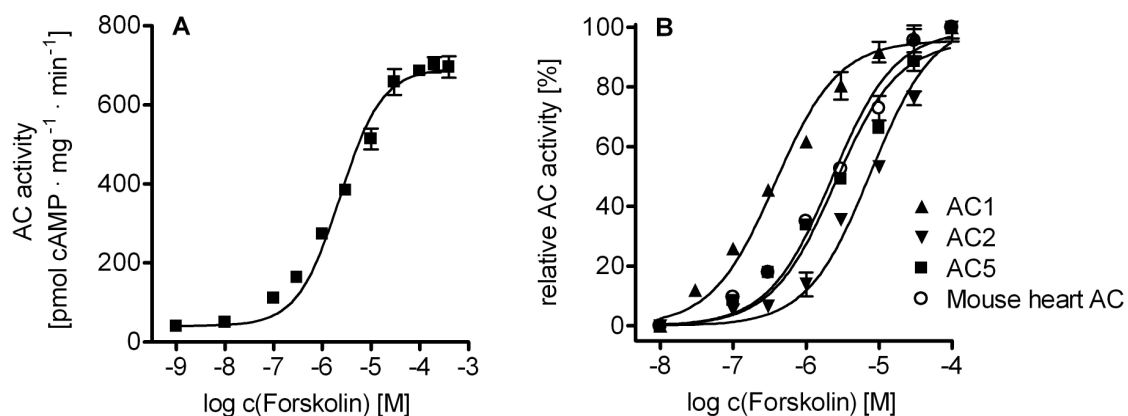
Fig. 4: Stimulation of mouse heart membrane AC and recombinant AC isoforms by FS. Reaction mixtures contained 7 mM Mn^{2+}, 40 μM ATP, [α-^{32}P]ATP (0.2-1.0 μCi/tube), 100 μM cAMP, 0.4 mg/mL creatine kinase, 9 mM phosphocreatine and 100 μM IBMX. Reactions were carried out for 10 min at 30°C as described in "Materials and Methods". **A:** Stimulation of heart membrane AC by FS. **B:** Comparison of FS concentration-response curves obtained for heart membrane AC and recombinant ACs 1, 2 and 5 expressed in Sf9 cells. Data shown are the means ± SD of representative experiments performed in duplicates. Summaries of the results of 3-4 independent experiments are shown in Tab. **2** and **3**.

FS increased basal AC activity in Sf9 cell membranes expressing ACs 1 and 2 by ~2 to 5-fold, whereas in Sf9 cell membranes expressing AC5 and mouse heart membranes, FS increased AC activity by ~15 to 20-fold. Thus, using FS as probe, there is a similarity of heart membrane with AC5. As outlined below, the situation with FS analogs is different.

In mouse heart membranes FS analogs activated AC in the order of potency BODIPY-FS > FS ~ 6A7DA-FS > DMB-FS > 7DA-FS ~ 9d-FS (Tab. **3**). The order of efficacy was DMB-FS > FS ~ 9d-FS ~ 7DA-FS > 6A7DA-FS > BODIPY-FS >> 1d-FS (ineffective). Tab. **3** also includes the pharmacological profile of FS analogs on

recombinant AC5. Note that the pharmacological profile of FS analogs on mouse heart AC and AC5 was assessed in the presence of Mn^{2+}. With respect to the EC_{50} values of FS analogs, we observed a significant correlation between mouse heart and AC5. However, the slope of the correlation was considerably steeper than 1.00, which value would have reflected pharmacological identity of the ACs studied (Fig. **5A**). With respect to the efficacies of FS analogs, the correlation between mouse heart and AC5 was not significant (Fig. **5B**). These data indicate that under Mn^{2+}-conditions, AC isoforms other than AC5 contribute to total AC activity in mouse heart membranes.

Tab. 2: EC_{50} values of FS for stimulation of mouse heart AC and AC isoforms and relative maximum stimulatory effect of FS on basal AC activity.

Parameter, cation	AC1	AC2	AC5	Cardiac AC
EC_{50} [µM], Mn^{2+}	0.42 ± 0.07	6.0 ± 2.1	4.0 ± 0.6	3.0 ± 0.2
EC_{50} [µM], Mg^{2+}	1.1 ± 0.4	11.4 ± 3.1	4.9 ± 1.0	2.3 ± 0.2
Relative maximum stimulatory effect [x-fold], Mn^{2+}	3.5 ± 0.1	5.2 ± 0.2	15.2 ± 0.05	22.8 ± 0.2
Relative maximum stimulatory effect [x-fold], Mg^{2+}	2.4 ± 0.02	3.0 ± 0.3	13.9 ± 0.9	18.0 ± 2.0

AC activities were determined as described under "Materials and Methods". Reaction mixtures contained 5 mM Mg^{2+} or Mn^{2+}, 40 µM ATP, [α-^{32}P]ATP (0.2-1.0 µCi/tube), 0.4 mg/mL creatine kinase, 9 mM phosphocreatine, 100 µM cAMP, 100 µM IBMX and FS at concentrations from 0.1-300 µM. Data were analyzed by non-linear regression and are the means ± SD of 3-4 independent experiments performed in duplicates.

Tab. 3: Potencies and efficacies of FS and FS analogs on mouse heart AC and AC5.

Diterpene	Cardiac AC EC$_{50}$ [μM]	Cardiac AC Efficacy [%]	AC5 EC$_{50}$ [μM]	AC5 Efficacy [%]
FS	3.0 ± 0.2	100	4.0 ± 0.6	100
6A7DA-FS	3.6 ± 0.5	76 ± 10	7.4 ± 2.8*	103 ± 11*
BODIPY-FS	1.4 ± 0.5	54 ± 6	2.3 ± 1.1*	48 ± 2*
7DA-FS	30.2 ± 10.2$^{\alpha}$	83 ± 5$^{\alpha}$	63.3 ± 10.6*	63 ± 4*
9d-FS	38.6 ± 19.2$^{\alpha}$	90 ± 12$^{\alpha}$	65.3 ± 9.0*	79 ± 10*
DMB-FS	17.4 ± 2.0$^{\alpha}$	118 ± 4$^{\alpha}$	48.0 ± 9.6*	95 ± 1*
1d-FS	ineffective		ineffective*	

AC activities were determined as described under "Materials and Methods". Reaction mixtures contained 10 mM Mn^{2+}, 40 μM ATP, [α-^{32}P]ATP (0.2-1.0 μCi/tube), 10 μM GTPγS, 0.4 mg/mL creatine kinase, 9 mM phosphocreatine, 100 μM cAMP and 100 μM IBMX. EC$_{50}$ values and efficacies were obtained by non-linear regression analysis and are the means ± SD of 3-4 independent experiments performed in duplicates. Values labelled with (*) were taken from (Pinto *et al.*, 2008).

$^{\alpha}$ For those FS analogs not reaching saturation of the concentration/response curves, the actual stimulatory effect at a concentration of 300 μM was used for calculation of efficacy. Extrapolated EC$_{50}$ values marked with an "$^{\alpha}$" were derived from concentration/response curves that did not reach saturation.
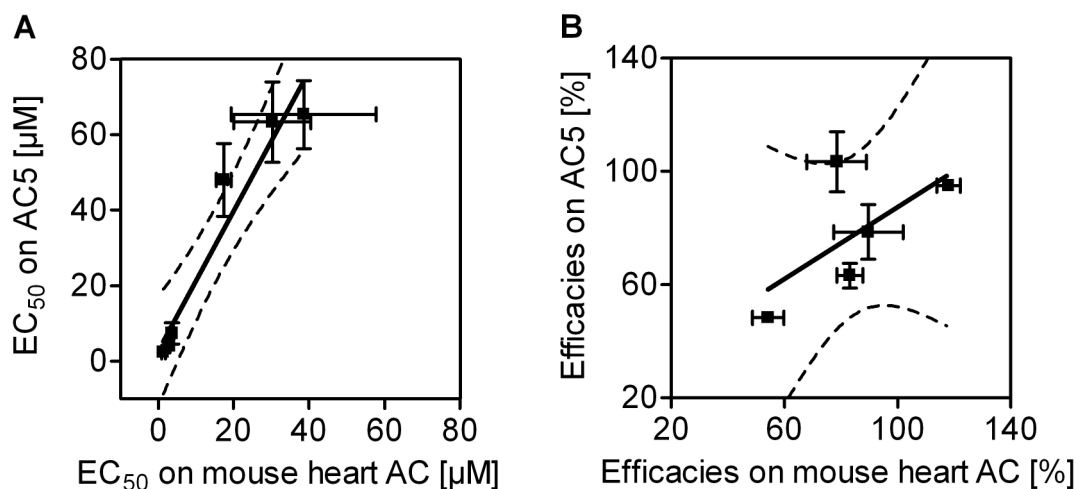
Fig. 5: Correlation of the potencies and efficacies of FS analogs on mouse heart AC and AC5. Data shown in Tab. **3** provide the basis for the correlations. Data were analyzed by linear regression. Dashed lines represent 95% confidence intervals of the linear regression lines. **A:** Correlation of potencies of FS analogs on mouse heart AC *vs.* AC5. Slope, 1.858 ± 0.2460; r^2, 0.9344; p, 0.0016. **B:** Correlation of efficacies of FS analogs on mouse heart AC *vs.* AC5. Slope, 0.6371 ± 0.4330; r^2, 0.4191; p, 0.2376 (not significant).

2.4.3 Regulation of Mouse Heart AC by GTPγS, GTP and Receptor Ligands

The non-hydrolysable GTP analog GTPγS activates AC through stimulation of $G_{s\alpha}$ (Eckstein, 1985; Gilman, 1987; Gille *et al.*, 2005). In the presence of Mg^{2+}, GTPγS increased AC activity 4-fold with an EC_{50} value of 80 nM (data not shown). In the presence of GTP (10 μM), the β-adrenoceptor agonist isoproterenol increased AC activity about 2-fold with an EC_{50} value of 12 nM (Fig. **6A**). Using a very similar heart membrane preparation as in the present study, Rohrer *et al.* (1996) reported that isoproterenol increased AC activity by 150% with 53 μM GTP. Thus, our results correspond well with the previous data, but Rohrer *et al.* (1996) did not report the absolute AC activities. Previous studies had already shown that in mouse heart, 72% of the β-adrenoceptors belong to the $β_1$-subtype, whereas 28% belong to the $β_2$-subtype (Rohrer *et al.*, 1996). In addition, studies with $β_1$-adrenoceptor knock-out mice showed that ~90% of the isoproterenol-stimulated AC activity is attributable to the $β_1$-adrenoceptor (Rohrer *et al.*, 1996).

Fig. **6B** shows the concentration/response curves for the effect of GTP on basal and isoproterenol-stimulated AC activity. GTP effectively supported isoproterenol-stimulated AC activity; the EC_{50} for GTP was 100 nM. GTP also exhibited a modest stimulatory effect on basal AC activity; the EC_{50} was 140 nM. GTP did not only increase isoproterenol-stimulated AC activity but also basal AC activity (Fig. **6B**).
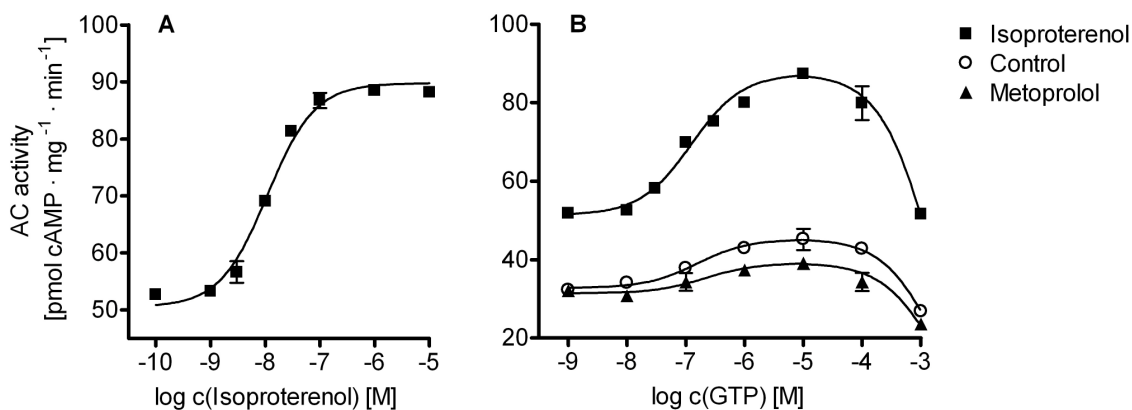
Fig. 6: Regulation of mouse heart membrane AC by isoproterenol, metoprolol and GTP. Reaction mixtures contained 7 mM Mg^{2+}, 40 μM ATP, [α-^{32}P]ATP (0.2-1.0 μCi/tube), 100 μM cAMP, 0.4 mg/mL creatine kinase, 9 mM phosphocreatine and 100 μM IBMX. Reactions were carried out for 10 min at 30°C as described in "Materials and Methods". **A:** Reaction mixtures contained isoproterenol at the concentrations indicated on the abscissa and GTP (10 μM). **B:** Reaction mixtures contained GTP at the concentrations indicated on the abscissa and water (control), isoproterenol or metoprolol (10 μM each). Data shown are means ± SD of 3 independent experiments performed in duplicates. The statistical significance of the effect of metoprolol on AC activity *vs.* control was assessed with the *t*-test. However, the effect of metoprolol was not significant.

In accordance with the literature (Engelhardt *et al.*, 2001), this basal GTP-dependent AC activity was reduced by the inverse agonist metoprolol. However, it should be emphasized that the inhibitory effect of metoprolol on GTP-stimulated AC activity did not reach statistical significance, indicating that the constitutive activity of the β_1-adrenoceptor at least in this system is small. The inhibitory effect of GTP >10 μM on AC activity is due to competition of GTP with ATP at the catalytic site of AC (Gille *et al.*, 2005). The stimulatory effect of isoproterenol on AC in the absence of added GTP is explained by nucleoside diphosphokinase-mediated conversion of endogenous GDP to GTP by ATP (Kimura and Shimada, 1988).

To identify GPCRs mediating stimulation (*via* G_s) or inhibition (*via* G_i) of AC in mouse heart, we examined several GPCR agonists in heart membranes (Fig. **7**). Histamine, serotonin, glucagon and neuropeptide Y did not exhibit significant effects on AC activity. In contrast, the full β-adrenoceptor agonists epinephrine, norepinephrine and isoproterenol increased AC activity about 2-fold, while dopamine showed partial β_1-adrenoceptor agonism. Partial agonism of dopamine has recently been reported for the recombinantly expressed β_1-adrenoceptor (Weitl and Seifert,

2008). As the histamine H_2-receptor is known to stimulate AC in human heart (Fryer *et al.*, 2006; Salazar *et al.*, 2007), we also examined the effects of the selective H_2-receptor agonists dimaprit and impromidine (Dove *et al.*, 2004) on AC activity in mouse heart membranes. However, impromidine and dimaprit did not exhibit a stimulatory effect on AC activity (data not shown).
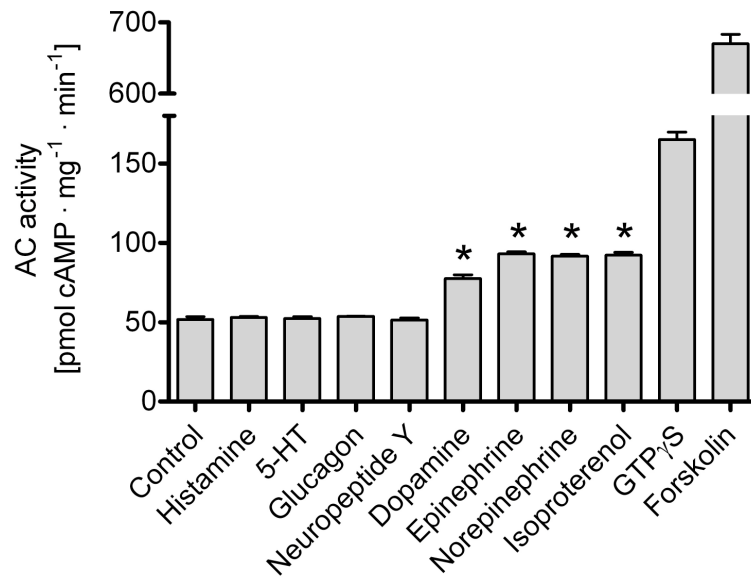
Fig. 7: Effects of various GPCR agonists on AC activity in mouse heart membranes. Reaction mixtures contained 7 mM Mg^{2+}, 40 μM ATP, [α-^{32}P]ATP (0.2-1.0 μCi/tube), 10 μM GTP, 100 μM cAMP, 0.4 mg/mL creatine kinase, 9 mM phosphocreatine and 100 μM IBMX. Reactions were carried out for 10 min at 30°C as described in "Materials and Methods". Reaction mixtures contained histamine, dopamine, (-)-epinephrine, (-)-norepinephrine, (-)-isoproterenol, GTPγS or FS (100 μM each) or serotonin (5-HT) and glucagon (10 μM each) or porcine neuropeptide Y (pNPY) (100 nM). Data shown are means ± SD of 3 independent experiments performed in duplicates. The statistical significance of the effects of receptor agonists on AC activity *vs.* control was assessed with the *t*-test. *, $p < 0.05$.

2.4.4 Enzyme Kinetics of Mouse Heart AC and Recombinant AC5

Substrate saturation experiments under maximum stimulatory conditions were performed for mouse heart membranes and recombinant AC5. Note the different scales of the y-axes in Fig. **8**, **A** and **B**, and the different scales of both the x- and y-axes in Fig. **8**, **C** and **D**. In the presence of Mg^{2+}, AC5 and mouse heart AC exhibited similar K_m and V_{max} values (Figs. **8A** and **8B**; Tab. **4**). Under Mn^{2+}-conditions, mouse heart AC showed 3- to 4-fold lower K_m and V_{max} values than recombinant AC5 (Figs. **8C** and **8D**; Tab. **5**).
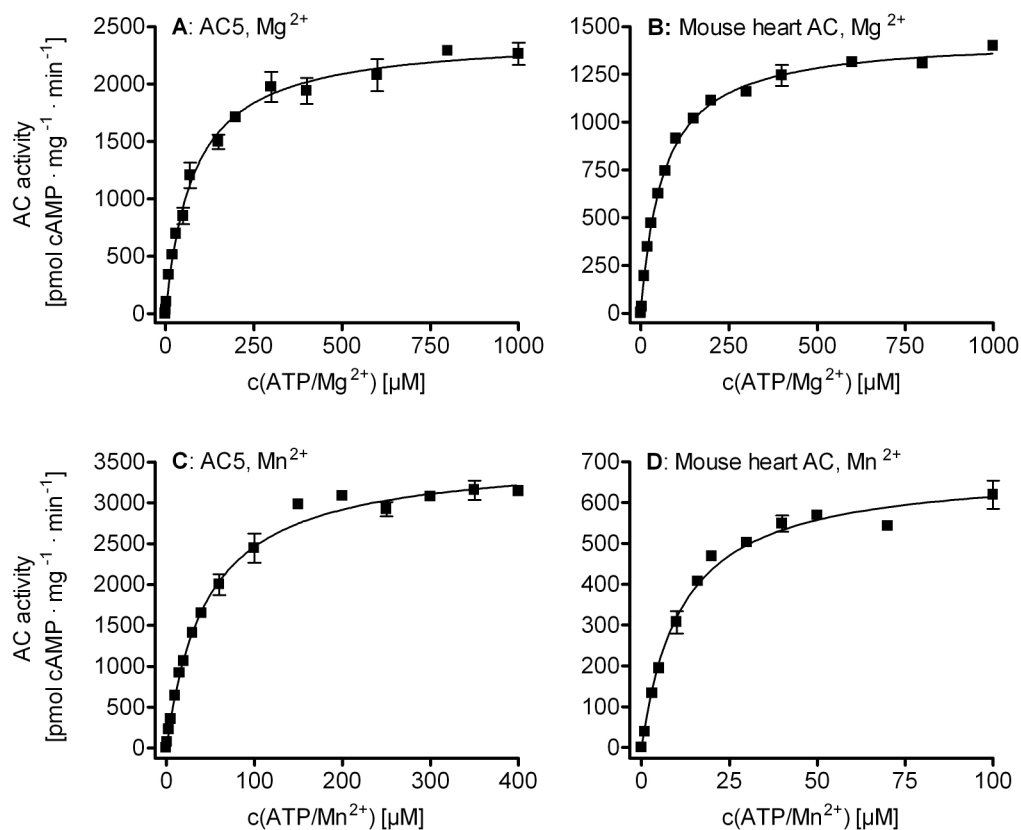
Fig. 8: Substrate saturation kinetics of recombinant AC5 and mouse heart membrane AC. Reaction mixtures contained 7 mM Mn^{2+} or Mg^{2+}, [α-^{32}P]ATP (0.2-1.0 µCi/tube), 10 µM GTP, 10 µM GTPγS, 100 µM cAMP, 0.4 mg/mL creatine kinase, 9 mM phosphocreatine, 100 µM IBMX, 10 µM isoproterenol and 100 µM FS. ATP/Mn^{2+} or ATP/Mg^{2+} (10 µM to 2 mM) plus 7 mM of free Mn^{2+} or Mg^{2+} were added to reaction mixtures. In order to ensure linear reaction progress, tubes were incubated for 10 min at 30°C. **A:** Substrate saturation curve for AC5 in the presence of Mg^{2+}. **B:** Substrate saturation curve for heart membrane AC in the presence of Mg^{2+}. **C:** Substrate saturation curve for AC5 in the presence of Mn^{2+}. **D:** Substrate saturation curve for heart membrane AC in the presence of Mn^{2+}. Experiments were performed as described in "Materials and Methods". Data shown are means ± SD of 3 independent experiments performed in duplicates.

2.4.5 Inhibitor Potencies at Mouse Heart AC and Recombinant AC Isoforms

MANT-nucleotides differentially inhibit AC isoforms (Gille *et al.*, 2004). We examined the inhibitory effects of 8 MANT-nucleotides on mouse heart AC and recombinant ACs. In the presence of Mg^{2+}, the rank order of inhibitory potency of MANT-nucleotides at mouse heart AC was MANT-ITP ~ MANT-ITPγS > MANT-GTPγS > MANT-ATPγS ~ MANT-GTP > MANT-UTP > MANT-ATP > MANT-CTP (Tab. **4**).

Tab. 4: Kinetic properties of mouse heart AC and ACs 1, 2 and 5 and potencies of MANT-nucleotides at ACs in the presence of Mg^{2+}.

Parameter	AC1	AC2	AC5	Cardiac AC
K_m [μM]	160 ± 20*	110 ± 30*	87 ± 31	68 ± 5
V_{max} [pmol · mg^{-1} · min^{-1}]	660 ± 90*	300 ± 70*	2,400 ± 760	1,600 ± 160
Nucleotide	K_i [nM]			
MANT-ITP	24	65	13	24
MANT-ITPγS	300*	450*	150*	26
MANT-GTP	1,500*	3,700*	760*	780
MANT-GTPγS	990*	1,800*	550*	340
MANT-ATP	3,200*	5,700*	2,000*	2,000
MANT-ATPγS	1,400	2,300	1,100	770
MANT-CTP	3,600	15,000	3,600	3,300
MANT-UTP	1,800	10,000	1,000	1,200

AC activities were determined as described under "Materials and Methods". K_m and V_{max} values were obtained by non-linear regression analysis of substrate-saturation experiments and are the means ± SD of 3-4 independent experiments performed in duplicates. Values labelled with (*) were taken from (Gille *et al.*, 2004). The K_i values for MANT-ITP, MANT-ATPγS, MANT-CTP and MANT-UTP on AC1, AC2 and AC5 were determined in this work as described (Gille *et al.*, 2004) and represent the means of at least three independent experiments. K_i values on cardiac AC were determined in this work as described in "Materials and Methods" and are the means of at least 3 independent experiments performed in duplicates. Standard deviations were generally smaller than 20% of the means. Inhibition curves were analyzed by non-linear regression.

The inhibitor profile of mouse heart AC was very similar to the inhibitor profile of AC5, with AC1 showing moderate and AC2 showing large differences relative to mouse heart AC (Tab. **4** and Fig. **9A**). A correlation of the K_i values of MANT-nucleotides on mouse heart AC and AC5 revealed a highly significant correlation with a slope close to 1.00, indicative for pharmacological identity between the two enzymes compared (Fig. **9B**). Note that this correlation concerns Mg^{2+}-conditions only.
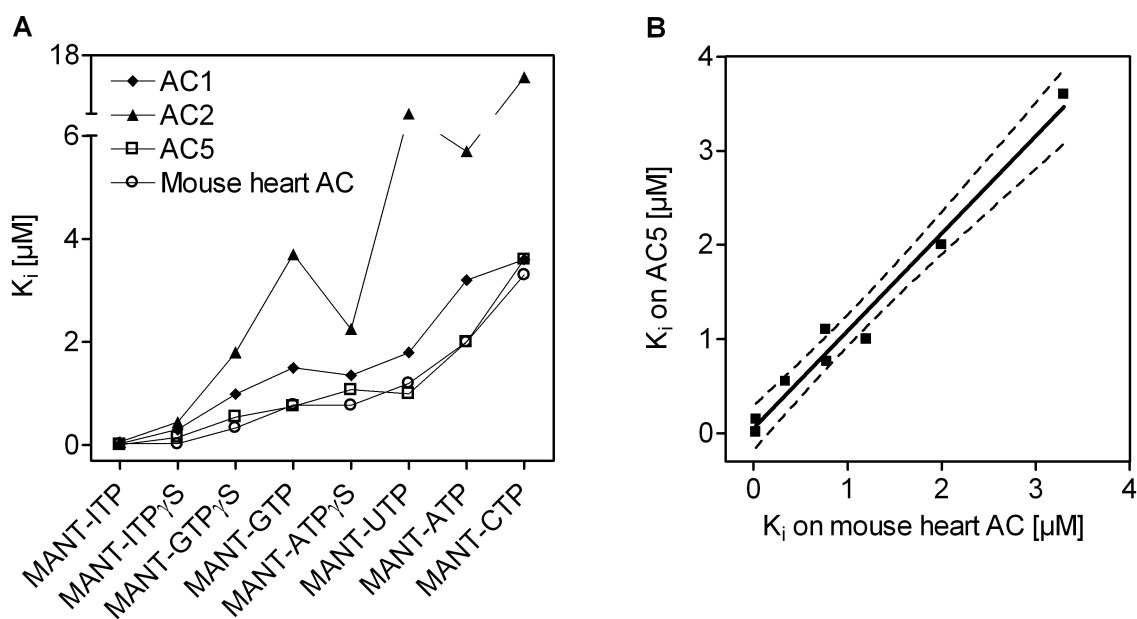
Fig. 9: Comparison of the inhibitory potencies of MANT-nucleotides on heart membrane AC and recombinant AC isoforms expressed in Sf9 cells in the presence of Mg^{2+}. A: K_i values of MANT-nucleotides on heart membrane AC and ACs 1, 2 and 5 shown in Tab. **4** were plotted. **B:** Correlation of the K_i values of MANT-nucleotides on mouse heart AC *vs.* AC5. Data were analyzed by linear regression. Dashed lines represent 95% confidence intervals of the linear regression lines. Slope, 1.033 ± 0.065; r^2, 0.9768; $p < 0.0001$.

In the presence of Mn^{2+}, the rank order of inhibitory potency of MANT-nucleotides at mouse heart AC was MANT-ITP > MANT-ITPγS > MANT-UTP > MANT-GTP ~ MANT-GTPγS ~ MANT-CTP > MANT-ATP ~ MANT-ATPγS (Tab. **5**). Overall, inhibitory potencies of MANT-nucleotides were higher in the presence of Mn^{2+} than in the presence of Mg^{2+}, but the potency-enhancing effect of Mn^{2+} ranged from just 3-fold for MANT-ITPγS to ~100-fold for MANT-CTP and MANT-UTP. Differential effects of Mg^{2+} and Mn^{2+} on inhibitor potency of MANT-nucleotides were also observed for recombinant ACs (Gille *et al.*, 2004). The inhibitor profile of mouse

heart AC in the presence of Mn^{2+} was clearly different from the profile of AC2, but we also noted several differences between mouse heart AC, on the one hand, and ACs 1, 5 and 6, on the other hand. Specifically, in the presence of Mn^{2+}, MANT-ITPγS, MANT-GTP, MANT-GTPγS, MANT-ATP, MANT-CTP and MANT-UTP were all more potent inhibitors of mouse heart AC than of the ACs 1, 5, and 6. Thus, heart membranes may contain an AC isoform that under Mn^{2+}-conditions is more potently inhibited by several MANT-nucleotides than AC5.

Tab. 5: Kinetic properties of mouse heart AC and ACs 1, 2, 5 and 6 and potencies of MANT-nucleotides at ACs in the presence of Mn^{2+}.

Parameter	AC1	AC2	AC5	AC6	Cardiac AC
K_m [µM]	110 ± 29*	99 ± 22*	40 ± 5	120 ± 42*	11 ± 2
V_{max} [pmol · mg^{-1} · min^{-1}]	1,500 ± 230*	1,200 ± 140*	3,200 ± 400	1,300 ± 260*	1,010 ± 370
Nucleotide	**K_i [nM]**				
MANT-ITP	3	14	1	3	4
MANT-ITPγS	41*	120*	31*	43*	8
MANT-GTP	90*	620*	55*	91*	21
MANT-GTPγS	62*	360*	35*	48*	23
MANT-ATP	210*	850*	200*	280*	64
MANT-ATPγS	160	380	77	72	67
MANT-CTP	150	690	150	280	29
MANT-UTP	46	460	32	71	12

AC activities were determined as described under "Materials and Methods". K_m and V_{max} values were obtained by non-linear regression analysis of substrate-saturation experiments and are the means ± SD of 3-4 independent experiments performed in duplicates. Values labelled with (*) were taken from (Gille *et al.*, 2004). The K_i values for MANT-ITP, MANT-ATPγS, MANT-CTP and MANT-UTP on AC1, AC2, AC5 and AC6 were determined in this work as described (Gille *et al.*, 2004) and represent the means of at least three independent experiments. K_i values on cardiac AC were determined in this work as described in "Materials and Methods" and are the means of at least 3 independent experiments performed in duplicates. Standard deviations were generally smaller than 20% of the means. Inhibition curves were analyzed by non-linear regression using the Prism 4.02 software (Graphpad, San Diego, CA).

All inhibition curves with MANT-nucleotides in heart membranes were monophasic (data not shown) so that we could not discriminate between various AC isoforms. In accordance with our previous study (Gille *et al.*, 2004), AC2 was less sensitive to inhibition by MANT-nucleotides than ACs 1, 5 and 6 (Tab. **5**). Unfortunately, the inhibitor profiles of ACs 1, 5 and 6 were very similar, allowing no differentiation between those three AC isoforms.

2.5   Discussion

The specific aim of this work was to characterize mouse heart AC, the long-term aim being the development of novel drugs for the treatment of chronic heart failure, particularly AC5 inhibitors. To achieve the specific aim of our work, we performed real-time PCR for the detection of AC mRNA, immunoblots and enzymological analysis of cardiac AC enzyme activity.

2.5.1   Real-Time PCR and Immunoblot Studies

In real-time PCR experiments, we obtained evidence for the expression of ACs 1, 3 to 7, and 9 (Fig. **2**). The threshold values for detection of AC5 and AC6 were lower than for the other AC isoforms indicating that AC5 and AC6 are the most prominent AC isoforms on mRNA level in the heart. These findings are in agreement with the literature pointing to high expression of ACs 5 and 6 in mammalian heart (Defer *et al.*, 2000; Hanoune and Defer, 2001; Beazely and Watts, 2006). There are reports on the expression of ACs1, 3, 4 and 7 in mammalian heart tissue (Manolopoulos *et al.*, 1995; Ferrand *et al.*, 1999; Defer *et al.*, 2000; Sunahara and Taussig, 2002; Risoe *et al.*, 2007). Our findings are consistent with the literature. Unfortunately, the functional roles of ACs 1, 3, 4, and 7 in the heart are much less understood than the roles of ACs 5 and 6. Furthermore, our data suggest that ACs 2 and 8 are not expressed in the heart. Despite numerous limitations of AC immunoblot analysis concerning antibody specificity and availability of recombinant ACs, positive immunoblot signals were obtained with the AC5/6 antibody in mouse heart membranes (Fig. **3A**). Therefore, our results from immunoblot analysis complement the results from RT-PCR experiments and indicate high expression of ACs 5 and 6 in the heart.

2.5.2 GPCR-Regulation of AC in Mouse Heart Membranes

Isoproterenol, GTPγS and FS effectively stimulated AC in mouse heart membranes, showing that the specific membrane preparation used in this work contained all components of the signaling cascade, i.e. β_1-adrenoceptors, G_s proteins and AC in a functionally intact form. In our hands, it was anything but trivial to obtain functionally active mouse heart membranes.

G_s-coupled histamine H_2-receptors and glucagon receptors are expressed in mammalian heart as well (Mery *et al.*, 1990; Matsuda *et al.*, 2004; Fryer *et al.*, 2006; Salazar *et al.*, 2007), but no modulation of murine cardiac AC activity was observed in this work using ligands for those GPCRs (Fig. **7**). The G_i protein-coupled NPY receptor subtypes Y_1, Y_2 and Y_5 are known to mediate functional responses in the heart as well (McDermott and Bell, 2007), but no response was detected with neuropeptide Y. In addition, functional G_s-coupled serotonin 5-HT$_4$-receptors are present in human ventricular myocardium (Levy *et al.*, 2008), but serotonin did not modulate cardiac AC activity. These findings suggest that in mouse heart, the β_1-adrenoceptor is the most important G_s-coupled GPCR, and we have no positive evidence for a G_i-coupled GPCR. In this study, we did not examine $G_{q/11}$- or $G_{12/13}$-mediated signal transduction pathways. The constitutive activity of the β_1-adrenoceptor was not significant in the native heart membranes (Fig. **6**) (Lefkowitz *et al.*, 1993; Zhou *et al.*, 2000; Engelhardt *et al.*, 2001; Wenzel-Seifert *et al.*, 2002). It cannot be excluded that G_s-coupled GPCRs other than the β_1-adrenoceptor play a functional role in the heart. Specifically, our crude heart membrane preparation predominantly consists of cardiomyocytes, but other cell types such as fibroblasts, vascular smooth muscle cells and endothelial cells contribute to the total cell mass, too. Thus, AC regulation by GPCRs in the latter three cell types may be below the detection limit of our global AC assay. We can also not exclude the possibility that the membrane preparation destroyed the integrity of some signaling pathways.

2.5.3 Regulation of Heart AC by FS and FS Analogs

FS analogs differentially regulate ACs 1, 2 and 5 (Pinto *et al.*, 2008). The EC_{50} values and relative maximum stimulatory effects of FS on heart AC and AC5 were similar, compatible with AC5 being the major cardiac AC isoform. Moreover, BODIPY-FS was a partial agonist on heart AC and AC5, whereas on AC2, BODIPY-FS was an inverse agonist. These data indicate that compared with AC5, AC2 is not of functional relevance in the heart, a conclusion in agreement with the real-time PCR experiments. Considering the low basal AC activity in mouse heart membranes and the very robust stimulation by FS as well as AC9 being FS-insensitive (Yan *et al.*, 1998), the contribution of AC9 to the AC activity in heart membranes seems to be of minor importance, too. Intriguingly, the correlations of potencies and particularly efficacies of FS analogs on heart AC and AC5 obtained in the presence of Mn^{2+} indicate that AC5 is not the only active AC isoform in heart membranes.

2.5.4 Regulation of Heart AC by Divalent Cations

Mg^{2+} is the physiological cation for AC activation *in vivo*. However, since with the non-physiological cation Mn^{2+} inhibitor potencies are higher than in the presence of Mg^{2+}, the former cation is often used for *in vitro* studies (Gille *et al.*, 2004, 2005; Taha *et al.*, 2009). For comparison with previous studies, we conducted some AC studies with heart membranes both in the presence of Mg^{2+} and Mn^{2+}. Regarding the effects of FS on AC, the exchange of Mg^{2+} against Mn^{2+} had little effect on potencies and relative maximum stimulatory effects on heart AC and recombinant ACs 1, 2 and 5 (Pinto *et al.*, 2008). However, as expected, MANT-nucleotides inhibited heart membrane more potently in the presence of Mn^{2+} than in the presence of Mg^{2+}.

With Mg^{2+} as physiological divalent cation, recombinant AC5 and mouse heart AC showed similar K_m and V_{max} values, supporting the notion that AC5 is an important AC isoform in mouse heart *in vivo*. However, under Mn^{2+}-conditions, AC5 showed a 4-fold higher K_m value than cardiac AC and V_{max} of AC5 was 3-fold higher than that of heart membranes. It is possible that under physiologically relevant Mg^{2+}-conditions, predominantly AC5 is activated in heart membranes, whereas under non-physiological Mn^{2+}-conditions, other AC isoforms than AC5 are activated as well, masking, at least partially, AC5. This interpretation is supported by the finding that under Mg^{2+}-conditions, the inhibitory profiles of MANT-nucleotides on mouse heart AC and AC5 were quite similar, whereas in the presence of Mn^{2+}, differences

between these ACs were noted. Under Mn^{2+}-conditions, the kinetics of mouse heart AC and the inhibitory profile of MANT-nucleotides on mouse heart AC do also not match the profiles of ACs 1, 2 and 6. Moreover, the correlations of the potencies and efficacies of FS analogs between mouse heart AC and AC5 in the presence of Mn^{2+} point to nonidentity of the enzymes studied. These data indicate that under Mn^{2+}-conditions, the relative contribution of AC5 to the total AC activity in mouse heart membranes is smaller than in the presence of Mg^{2+}. The elusive Mn^{2+}-activated mouse heart AC isoform is more sensitive to inhibition by most MANT-nucleotides than recombinant AC5.

A further limitation of our study concerns the lack of pharmacological and immunological discrimination between ACs 5 and 6, both of which are functionally important in the heart (Okumura *et al.*, 2003a, b; Takahashi *et al.*, 2006). To learn more on the properties of AC5 in a native membrane environment, it will be important to examine tissues that are highly enriched in AC5 relative to other tissues. The striatum may represent such a tissue (Glatt and Snyder, 1993).

2.5.5 Conclusions

The real-time PCR experiments, immunoblot studies, FS analog stimulation experiments, enzyme kinetics and MANT-nucleotide inhibition experiments under Mg^{2+}-conditions as well as our previous electrophysiological studies (Rottländer *et al.*, 2007) indicate that AC5 is an important cardiac AC isoform, provided Mg^{2+}-conditions are considered. To the best of our knowledge, MANT-ITP is the most potent competitive AC5 and cardiac AC inhibitor reported so far. Thus, hypoxanthine nucleotides provide an excellent starting point for the future development of AC5 inhibitors. However, a major as yet unresolved issue is the fact that immunologically and pharmacologically, ACs 5 and 6 are difficult to discriminate although at the organ level, they have different functions (Okumura *et al.*, 2003a, b; Takahashi *et al.*, 2006). Moreover, Mn^{2+} reduces the contribution of AC5 to overall AC activity in heart membranes and unmasks an elusive AC isoform. Thus, future AC studies in native membranes should be preferably conducted in the presence of Mg^{2+} although Mn^{2+} is very popular in AC studies.

With respect to *in vivo* application, AC5 inhibitors with high stability against enzymatic degradation are required. By analogy to antiviral drugs, lipophilic nucleotide prodrugs with high bioavailability have to be designed. Conversion of the nucleotide prodrug to the active nucleoside 5´-triphosphate by phosphorylation is then accomplished by specific kinases (Laux *et al.*, 2004). It is noteworthy that MANT-NTPs and the corresponding MANT-NTPγSs possess comparable potencies on heart AC. The advantage of MANT-NTPγSs relative to MANT-NTPs is that the phosphorothioates are resistant to cleavage by phosphatases (Eckstein, 1985), rendering them valuable experimental tools for electrophysiological studies in which nucleotides diffuse into the cytosol *via* the patch pipette (Rottländer *et al.*, 2007).

2.6   References

Beazely MA and Watts VJ (2006) Regulatory properties of adenylate cyclases type 5 and 6: A progress report. *Eur J Pharmacol* **535**:1-12.

Bristow MR (2000) β-adrenergic receptor blockade in chronic heart failure. *Circulation* **101**:558-569.

Defer N, Best-Belpomme M and Hanoune J (2000) Tissue specificity and physiological relevance of various isoforms of adenylyl cyclase. *Am J Physiol Renal Physiol* **279**:F400-416.

Devic E, Xiang Y, Gould D and Kobilka B (2001) β-adrenergic receptor subtype-specific signaling in cardiac myocytes from β_1- and β_2-adrenoceptor knockout mice. *Mol Pharmacol* **60**:577-583.

Dove S, Elz S, Seifert R and Buschauer A (2004) Structure-activity relationships of histamine H_2-receptor ligands. *Mini Rev Med Chem* **4**:941-954.

Eckstein F (1985) Nucleoside phosphorothioates. *Annu Rev Biochem* **54**:367-402.

El-Armouche A, Zolk O, Rau T and Eschenhagen T (2003) Inhibitory G proteins and their role in desensitization of the adenylyl cyclase pathway in heart failure. *Cardiovasc Res* **60**:478-487.

Engelhardt S, Grimmer Y, Fan GH and Lohse MJ (2001) Constitutive activity of the human β_1-adrenergic receptor in β_1-receptor transgenic mice. *Mol Pharmacol* **60**:712-717.

Ferrand N, Pessah M, Frayon S, Marais J and Garel JM (1999) Olfactory receptors, $G\alpha_{olf}$ and adenylyl cyclase mRNA expressions in the rat heart during ontogenic development. *J Mol Cell Cardiol* **31**:1137-1142.

Fonarow GC (2008) Epidemiology and risk stratification in acute heart failure. *Am Heart J* **155**:200-207.

Fryer RM, Reinhart GA and Esbenshade TA (2006) Histamine in cardiac sympathetic ganglia: A novel neurotransmitter? *Mol Interv* **6**:14-19, 12.

Gille A, Guo J, Mou TC, Doughty MB, Lushington GH and Seifert R (2005) Differential interactions of G proteins and adenylyl cyclase with nucleoside 5´-triphosphates, nucleoside 5´-[γ-thio]triphosphates and nucleoside 5´-[β,γ-imido]triphosphates. *Biochem Pharmacol* **71**:89-97.

Gille A, Lushington GH, Mou TC, Doughty MB, Johnson RA and Seifert R (2004) Differential inhibition of adenylyl cyclase isoforms and soluble guanylyl cyclase by purine and pyrimidine nucleotides. *J Biol Chem* **279**:19955-19969.

Gilman AG (1987) G proteins: Transducers of receptor-generated signals. *Annu Rev Biochem* **56**:615-649.

Glatt CE and Snyder SH (1993) Cloning and expression of an adenylyl cyclase localized to the corpus striatum. *Nature* **361**:536-538.

Hanoune J and Defer N (2001) Regulation and role of adenylyl cyclase isoforms. *Annu Rev Pharmacol Toxicol* **41**:145-174.

Houston C, Wenzel-Seifert K, Burckstummer T and Seifert R (2002) The human histamine H_2-receptor couples more efficiently to Sf9 insect cell G_s proteins than to insect cell G_q proteins: Limitations of Sf9 cells for the analysis of receptor/G_q protein coupling. *J Neurochem* **80**:678-696.

Iwatsubo K, Minamisawa S, Tsunematsu T, Nakagome M, Toya Y, Tomlinson JE, Umemura S, Scarborough RM, Levy DE and Ishikawa Y (2004) Direct inhibition of type 5 adenylyl cyclase prevents myocardial apoptosis without functional deterioration. *J Biol Chem* **279**:40938-40945.

Kimura N and Shimada N (1988) Direct interaction between membrane-associated nucleoside diphosphate kinase and GTP-binding protein (G_s), and its regulation by hormones and guanine nucleotides. *Biochem Biophys Res Commun* **151**:248-256.

Laux WHG, Pande P, Shoshani I, Gao JY, Boudou-Vivet V, Gosselin G and Johnson RA (2004) Pro-nucleotide inhibitors of adenylyl cyclases in intact cells. *Journal of Biological Chemistry* **279**:13317-13332.

Lefkowitz RJ, Cotecchia S, Samama P and Costa T (1993) Constitutive activity of receptors coupled to guanine nucleotide regulatory proteins. *Trends Pharmacol Sci* **14**:303-307.

Levy FO, Qvigstad E, Krobert KA, Skomedal T and Osnes JB (2008) Effects of serotonin in failing cardiac ventricle: Signalling mechanisms and potential therapeutic implications. *Neuropharmacology*.

Liu X, Thangavel M, Sun SQ, Kaminsky J, Mahautmr P, Stitham J, Hwa J and Ostrom RS (2007) Adenylyl cyclase type 6 overexpression selectively enhances β-adrenergic and prostacyclin receptor-mediated inhibition of

cardiac fibroblast function because of colocalization in lipid rafts. *Naunyn Schmiedebergs Arch Pharmacol*.

Lohse MJ, Engelhardt S and Eschenhagen T (2003) What is the role of β-adrenergic signaling in heart failure? *Circ Res* **93**:896-906.

Manolopoulos VG, Liu J, Unsworth BR and Lelkes PI (1995) Adenylyl cyclase isoforms are differentially expressed in primary cultures of endothelial cells and whole tissue homogenates from various rat tissues. *Biochem Biophys Res Commun* **208**:323-331.

Matsuda N, Jesmin S, Takahashi Y, Hatta E, Kobayashi M, Matsuyama K, Kawakami N, Sakuma I, Gando S, Fukui H, Hattori Y and Levi R (2004) Histamine H_1- and H_2-receptor gene and protein levels are differentially expressed in the hearts of rodents and humans. *J Pharmacol Exp Ther* **309**:786-795.

Matzdorf C, Kurtz A and Höcherl K (2007) COX-2 activity determines the level of renin expression but is dispensable for acute upregulation of renin expression in rat kidneys. *Am J Physiol Renal Physiol* **292**:F1782-1790.

McDermott BJ and Bell D (2007) NPY and cardiac diseases. *Curr Top Med Chem* **7**:1692-1703.

Mery PF, Brechler V, Pavoine C, Pecker F and Fischmeister R (1990) Glucagon stimulates the cardiac Ca^{2+} current by activation of adenylyl cyclase and inhibition of phosphodiesterase. *Nature* **345**:158-161.

Okumura S, Kawabe J, Yatani A, Takagi G, Lee MC, Hong C, Liu J, Takagi I, Sadoshima J, Vatner DE, Vatner SF and Ishikawa Y (2003a) Type 5 adenylyl cyclase disruption alters not only sympathetic but also parasympathetic and calcium-mediated cardiac regulation. *Circ Res* **93**:364-371.

Okumura S, Takagi G, Kawabe J, Yang G, Lee MC, Hong C, Liu J, Vatner DE, Sadoshima J, Vatner SF and Ishikawa Y (2003b) Disruption of type 5 adenylyl cyclase gene preserves cardiac function against pressure overload. *Proc Natl Acad Sci USA* **100**:9986-9990.

Pinto C, Papa D, Hubner M, Mou TC, Lushington GH and Seifert R (2008) Activation and inhibition of adenylyl cyclase isoforms by forskolin analogs. *J Pharmacol Exp Ther* **325**:27-36.

Risoe PK, Wang Y, Stuestol JF, Aasen AO, Wang JE and Dahle MK (2007) Lipopolysaccharide attenuates mRNA levels of several adenylyl cyclase isoforms *in vivo*. *Biochim Biophys Acta* **1772**:32-39.

Rohrer DK, Desai KH, Jasper JR, Stevens ME, Regula DP, Jr., Barsh GS, Bernstein D and Kobilka BK (1996) Targeted disruption of the mouse β_1-adrenergic receptor gene: Developmental and cardiovascular effects. *Proc Natl Acad Sci USA* **93**:7375-7380.

Rottländer D, Matthes J, Vatner SF, Seifert R and Herzig S (2007) Functional adenylyl cyclase inhibition in murine cardiomyocytes by 2´(3´)-*O*-(*N*-methylanthraniloyl)-guanosine 5´-[γ-thio]triphosphate. *J Pharmacol Exp Ther* **321**:608-615.

Salazar NC, Chen J and Rockman HA (2007) Cardiac GPCRs: GPCR signaling in healthy and failing hearts. *Biochim Biophys Acta* **1768**:1006-1018.

Sunahara RK and Taussig R (2002) Isoforms of mammalian adenylyl cyclase: Multiplicities of signaling. *Mol Interv* **2**:168-184.

Taha HM, Schmidt J, Göttle M, Suryanarayana S, Shen Y, Tang WJ, Gille A, Geduhn J, König B, Dove S and Seifert R (2009) Molecular analysis of the interaction of anthrax adenylyl cyclase toxin, edema factor, with 2´(3´)-*O*-(*N*-(methyl)anthraniloyl)-substituted purine and pyrimidine nucleotides. *Mol Pharmacol* **75**:693-703.

Takahashi T, Tang T, Lai NC, Roth DM, Rebolledo B, Saito M, Lew WY, Clopton P and Hammond HK (2006) Increased cardiac adenylyl cyclase expression is associated with increased survival after myocardial infarction. *Circulation* **114**:388-396.

Weitl N and Seifert R (2008) Distinct interactions of human β_1- and β_2-adrenoceptors with isoproterenol, epinephrine, norepinephrine, and dopamine. *J Pharmacol Exp Ther* **327**:760-769.

Wenzel-Seifert K, Liu HY and Seifert R (2002) Similarities and differences in the coupling of human β_1- and β_2-adrenoceptors to Gα_s splice variants. *Biochem Pharmacol* **64**:9-20.

Yan L, Vatner DE, O´Connor JP, Ivessa A, Ge H, Chen W, Hirotani S, Ishikawa Y, Sadoshima J and Vatner SF (2007) Type 5 adenylyl cyclase disruption increases longevity and protects against stress. *Cell* **130**:247-258.

Yan SZ, Huang ZH, Andrews RK and Tang WJ (1998) Conversion of forskolin-insensitive to forskolin-sensitive (mouse-type 9) adenylyl cyclase. *Mol Pharmacol* **53**:182-187.

Yu DS, Lee DT, Kwong AN, Thompson DR and Woo J (2008) Living with chronic heart failure: A review of qualitative studies of older people. *J Adv Nurs* **61**:474-483.

Zhou YY, Yang D, Zhu WZ, Zhang SJ, Wang DJ, Rohrer DK, Devic E, Kobilka BK, Lakatta EG, Cheng H and Xiao RP (2000) Spontaneous activation of β_2- but not β_1-adrenoceptors expressed in cardiac myocytes from $\beta_1\beta_2$ double knockout mice. *Mol Pharmacol* **58**:887-894.

Chapter 3

Molecular Analysis of the Interaction of *Bordetella pertussis* Adenylyl Cyclase with Fluorescent Nucleotides

3.1   Abstract

The calmodulin (CaM)-dependent adenylyl cyclase (AC) toxin from *Bordetella pertussis* (CyaA) substantially contributes to the pathogenesis of whooping cough. Thus, potent and selective CyaA inhibitors may be valuable drugs for prophylaxis of this disease. We examined the interactions of fluorescent 2´,3´-*N*-methylanthraniloyl (MANT)-, anthraniloyl (ANT)- and trinitrophenyl (TNP)-substituted nucleotides with CyaA. Compared to mammalian AC isoforms and *Bacillus anthracis* AC toxin edema factor, nucleotides inhibited catalysis by CyaA less potently. Introduction of the MANT-substituent resulted in 5- to 170-fold increased potency of nucleotides. K_i values of 3´MANT-2´d-ATP and 2´MANT-3´d-ATP in the AC activity assay using Mn^{2+} were 220 nM and 340 nM, respectively. Natural nucleoside 5´-triphosphates, guanine-, hypoxanthine- and pyrimidine-MANT- and TNP-nucleotides and di-MANT-nucleotides inhibited CyaA, too. MANT-nucleotide binding to CyaA generated fluorescence resonance energy transfer (FRET) from tryptophans W69 and W242 and multiple tyrosine residues, yielding K_d values of 300 nM for 3´MANT-2´d-ATP and 400 nM for 2´MANT-3´d-ATP. Fluorescence experiments and docking approaches indicate that the MANT- and TNP-groups interact with F306. Increases of FRET and direct fluorescence with MANT-nucleotides were strictly CaM-dependent, whereas TNP-nucleotide fluorescence upon binding to CyaA increased in the absence of CaM and was actually reduced by CaM. In contrast to low-affinity MANT-nucleotides, even low-affinity TNP-nucleotides generated strong fluorescence increases upon binding to CyaA. We conclude that the catalytic site of CyaA possesses substantial conformational freedom to accommodate structurally diverse ligands and that certain ligands bind to CyaA even in the absence of CaM, facilitating future inhibitor design.

3.2   Introduction

Bordetella pertussis toxin CyaA is a 1706-amino acid virulence factor interacting with surface receptors of eukaryotic host cells and translocating its AC domain into the cytosol (Confer and Eaton, 1982; Hewlett *et al.*, 1989; Ladant and Ullmann, 1999). After activation by calmodulin (CaM), an endogenous calcium sensor, CyaA catalyzes massive synthesis of cAMP (Mock and Ullmann, 1993; Shen *et al.*, 2002; Ahuja *et al.*, 2004). cAMP inhibits phagocyte function and facilitates respiratory tract infection by *Bordetella pertussis* (Boyd *et al.*, 2005; Carbonetti *et al.*, 2005; Hewlett *et al.*, 2006). Substrate analogs may be used to inhibit the catalytic activity of CyaA (Johnson and Shoshani, 1990; Soelaiman *et al.*, 2003; Gille *et al.*, 2004) and for prophylaxis of *Bordetella pertussis* infection. We have discovered *N*-methylanthraniloyl (MANT)-substituted NTPs as competitive inhibitors of mammalian and bacterial ACs including CyaA (Gille *et al.*, 2003, 2004). Additionally, 2´,3´-(2,4,6-trinitrophenyl) (TNP)-substituted NTPs are potent inhibitors of mammalian AC (Mou *et al.*, 2006). Furthermore, adefovir, a drug for the treatment of chronic hepatitis B virus infection, is a potent CyaA inhibitor (Shen *et al.*, 2004).

Mammals express nine membranous AC isoforms (ACs 1-9) and a soluble AC. We have employed the cytosolic catalytic domains C1 of type 5 AC and C2 of type 2 AC for molecular AC analysis (Gille *et al.*, 2004; Mou *et al.*, 2005, 2006). Comparing the crystal structures of C1:C2 bound to MANT-GTP, MANT-ATP and TNP-ATP, we found the catalytic site of AC to consist of three binding pockets, accommodating the base, the 2´,3´-ribosyl substituent and the phosphate chain. We have also reported the crystal structure of CyaA in complex with CaM and PMEApp, the active metabolite of adefovir (Guo *et al.*, 2005). Forty-nine amino acid residues of CyaA and 41 residues of CaM form salt bridges, hydrogen bonds and hydrophobic contacts, resulting in high affinity of CyaA for CaM (K_d = 0.2 nM). However, the precise conformational changes in the catalytic site of CyaA underlying its activation by CaM are still unknown. An understanding of these processes will greatly facilitate future inhibitor design.

To monitor nucleotide binding to and conformational changes in CyaA, different approaches can be employed. First, MANT- and ANT-nucleotides are environmentally sensitive probes displaying increased fluorescence and blue-shift of the emission maximum upon exposure to a hydrophobic environment (Hiratsuka,

1983; Jameson and Eccleston, 1997). As is obvious from the CyaA crystal structure in complex with PMEApp (Shen *et al.*, 2004; Guo *et al.*, 2005), the catalytic site contains the hydrophobic residue F306. Nucleotide binding to CyaA allows hydrophobic interactions between the MANT-/ANT-group and F306, resulting in an increased fluorescence signal (Sarfati *et al.*, 1990; Guo *et al.*, 2005). This notion is supported by the fact that CyaA-F306A does not increase the fluorescence signal of 3´ANT-2´d-ATP. Second, the catalytic domain of CyaA bears two tryptophan residues, W69 located 21 Å and W242 38 Å away from the catalytic site (Guo *et al.*, 2005). These distances allow fluorescence resonance energy transfer (FRET) (Lakowicz, 1999) from tryptophan (excitation wavelength, 280 nm; emission wavelength, 350 nm) to MANT (excitation wavelength, 350 nm; emission wavelength, 450 nm) (Gilles *et al.*, 1990; Sarfati *et al.*, 1990; Mou *et al.*, 2005, 2006). Third, TNP-nucleotides are environmentally sensitive fluorescence probes, too (Hiratsuka, 2003). Like MANT-nucleotides, TNP-nucleotides show a blue-shift in emission in a hydrophobic environment (Hiratsuka, 2003). Compared to MANT-/ANT-nucleotides, TNP-nucleotides are more rigid since the fluorophore is attached through both the 2´- and 3´-ribosyl position (Jameson and Eccleston, 1997; Hiratsuka, 2003). A potential advantage of TNP-nucleotides compared to MANT-nucleotides is the fact that the relative fluorescence increases can be substantially larger, depending on the specific protein studied (Jameson and Eccleston, 1997; Hiratsuka, 2003; Mou *et al.*, 2005, 2006).

In the present study, we used MANT-/ANT- and TNP-nucleotides as probes to determine their potencies at inhibiting CyaA and to investigate conformational changes in the catalytic site. Nucleotides **12**, **14**, **15**, **18**, **19**, **20**, **25**, **30** and **31** (Tab. **1**) represent newly synthesized fluorescent probes. Moreover, the binding mode of nucleotides was explored by docking of representative derivatives to a CyaA model derived from the crystal structure in complex with PMEApp (Shen *et al.*, 2004; Guo *et al.*, 2005).

3.3   Materials and Methods

Materials. MANT- and ANT-substituted NTPs of adenosine, cytidine, inosine and uridine were synthesized according to a documented procedure (Hiratsuka, 1983). The modification of the synthesis by lowering the pH value from 9.6 to 8.6 induced higher yields. In case of the starting material methyl-isatoic anhydride, the major portion of the excessive compound was removed by $CHCl_3$-extraction. In general, the separation of starting materials could be achieved by using size exclusion chromatography with Sephadex® LH-20 in water. However, HPLC-analysis and liquid chromatography/mass spectrometry coupling still showed by-product of the corresponding (M)ANT-diphosphate residue. Pure MANT-nucleotides were obtained by preparative reversed-phase HPLC with a Phenomenex Luna C18(2) column (particle size, 10 μm; length, 250 mm; inner diameter, 21.2 mm). The nucleoside 5´-diphosphates were also collected because of their putative inhibitory effects. (M)ANT-nucleoside 5´-diphosphates and triphosphates were obtained in high purity of 99%. Di-MANT-IMP (**31**) bearing two MANT-groups at the 2´,3´-ribosyl position was also found as a by-product of our synthesis and was purified to 99% content, too. MANT-ATP (**8**), MANT-GTP (**10**), ANT-GTP (**24**), 3´MANT-2´d-ATP (**21**), 2´MANT-3´d-ATP (**22**), TNP-CTP (**28**), TNP-UTP (**29**) and γS-substituted MANT-nucleotides (**9**, **11**, **13**) were obtained from Jena Bioscience, Jena, Germany. In case of MANT-ATP, the MANT-group isomerizes between the 2´- and 3´-position of the ribose ring, whereas in 2´MANT-3´d-ATP and 3´MANT-2´d-ATP the MANT-group is fixed to the corresponding position due to the absence of the neighboring hydroxyl group. PMEApp (**1**) was supplied by Gilead Sciences, Foster City, CA, USA. TNP-ATP (**26**) and TNP-GTP (**27**) were from Molecular Probes, Eugene, OR, USA. ITP was from Sigma-Aldrich, Seelze, Germany; GTP was from Roche, Mannheim, Germany. UTP and CTP were from Boehringer, Ingelheim, Germany. The catalytic domain of *Bordetella pertussis* AC protein (CyaA, amino acids 1 to 373) was purified as described (Shen *et al.*, 2002). Lyophilized calmodulin from bovine brain was purchased from EMD Biosciences, Calbiochem, Darmstadt, Germany. [α-^{32}P]ATP (800 Ci/mmol) was purchased from PerkinElmer, Wellesley, MA, USA. Aluminum oxide 90 active, neutral (activity 1, particle size 0.06 - 0.2 mm) was purchased from Merck, Darmstadt, Germany. Albumin from bovine serum, fraction V, highest quality,

was from Sigma-Aldrich. $MnCl_2$ tetrahydrate and $MgCl_2$ hexahydrate (highest quality) were from Merck.

FRET and Direct Fluorescence Experiments with MANT-Nucleotides. Experiments were performed using a quartz UV ultra-microcuvette from Hellma, Müllheim, Germany (type 105.251-QS; light path length, 3 mm; center, 15 mm; total volume, 70 μL). Measurements were performed in a Varian Cary Eclipse fluorescence spectrometer at a constant temperature of 25°C (slit width, 5 nm; scan rate, 120 nm/min; averaging time, 0.5 s; data interval, 1 nm; PMT voltage, 700 V). The cuvette contained at first 64 μL of 75 mM Hepes/NaOH buffer, 100 μM $CaCl_2$, 100 mM KCl and 5 mM $MnCl_2$, pH 7.4. Next, nucleotide, CyaA and CaM were added in sequence. The cuvette content (final volume, 70 μL) was mixed after each addition. In FRET experiments, nucleotides were used at final concentrations from 10 nM to 2 μM, and CyaA and CaM were 300 nM each. The excitation wavelength was 280 nm, and emission was scanned from 300 nm to 550 nm. To investigate the kinetics of CyaA interaction with MANT-nucleotides, the excitation wavelength was 280 nm and changes in fluorescence intensity were measured over time at 430 nm. Nucleotides, CyaA and CaM were applied at a final concentration of 300 nM. MANT-nucleotides were finally displaced from CyaA using PMEApp (10 nM to 3 μM). In saturation studies, independent FRET experiments were performed using MANT-nucleotides from 10 nM to 2 μM final concentration; CyaA and CaM were 300 nM each. Saturation curves were obtained by subtracting the fluorescence intensity at 430 nm after the addition of CyaA from the maximal fluorescence (FRET) after the addition of CyaA/CaM.

In direct fluorescence experiments, MANT-nucleotides were excited at 350 nm and emission spectra were recorded from 380 nm to 550 nm. In order to obtain large increases in direct fluorescence, CyaA and CaM (final concentrations, 2.4 μM) were used in excess relative to MANT-nucleotides (final concentration, 100 nM). For an estimation of the hydrophobic properties of the binding site interacting with the MANT-group, direct fluorescence of the nucleotides was determined in water and in 30% (v/v) dimethyl sulfoxide.

Fluorescence Studies with TNP-Nucleotides. Fluorescence studies with TNP-nucleotides were essentially performed as for MANT-nucleotides with some modifications. Specifically, the concentrations of TNP-nucleotides, CyaA and CaM were 5 μM each. The higher protein concentrations were necessary to compensate for the lower quantum yield with TNP-nucleotides compared to MANT-nucleotides (Jameson and Eccleston, 1997; Hiratsuka, 2003).The excitation wavelength was 405 nm, and emission was scanned from 480 to 620 nm.

AC Activity Assay. For the determination of the potency of CyaA inhibitors, assay tubes contained 10 μL of inhibitor at final concentrations from 10 nM to 100 μM and 20 μL of CyaA protein (10 pM final concentration) in 75 mM Hepes/NaOH, pH 7.4, containing 0.1% (m/v) bovine serum albumin. Tubes were preincubated for 2 min at 25°C, and reactions were initiated by the addition of 20 μL of reaction mixture consisting of the following components to yield the given final concentrations: 100 mM KCl, 10 μM free Ca^{2+}, 5 mM free Mn^{2+} or Mg^{2+}, 100 μM EGTA, 100 μM cAMP, 100 nM CaM. ATP was added as non-labeled substrate at a final concentration of 40 μM and as radioactive tracer [α-^{32}P]ATP (0.2 μCi/tube). For the determination of K_m and V_{max} values, 10 μM to 2 mM ATP/Mn^{2+} or ATP/Mg^{2+} were added, plus 5 mM of free Mn^{2+} or Mg^{2+}. In order to ensure linear reaction progress, tubes were incubated for 10 min at 25°C, and reactions were stopped by the addition of 20 μL of 2.2 N HCl. Denaturated protein was sedimented by a 1-min centrifugation at 12,000 x g. [^{32}P]cAMP was separated from [α-^{32}P]ATP by transferring the samples to columns containing 1.4 g of neutral alumina. [^{32}P]cAMP was eluted by the addition of 4 mL 0.1 M ammonium acetate solution, pH 7.0. Blank values were about 0.02% of the total added amount of [α-^{32}P]ATP; substrate turnover was < 3% of the total added [α-^{32}P]ATP. Samples collected in scintillation vials were filled up with 10 mL of double-distilled water and Čerenkov radiation was measured in a PerkinElmer Tricarb 2800TR liquid scintillation analyzer. Free concentrations of divalent cations were calculated with WinMaxC (http://www.stanford.edu/~cpatton/maxc.html). K_i values reported in Tab. **1** and K_d values obtained from saturation experiments were calculated using the Prism 4.02 software (Graphpad, San Diego, CA, USA).

Modeling of the Nucleotide Binding Mode to CyaA. Docking studies were performed with the molecular modeling package SYBYL 7.3 (Tripos Inc., St. Louis, MO, USA) on a Silicon Graphics Octane workstation. An initial computer model of CyaA in complex with PMEApp was generated from the PDB crystal structure 1zot (Guo *et al.*, 2005). Hydrogens were added and AMBER_FF99 charges were assigned to the protein and the water molecules, followed by a rough pre-optimization of the model (100 cycles) with the AMBER_FF99 force field (Cornell *et al.*, 1995) and fixed PMEApp. The three Mg^{2+} ions received formal charges of 2. Starting conformations of 3´MANT-2´d-ATP (**21**), 2´MANT-3´d-ATP (**22**) and TNP-ATP (**26**) were derived from complexes of 3´MANT-ATP and TNP-ATP with mammalian AC (PDB structures 2gvz and 2gvd, respectively) (Mou *et al.*, 2005, 2006). PMEApp and the ligands **21**, **22** and **26** were provided with Gasteiger-Hueckel charges. Initial docking positions resulted from superposition of roughly optimized conformations with PMEApp, allowing the modification of rotatable bonds, and from consideration of the fluorescence data (interaction of the MANT- and TNP-groups with F306). Water molecules in the catalytic site were removed. Each complex was refined in a stepwise approach. First, ~50 minimization cycles with fixed ligand (AMBER_FF99 force field, steepest descent method) were performed, second, ~100 minimization cycles of the ligand and the surrounding (distance up to 6 Å) protein residues (Tripos force field) (Clark *et al.*, 1989), and third, ~100 minimization cycles with fixed ligand (AMBER_FF99 force field, Powell conjugate gradient). The second and third steps were repeated with larger number of cycles until a root mean square (RMS) force of 0.05 kcal mol^{-1} $Å^{-1}$ was approached. In order to avoid overestimation of electrostatic interactions, a distance-dependent dielectric constant of 4 was applied. Molecular surfaces and lipophilic potentials (protein variant with the new Crippen parameter table (Heiden *et al.*, 1993; Ghose *et al.*, 1998)) were calculated and visualized by the program MOLCAD (J. Brickmann *et al.*, Technical University of Darmstadt, Germany) contained within SYBYL.

3.4 Results

3.4.1 Overview on Nucleotide Structures

We examined the inhibitory effects of 31 nucleotides on the catalytic activity of CyaA (Tab. **1**). Nucleotides differed from each other in base, phosphate chain length, phosphate chain substitution, and MANT-, ANT- or TNP-substituents at the 2´,3´-ribosyl position. In compounds **8-20**, **23-25** and **30**, the MANT- or ANT-group undergoes spontaneous isomerization between the 2´- and 3´-ribosyl position (Jameson and Eccleston, 1997). In **21** and **22**, the MANT-group is fixed to the 2´- or 3´-position because the neighboring ribosyl position is deoxygenated, thus preventing isomerization. In **23-25**, an ANT-group is attached to the ribosyl residue instead of the MANT-group. Compounds **26-29** contain TNP-substituents. In **31**, two MANT-substituents are attached to the 2´- and 3´-ribosyl position. In **9**, **11** and **13**, the γ-phosphate group is substituted by a γ-thiophosphate group. The potencies of the different nucleotides were determined in the AC activity assay in the presence of either Mn^{2+} or Mg^{2+}.

3.4.2 Structure/Activity Relationships under Mn^{2+}-Conditions

Under Mn^{2+}-conditions, MANT-ITP (**12**) displayed the highest potency of all MANT-NTPs examined, exhibiting 7-fold higher potency than MANT-ATP (**8**). The rank order of potencies was MANT-ITP > MANT-CTP > MANT-UTP > MANT-ATP > MANT-GTP. MANT-GTP (**10**) exhibited 10-fold lower potency compared to MANT-ITP. For MANT-NDPs, the order of potency was MANT-IDP ~ MANT-ADP > MANT-CDP > MANT-UDP; MANT-IDP was 4-fold more potent than MANT-UDP. For ANT-nucleotides, the adenine base was advantageous compared with guanine; ANT-ATP (**23**) was 22-fold more potent than ANT-GTP (**24**). Among γS-substituted MANT-nucleotides, the rank order of potency was MANT-ATPγS > MANT-ITPγS > MANT-GTPγS; MANT-ATPγS (**9**) was 4 to 5-fold more potent than MANT-GTPγS (**11**).

TNP-ATP (**26**) was the most potent TNP-nucleotide; the rank order was TNP-ATP > TNP-CTP > TNP-GTP > TNP-UTP. Among the nucleotides bearing no fluorescent substituent at the 2´,3´-ribosyl position, GTP (**2**) displayed the highest affinity, which was 4-fold higher than the affinity of ITP (**3**) and UTP (**6**). Interestingly, the K_i constants of GTP and CTP were lower than the K_m value of the natural substrate ATP. Compared to the non-substituted NTPs, the MANT-group increased

inhibitor potency 5-fold, 31-fold, 45-fold and 166-fold for MANT-GTP, MANT-CTP, MANT-UTP and MANT-ITP, respectively. The TNP-group increased inhibitory potency in case of TNP-CTP and TNP-UTP just by factors of 3 and 2, respectively, and TNP-GTP (**27**) was only slightly more potent than GTP (**2**). MANT-substituted nucleotides were 2, 3, 9 and 22 times more potent in inhibiting CyaA compared with TNP-nucleotides (**8** *vs.* **26**, **10** *vs.* **27**, **14** *vs.* **28**, and **15** *vs.* **29**). While ANT-ATP (**23**) was 3-fold more potent than MANT-ATP (**8**), the potency of ANT-GTP (**24**) was 5-fold lower compared with MANT-GTP (**10**). Omission of the γ-phosphate group resulted in substantially decreased potencies at all nucleotides. Specifically, MANT-ADP (**16**) was 3-fold less potent than MANT-ATP (**8**), MANT-GDP (**17**) 10-fold less than MANT-GTP (**10**) (Gille *et al.*, 2004), MANT-CDP (**19**) 15-fold less than MANT-CTP (**14**), MANT-UDP (**20**) 17-fold less than MANT-UTP (**15**) and MANT-IDP (**18**) 18-fold less than MANT-ITP (**12**). ANT-ADP (**25**) was 9-fold less potent than ANT-ATP (**23**). Adding the γS-substitution to MANT-NTPs decreased potency of MANT-ITP 3-fold (**12** *vs.* **13**), increased potency of MANT-ATP 4-fold (**8** *vs.* **9**) and left the potency of MANT-GTP unchanged (**10** *vs.* **11**). Most strikingly, 3´MANT-2´d-ATP (**21**) and 2´MANT-3´d-ATP (**22**) were 22-fold and 14-fold more potent, respectively, than MANT-ATP (**8**).

3.4.3 Structure/Activity Relationships under Mg^{2+}-Conditions

The exchange of Mn^{2+} by Mg^{2+} increased K_m and V_{max} 14-fold and 5-fold, respectively. Inhibitory potencies of all tested nucleotides were differentially lowered when Mg^{2+} was used instead of Mn^{2+}. While the potency of MANT-GTPγS was only minimally reduced, 3´MANT-2´d-ATP and 2´MANT-3´d-ATP showed ~160-fold and ~70-fold lower potency with Mg^{2+}. The rank order of potency for MANT-substituted NTPs was MANT-GTP = MANT-ITP > MANT-CTP > MANT-UTP > MANT-ATP. While MANT-GTP (**10**) displayed the lowest potency of all MANT-NTPs under Mn^{2+}-conditions, it was - together with MANT-ITP (**12**) - the most potent MANT-NTP when Mg^{2+} was used. ANT-ATP (**23**) was 3-fold more potent than MANT-ATP (**8**) and exceeded ANT-GTP (**24**) in potency. MANT-GTPγS (**11**) was the most potent γS-substituted nucleotide tested, being 2-fold more potent than MANT-ATPγS (**9**) and 4-fold more potent than MANT-ITPγS (**13**). The introduction of the MANT-group increased the potency of CTP, UTP and GTP 7- to 16-fold. Most strikingly, MANT-ITP (**12**) was ~70-fold more potent than ITP (**3**). Among TNP-nucleotides, potency

decreased in the order TNP-ATP, TNP-GTP, TNP-CTP, TNP-UTP. It is noteworthy that the TNP-group did not increase potency compared to non-substituted NTPs; potency even decreased (**2** *vs.* **27**, **5** *vs.* **28** and **6** *vs.* **29**).

Tab. 1: Potencies of inhibitors at CyaA.

Cpd.		Mn^{2+}	Mg^{2+}
	K_m	45 ± 6	609 ± 62
	V_{max}	165 ± 21	861 ± 106
1	PMEApp	0.001 ± 0.0003	0.025 ± 0.002
2	GTP	27 ± 6	260 ± 32
3	ITP	100 ± 20	$1,100 \pm 220$
4	ITPγS	77	ND
5	CTP	35 ± 1	270 ± 43
6	UTP	120 ± 14	330 ± 80
7	UTPγS	36	ND
8	MANT-ATP	4.3 ± 0.4	51 ± 1
9	MANT-ATPγS	1.2 ± 0.4	15 ± 2
10	MANT-GTP	5.9 ± 1.0	16 ± 2
11	MANT-GTPγS	5.4 ± 0.5	7.4 ± 0.1
12	MANT-ITP	0.6 ± 0.1	16 ± 4
13	MANT-ITPγS	1.8 ± 0.3	31 ± 2
14	MANT-CTP	1.1 ± 0.1	36 ± 4
15	MANT-UTP	2.6 ± 0.3	42 ± 9
16	MANT-ADP	12 ± 2	91 ± 16
17	MANT-GDP	60	ND
18	MANT-IDP	11 ± 3	> 100
19	MANT-CDP	18 ± 3	> 100
20	MANT-UDP	43 ± 1	> 100
21	3´MANT-2´d-ATP	0.2 ± 0.04	32 ± 7
22	2´MANT-3´d-ATP	0.3 ± 0.04	22 ± 4
23	ANT-ATP	1.3 ± 0.1	20 ± 3
24	ANT-GTP	29 ± 0.3	> 100
25	ANT-ADP	11 ± 1	> 100
26	TNP-ATP	6.5 ± 0.2	110 ± 23
27	TNP-GTP	20 ± 3	320 ± 7
28	TNP-CTP	10 ± 0.4	410 ± 9
29	TNP-UTP	58 ± 8	780 ± 38
30	MANT-IMP	> 100	> 100
31	Di-MANT-IMP	20 ± 3	37 ± 3

AC toxin activities were determined as described under "Materials and Methods". Apparent K_m and V_{max} values were obtained by non-linear regression analysis of substrate-saturation experiments and are the means ± SEM of 3-5 independent experiments. K_m values are given in μM, V_{max} values are given as molar turnover numbers (s^{-1}). K_i values are given in μM and are the means ± SEM of at least 3 experiments performed in duplicates. For determination of the inhibitory potencies of various purine and pyrimidine nucleotides, reaction mixtures contained 100 mM KCl, 10 μM free Ca^{2+}, 5 mM free Mn^{2+} or Mg^{2+}, 100 μM EGTA, 40 μM ATP, 0.2 μCi/tube [α-^{32}P]ATP, 100 μM cAMP, 100 nM CaM, 10 pM CyaA in 75 mM Hepes/NaOH, pH 7.4, and nucleotides at concentrations from 100 pM to 2 mM as appropriate to construct concentration-response curves. The K_i value for **1** under Mg^{2+}-conditions was taken from (Shen *et al.*, 2004). The K_i values for **4**, **7** and **17** under Mn^{2+}-conditions were taken from (Gille *et al.*, 2004). Inhibition curves were analyzed by non-linear regression using the Prism 4.02 software (Graphpad, San Diego, CA). Cpd., compound.

3.4.4 FRET Experiments with MANT-Nucleotides

In FRET experiments, 2´MANT-3´d-ATP, 3´MANT-2´d-ATP and MANT-ATP (final concentrations, 300 nM each) were added first to the buffer, and fluorescence of MANT-nucleotides as a result of excitation at 280 nm was detected at 450 nm (Fig. **1**, dotted line). When CyaA was added, tryptophan and tyrosine fluorescence occurred at 350 nm (Fig. **1**, solid line). Upon addition of CaM, fluorescence intensity at 430 nm considerably increased due to FRET using 2´MANT-3´d-ATP and 3´MANT-2´d-ATP (Fig. **1**, **A** and **B**, dashed lines), but not using MANT-ATP (Fig. **1C**), MANT-GTP, MANT-ITP, MANT-CTP and MANT-UTP (data not shown). When FRET experiments were performed using the tryptophan-specific excitation wavelength of 295 nm (Lakowicz, 1999), fluorescence intensity at 350 nm decreased about 3-fold. The relative magnitude of FRET with 2´MANT-3´d-ATP and 3´MANT-2´d-ATP remained unchanged upon tryptophan-selective excitation (data not shown). Thus, FRET resulted from excitation of W69 and W242 and tyrosine residues. Y75, Y122, Y263, Y333, Y345 and Y350 are located in a distance of less than 20 Å from the catalytic site. Thus, in order to obtain high FRET signals, it is favorable to excite both tyrosine and tryptophan residues.

PMEApp (**1**) inhibited FRET in a concentration-dependent manner (Fig. **2**). Half-maximal displacement of 300 nM 3´MANT-2´d-ATP occurred at a PMEApp concentration of approximately 50 nM, which is compatible with the notion that PMEApp is a much more potent CyaA inhibitor than 3´MANT-2´d-ATP (Tab. **1**). Kinetics of CyaA FRET stimulation by CaM and inhibition by PMEApp occurred within mixing time (few seconds). These data show that FRET was specific and reversible.

By determining FRET with MANT-nucleotides at increasing concentrations after addition of CaM, saturation curves were obtained (Fig. **3**). Apparent K_d values were 400 nM for 2´MANT-3´d-ATP (**A**) and 300 nM for 3´MANT-2´d-ATP (**B**). For MANT-ATP, MANT-GTP, MANT-ITP, MANT-CTP, and MANT-UTP, K_d values could not be determined because of absent or minimal FRET (data not shown).
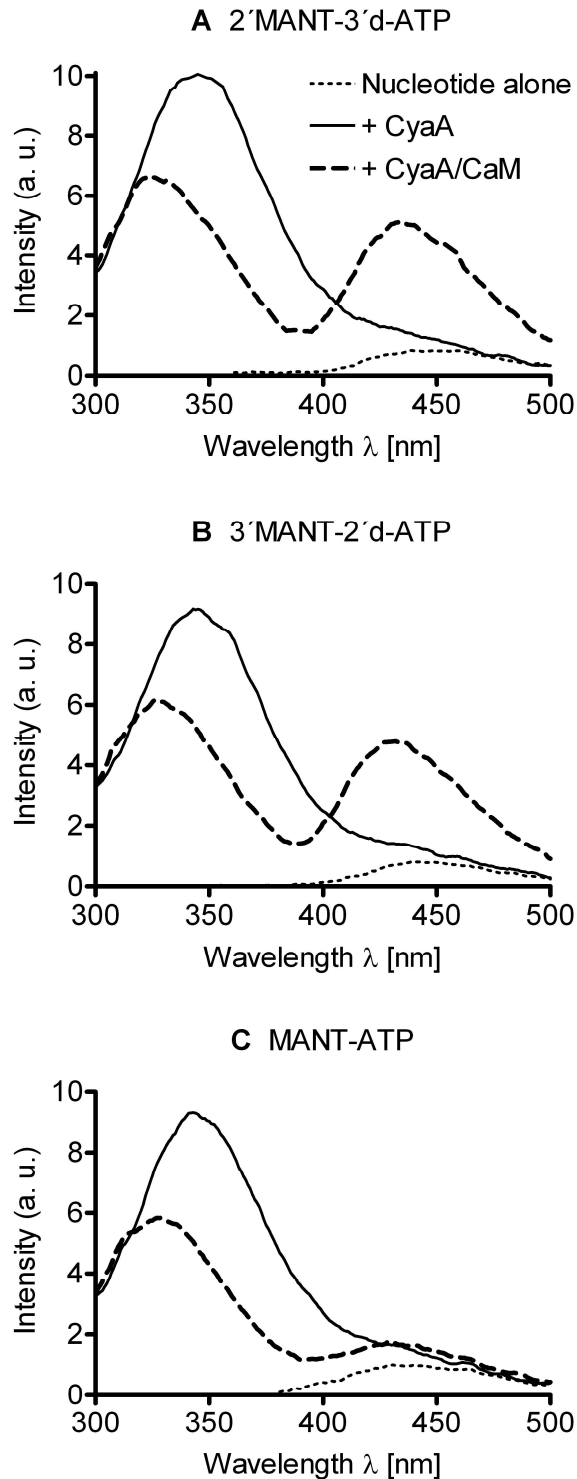
Fig. 1: Monitoring of MANT-nucleotide binding to the catalytic site of CyaA using FRET. The assay buffer consisted of 75 mM Hepes/NaOH, 100 μM CaCl$_2$, 100 mM KCl and 5 mM MnCl$_2$, pH 7.4. Nucleotides (**A:** 2′MANT-3′d-ATP; **B:** 3′MANT-2′d-ATP; **C:** MANT-ATP) were added to the buffer to yield a final concentration of 300 nM, and emission was scanned at an excitation wavelength of 280 nm. CyaA protein and CaM were added in sequence to yield a final concentration of 300 nM. Shown are superimposed recordings of a representative experiment. Similar data were obtained in 3 independent experiments. a.u., arbitrary unit.
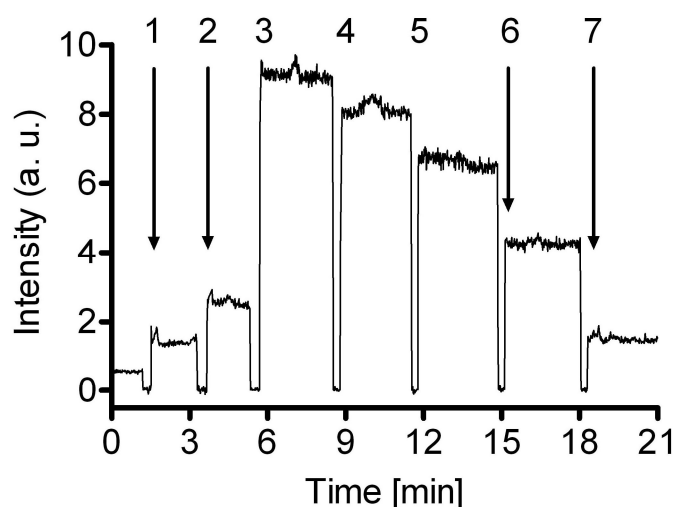
Fig. 2: Time-resolved activation of CyaA by CaM and stepwise abolishment of FRET by PMEApp. Excitation wavelength was 280 nm and emission was detected at 430 nm over time. 300 nM 3′MANT-2′d-ATP (**1**), 300 nM CyaA protein (**2**), 300 nM CaM (**3**) and PMEApp in the given final concentrations (addition steps **4**, 10 nM; **5**, 30 nM; **6**, 70 nM; **7**, 1.6 μM) were added in sequence. A recording of a representative experiment is shown. Similar data were obtained in 4 independent experiments. a.u., arbitrary unit.
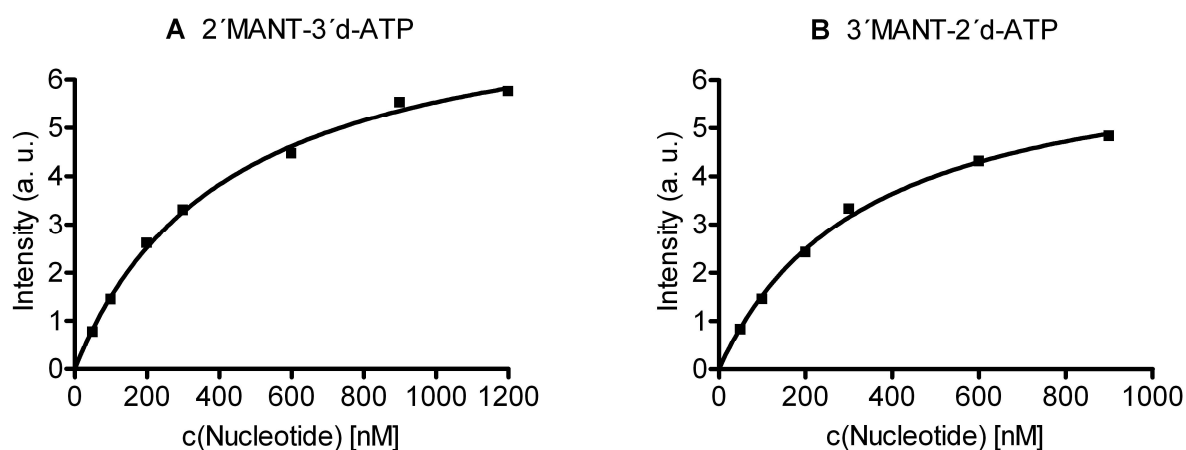
Fig. 3: Saturation curves of 2′MANT-3′d-ATP and 3′MANT-2′d-ATP binding to activated CyaA. Each data point was determined in an independent experiment as described under "Materials and Methods". Final concentrations of CyaA and CaM were 300 nM each. The fluorescence increase at 430 nm was calculated by subtracting the fluorescence at 430 nm after addition of CyaA from the maximal fluorescence at 430 nm after addition of CyaA/CaM. Data were analyzed by non-linear regression using the Prism 4.02 software. Similar data were obtained in 3 independent experiments. a.u., arbitrary unit.

We used CyaA at a final concentration of just 300 nM in an assay volume of 70 μL in FRET studies, corresponding to 0.8 μg of CyaA for one measurement. As the consumption of protein is low, as the production of CyaA can be accomplished at large scale (Shen *et al.*, 2002) and as kinetics occur within seconds (Fig. **2**), fluorimetric high-throughput screening of potential novel inhibitors is feasible, avoiding the use of radioactive AC assays. Since fluorescent nucleotides (e.g. 3´MANT-2´d-ATP) were competitively displaced from CyaA by PMEApp (Fig. **2**), the affinity of non-labeled inhibitors may also be estimated using this approach. In saturation experiments (Fig. **3**), apparent K_d values were estimated to be 400 nM for 2´MANT-3´d-ATP (**A**) and 300 nM for 3´MANT-2´d-ATP (**B**). The results from FRET experiments are in good agreement with the corresponding K_i values determined in the AC activity assay (Tab. **1**).

3.4.5 Direct Fluorescence Experiments with MANT-Nucleotides

Nucleotides were excited at 350 nm and emission was scanned from 380 nm to 550 nm. Addition of CyaA to cuvettes containing 2´MANT-3´d-ATP or 3´MANT-2´d-ATP did not increase their intrinsic fluorescence (Fig. **4, A** and **B**). However, upon addition of CaM, fluorescence increased by 120% and 130%, respectively. Moreover, the emission maximum of 2´MANT-3´d-ATP and 3´MANT-2´d-ATP showed a shift to shorter wavelengths (blue shift). Under these conditions, MANT-ATP fluorescence increased by only approximately 40% (data not shown). For comparison, direct fluorescence of nucleotides was determined in a polar environment (water) and a hydrophobic environment [30% (v/v) dimethyl sulfoxide]. Fluorescence of 100 nM 3´MANT-2´d-ATP increased by 160% when exposed to dimethyl sulfoxide (Fig. **4C**). In addition, the emission maximum shifted to shorter wavelengths. Thus, binding of MANT-nucleotides to CyaA transferred the MANT-group into a hydrophobic environment, probably facilitating interaction with F306 (Guo *et al.*, 2005).

A 2′MANT-3′d-ATP

B 3′MANT-2′d-ATP

C 3′MANT-2′d-ATP
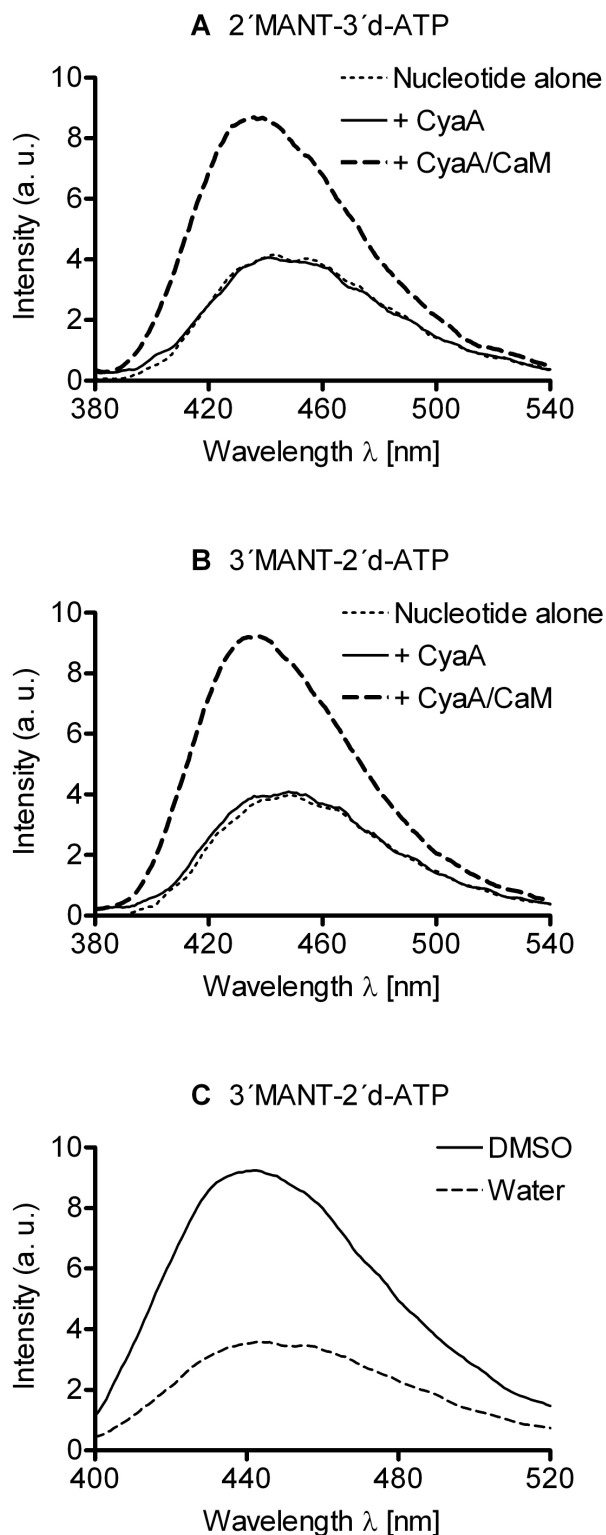
Fig. 4: Direct fluorescence of MANT-nucleotides. The excitation wavelength was 350 nm, and emission was scanned from 380 nm to 550 nm. 100 nM nucleotide, 2.4 μM CyaA and 2.4 μM CaM were added to cuvettes (**A**) and (**B**) in sequence. To mimic binding of the MANT-group to a hydrophobic binding pocket, 3′MANT-2′d-ATP was directly excited in water plus dimethyl sulfoxide (DMSO) 30% (v/v) (**C**). Shown are superimposed recordings of a representative experiment. Similar data were obtained in 5 independent experiments. a.u., arbitrary unit.

3.4.6 Fluorescence Experiments with TNP-Nucleotides

When excited at a wavelength of 405 nm, TNP-ATP, TNP-GTP, TNP-CTP and TNP-UTP showed a fluorescence peak at ~550 nm (Fig. **5**) The addition of CyaA to cuvettes containing TNP-nucleotides increased fluorescence 3- to 5-fold, with TNP-ATP and TNP-GTP showing the largest increases (Fig. **5, A** and **B**). The fluorescence increases with TNP-nucleotides were virtually instantaneous after CyaA addition (data not shown), indicative for rapid nucleotide/protein interaction. Moreover, we observed a blue-shift of the emission maximum of TNP-nucleotides to ~540 nm. These data indicate that binding of TNP-nucleotides to CyaA transfers the TNP-group into a hydrophobic environment. Furthermore, and in striking contrast to the results obtained with MANT-nucleotides (Figs. **2**-**4**), addition of CaM to CyaA reduced TNP-nucleotide fluorescence. This reduction in fluorescence was dependent on the specific nucleotide studied; TNP-ATP showed the smallest relative reduction (Fig. **5A**), and TNP-CTP and TNP-UTP showed the largest relative reductions (Fig. **5, C** and **D**).
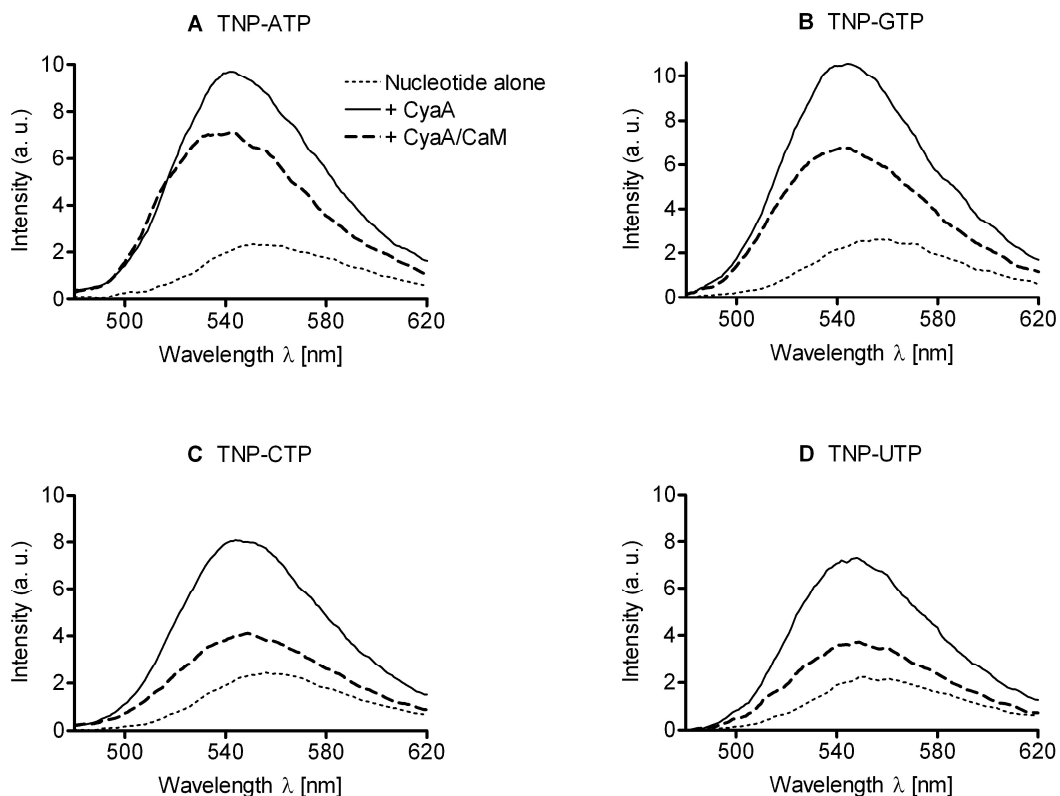
Fig. 5: Fluorescence analysis of the interactions of TNP-nucleotides with CyaA. The excitation wavelength was 405 nm, and emission was scanned from 480 nm to 620 nm. 5 μM nucleotide, 5 μM CyaA and 5 μM CaM were added to the cuvette in sequence. **A:** TNP-ATP; **B:** TNP-GTP; **C:** TNP-CTP; **D:** TNP-UTP. Shown are superimposed recordings of a representative experiment. Similar data were obtained in 3-5 independent experiments. a.u., arbitrary unit.

3.4.7 Modeling of the Binding Modes of MANT- and TNP-Nucleotides to CyaA

The crystal structure of CyaA in complex with CaM and PMEApp (Guo *et al.*, 2005) offered us the possibility to predict the binding mode of MANT- and TNP-nucleotides. The AC domain of CyaA contains the catalytic site at the interface of two structural domains, C_A (M1-G61, A187-A364) and C_B (V62-T186). Compared with PMEApp, the substrate ATP and the fluorescent nucleotides are conformationally restricted due to the semirigid ribosyl moiety. However, the spacious cavity between C_A and C_B may accomodate the different scaffolds so that an alignment of the adenine base and the terminal phosphates is possible (Fig. **6A**). It becomes obvious that hydrophobic interactions, especially of the lipophilic edge of the deoxyribosyl moiety with L60 and of the 3′MANT-group with F306, significantly contribute to the binding of 3′MANT-2′d-ATP (**21**) to CyaA (Tab. **1** and Fig. **3B**). In fact, non-substituted NTPs exhibited 5- to 170-fold lower affinities than their MANT-substituted analogs (e.g. ITP *vs.* MANT-ITP), and CyaA-F306A failed to increase the fluorescence signal of 3′ANT-2′d-ATP (Guo *et al.*, 2005).

However, the question arises why PMEApp (**1**) is four orders of magnitude more potent at inhibiting CyaA than the natural and γS-substituted NTPs (**2-7**) if the alignment indicates similar interactions. First, a reasonable superposition of the phosphates and the adenine bases as shown in Fig. **6A** is only possible if the conformation of the nucleotide moiety retains a certain strain of approximately 3 kcal/mol. A complete minimization would displace the adenine base and, in particular, the phosphate groups from their optimal positions. Therefore, the "true" fit must be a balance between conformational strain and binding energy. Second, the ethoxy oxygen of PMEApp strongly interacts with E301 and N304 *via* a water molecule, and the ethylene bridge is also in close contact with the edge of F306.

Fig. **6B** represents the docking of 3′MANT-2′d-ATP (**21**) into CyaA in more detail. The deoxyribosyl ring adopts a 3′-exo conformation like the ribosyl moiety of MANT-ATP in complex with mammalian AC (Mou *et al.*, 2006). The three Mg^{2+} ions are in positions similar to those in the CyaA-PMEApp complex and form the same interactions. Two of them are coordinated with D188 and D190, one additionally with H298, and the third with the α- and β-phosphate. The imidazolyl-NH of H298 may be H-bonded with an oxygen of the α-phosphate. The γ-phosphate contacts the lysine residues K65 and K58 (O-N distances, ~2.8 Å).
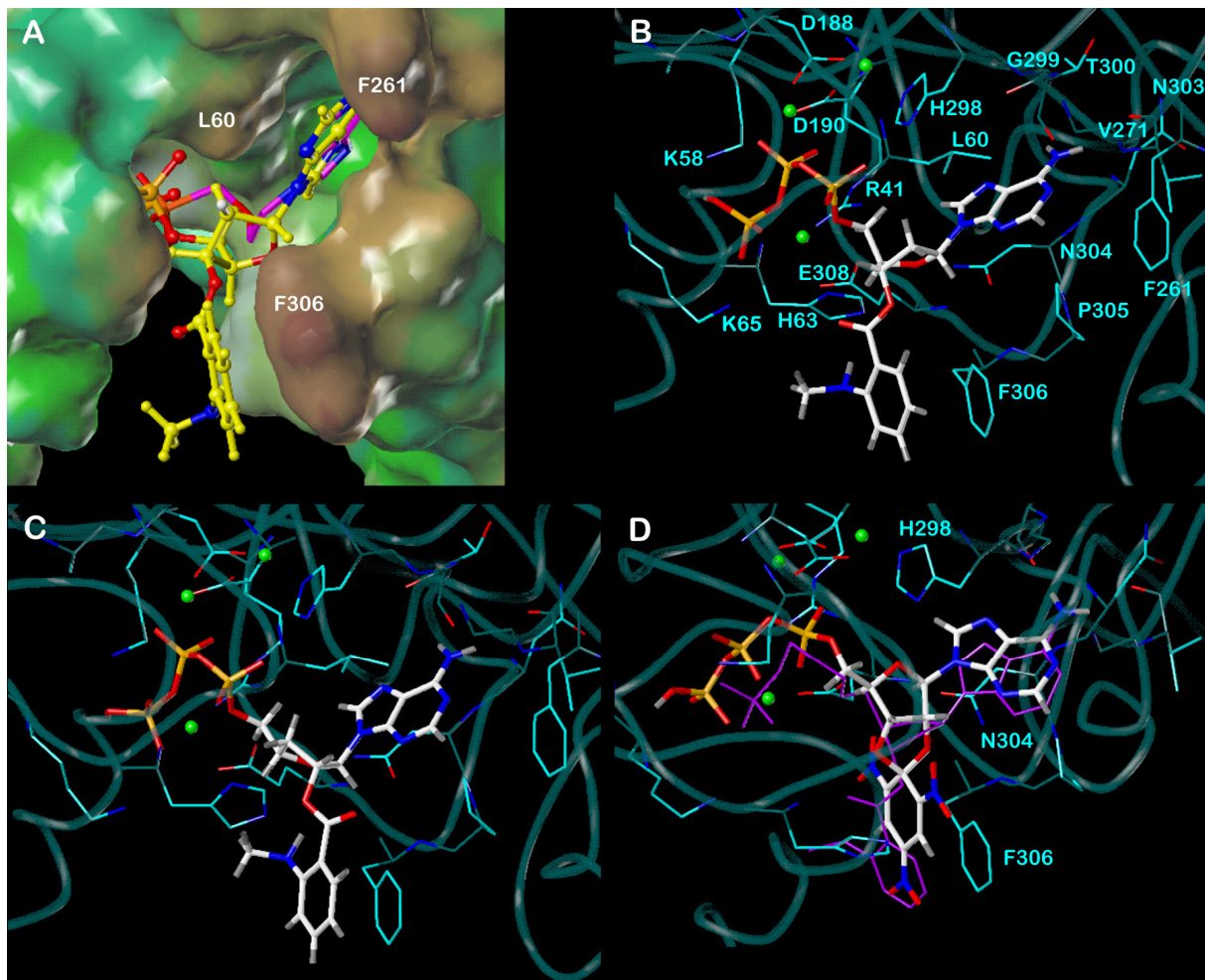
Fig. 6: Docking of representative MANT- and TNP-nucleotides to CyaA. The models are based on the crystal structure of CyaA in complex with PMEApp, PDB 1zot (Guo *et al.*, 2005; Moreland *et al.*, 2005). Colors of atoms, unless otherwise indicated: orange, phosphorous; red, oxygen; blue, nitrogen; white, carbon; green spheres, magnesium. **A:** Overview of the binding site, represented by the lipophilic potential mapped onto a MOLCAD Connolly surface (brown, hydrophobic areas; green and blue, polar areas). Docked ligands: PMEApp (carbon atoms in magenta); 3´MANT-2´d-ATP (carbon and hydrogen atoms in yellow). **B:** Docking of 3´MANT-2´d-ATP (**21**). Amino acids within a sphere of ~3 Å around the ligand are labeled. The protein backbone is schematically represented by a tube. Carbon atoms of the backbone are colored in dark cyan, carbon atoms of the side chains are in light cyan. **C:** Docking of 2´MANT-3´d-ATP (**22**). Representation of the backbone and the side chains as in B. For clarity, some labels are omitted (see B). **D:** Docking of TNP-ATP (**26**). For comparison, 3´MANT-2´d-ATP is shown in the same position like in B (all atoms colored in magenta). Only amino acids with suggested interactions specific for TNP-ATP are labeled. Representation of the backbone and the side chains as in B.

These interactions account for the higher inhibitory potencies of the triphosphates compared with the diphosphate and monophosphate analogs in Tab. **1**. The adenine moiety is sandwiched between the side chains of H298 and N304 whose amide NH_2 group may form an additional H bond with the deoxyribosyl ring oxygen. The 6-amino substituent is in proximity to the backbone oxygens of V271, G299 and T300. However, the loop between G299 and N304 may align all of the nucleobases in similar position. In the case of GTP, ITP, UTP and their MANT- and TNP-derivatives, backbone NH functions of, for example, G299 and V271 could serve as hydrogen donors for the carbonyl oxygens in 6 and 4 position, respectively. This diversity of possible interactions may account for the relatively small and inconsistent potency differences when comparing the impact of base substitution in different subsets of nucleotides [i.e., natural NTPs, MANT-NTPs, MANT-NDPs and TNP-NTPs (see Tab. **1**)]. In addition, the affinity of each nucleotide may be affected by a specific arrangement of water molecules that cannot be simply transferred from the PMEApp-bound CyaA structure.

Fig. **6B** also shows that the high potency of 3′MANT-2′d-ATP (**21**) is particularly due to ideal stacking of the phenyl rings of the inhibitor and F306. This stacking also accounts for the efficient FRET and direct fluorescence observed with 3′MANT-2′d-ATP (Figs. **1-4**). The axial position of the hydrogen atom corresponding to the 2′-OH group in 3′MANT-ATP suggests that even the 2′,3′di-MANT-ATP derivative will be similarly potent since the 2′-MANT-moiety may fit into a hydrophobic site consisting of P305 and F261.

This site would also be occupied by the 2′-MANT-group in 2′MANT-3′d-ATP (**22**) if the deoxyribosyl ring adopts a 3′-exo conformation. However, similar potencies of the positional isomers **21** and **22** in the AC assay (Tab. **1**) and fluorescence assay (Fig. **3**) as well as similar magnitudes of FRET and direct fluorescence (Figs. **1** and **4**) rather indicate analogous interactions between the MANT-group and F306 in the complexes of CyaA with 2′MANT-3′d-ATP and 3′MANT-2′d-ATP, respectively. Fig. **6C** illustrates that docking of 2′MANT-3′d-ATP may indeed reproduce the interaction pattern of 3′MANT-2′d-ATP with CyaA shown in Fig. **6B**. The only difference is a 3′-endo conformation of the deoxyribosyl moiety as is present, e.g., in A-DNA.

Fig. **6D** shows the predicted binding mode of TNP-ATP (**26**) which has a potency similar to that of the isomerizing MANT-ATP derivative (**8**). Despite the rigidity of the tricyclic TNP-ATP scaffold containing a spiro junction, a sufficient alignment with 3´MANT-2´d-ATP is possible so that the phosphate groups, the adenine base, and the phenyl moieties may interact with the same CyaA sites. This superposition implies a relatively deep position of TNP-ATP in the cavity. The interaction of F306 with the TNP-group is weaker than with MANT (no optimal position, lower hydrophobicity). However, hydrogen bonds of two ribosyl oxygens with the side chains of H298 and N304, respectively, may counterbalance, in part, the reduced hydrophobic interactions and higher conformational strain. In addition, the intrinsic fluorescence properties of TNP-nucleotides, i.e. higher fluorescence increases upon transfer into a hydrophobic environment than with MANT-nucleotides (Jameson and Eccleston, 1997; Hiratsuka, 2003), more than compensate for the suboptimal positioning of the TNP-group relative to F306 (Figs. **4** and **5**). It is noteworthy that the inhibitory potency of TNP-derivatives **26-29** is more dependent on the specific nucleobase than in the corresponding subseries of MANT-nucleotides **8**, **10**, **14** and **15** and the non-substituted NTPs GTP (**2**), CTP (**5**) and UTP (**6**). The rigid scaffold of the TNP-nucleotides probably does not enable an optimal fit of guanine and the pyrimidines to the backbone of the loop between G299 and N304.

The lower substrate K_m and V_{max} values as well as the generally 5- to 40-fold higher potency of the inhibitors under Mn^{2+}-conditions than under Mg^{2+}-conditions clearly point to considerably tighter binding with the former cation. This increase in the free energy of binding of up to ~2 kcal/mol should be due mainly to stronger Mn^{2+}-phosphate binding. No further conclusions can be drawn from the docking approaches based on force field methods and without a CyaA crystal structure with Mn^{2+} instead of Mg^{2+}.

3.5   Discussion

3.5.1   Spacious Catalytic Site of CyaA

The catalytic site of CyaA forms a large cavity with substantial conformational freedom to accommodate structurally diverse ligands. In particular, not only adenine nucleotides, but also other purine and even pyrimidine nucleotides reduce the catalytic activity of CyaA (Tab. **1**) because of flexible fit to the backbone of the loop between G299 and N304 (Fig. **6**). Effective interaction of CyaA with purine and pyrimidine nucleotides is also clearly documented in the fluorescence experiments with TNP-ATP, TNP-GTP, TNP-CTP and TNP-UTP (Fig. **5**), monitoring interaction of the TNP-group with F306 (Fig. **6D**). The distinct fluorescence responses upon interaction of CyaA with various TNP-nucleotides in the absence and presence of CaM are indicative for slightly different orientations of TNP-nucleotides in the catalytic site of CyaA. Moreover, various MANT-nucleotides (**12**-**15**) exhibiting higher affinity for CyaA than TNP-nucleotides (Tab. **1**) did not give rise to FRET with CyaA. These findings suggest that differences in affinity do not account for the different fluorescence responses with various nucleotides. Rather, the differences in fluorescence properties point to differences in orientation of the nucleotides in the catalytic site. Taken together, all those findings are in accordance with the modeling data and support the notion of a spacious catalytic site of CyaA.

3.5.2   Towards the Development of Selective CyaA Inhibitors

Because the inhibitory profile of CyaA differs considerably from that of mammalian ACs (Gille *et al.*, 2004; Mou *et al.*, 2005, 2006), development of more potent and selective CyaA inhibitors is feasible. For all inhibitors studied, the TNP-substituent was substantially less effective in increasing nucleotide affinity than MANT/ANT. Whereas ANT-ATP was more potent than MANT-ATP, the MANT-group was superior to ANT in case of MANT-GTP *vs.* ANT-GTP. The additional methyl group in MANT compared with ANT may reduce mobility of the fluorescent group and, thereby, facilitate alignment with F306, depending on the specific nucleobase present.

For all MANT-NDP/NTP pairs studied so far, elimination of the γ-phosphate group substantially decreased inhibitor affinity. As an example, MANT-IDP (**18**) was almost 20-fold less potent than MANT-ITP (**12**), and the omission of the β-phosphate

in MANT-IMP (**30**) further reduced affinity compared with MANT-IDP. The importance of the polyphosphate chain for effective interaction of nucleotides with the catalytic site is also supported by our modeling data (Fig. **6B**). For future applications of MANT-nucleotides in intact-cell assays, nucleotides with a phosphate tail resistant to hydrolysis are needed (Rottländer *et al.*, 2007). As the potency of γS-substituted MANT-nucleotides was higher in case of MANT-ATPγS *vs.* MANT-ATP and MANT-GTPγS *vs.* MANT-GTP, the design of potent nucleotides resistant to hydrolysis is feasible.

An unexpected side product in our synthesis scheme of MANT-ITP (**12**) was di-MANT-IMP (**31**). Even more unexpectedly, addition of a second MANT-group to the ribosyl ring in di-MANT-IMP (**31**) caused an increase in affinity compared with MANT-IMP (**30**) under Mn^{2+}- and Mg^{2+}-conditions (Tab. **1**) that may be attributed to interactions of the 2′MANT-group with a hydrophobic site consisting of P305 and F261 (Fig. **6B**). Thus, the introduction of a second MANT-/ANT-group or other bulky substituents should be considered in future inhibitor design projects to increase inhibitor affinity. In addition, given the surprising differences in fluorescence responses between MANT- and TNP-nucleotides, di-MANT-nucleotides may provide valuable conformational probes to better understand the mechanisms of CyaA activation.

Considering the bases, hypoxanthine is superior to other purine and pyrimidine bases (Tab. **1**). Moreover, 2′MANT-3′d-ATP and 3′MANT-2′d-ATP are considerably more potent than MANT-ATP. Therefore, 2′MANT-3′d-ITP and 3′MANT-2′d-ITP are interesting future candidates as potential novel CyaA inhibitors. Further increase in potency and selectivity of PMEApp may be achieved by changing the adenine base to hypoxanthine and by introducing a MANT-/ANT-substituent.

Like CyaA, *Bacillus anthracis* AC toxin edema factor also bears a phenylalanine residue close to the catalytic site (Guo *et al.*, 2005). Structural comparison of CyaA with edema factor revealed that F306 of CyaA is the analog of F586 in edema factor, forming hydrophobic interactions with the MANT-group, thus increasing direct fluorescence of MANT-nucleotides. The inhibitory profile of edema factor differs considerably from that of CyaA. In particular, MANT-ATP inhibits the catalytic activity of CyaA with almost 25-fold lower potency than catalysis by edema factor (Gille *et al.*, 2004). In case of 3′MANT-2′d-GTP, 3′MANT-2′d-ATP and MANT-ADP, the decreases in potency of CyaA inhibition compared to edema factor

inhibition were 22-fold, 25-fold and 40-fold, respectively. Based on these differences in enzymological properties, it is also reasonable to assume that the fluorescence analysis of edema factor with MANT- and TNP-nucleotides will give very different results than with CyaA.

We have solved the crystal structure of mammalian C1:C2 AC in complex with MANT-GTP, MANT-ATP and TNP-ATP (Mou *et al.*, 2005, 2006). Based on crystallographic studies, we have developed a tripartite model for mammalian AC with a binding site for the base, the ribosyl substituent and the phosphate tail (Mou *et al.*, 2005, 2006). In this model, the base site possesses the smallest influence, whereas the ribosyl substituent has a strong impact. This model can also be applied to CyaA (Fig. **6**). Specifically, a variety of purine and pyrimidine nucleotides inhibit CyaA, suggesting that the base does not greatly determine the potency of 2´,3´-ribosyl substituted inhibitors. In contrast, introduction of a MANT-/ANT-group increased inhibitor potency at CyaA up to 170-fold (e.g. ITP *vs.* MANT-ITP), pointing to the critical importance of the ribosyl substituent. However, TNP-substitution showed a much smaller effect on inhibitor affinity for CyaA than for C1:C2 (Mou *et al.*, 2006) (Tab. **1**), highlighting the substantial structural differences between the binding. In particular, mammalian AC possesses a large hydrophobic pocket consisting of several amino acids accommodating the 2´,3´-ribosyl substituent (Mou *et al.*, 2005, 2006), whereas in case of CyaA, just one amino acid, F306, participates in hydrophobic interactions with MANT- and TNP-nucleotides (Fig. **6**).

3.5.3   The Role of Divalent Cations

It is also important to emphasize that in future studies, inhibitors should be studied both under Mg^{2+}- and Mn^{2+}-conditions because there are differences in the rank order of potency of compounds under those conditions. Moreover, exchange of Mn^{2+} against Mg^{2+} increases V_{max} and K_m (Tab. **1**). Crystallographic studies are required to understand those substantial differences between Mn^{2+} and Mg^{2+}. It is reasonable to assume that under physiological conditions, Mg^{2+} rather than Mn^{2+} is relevant. It is most likely that Mn^{2+} is only an (important) experimental tool to facilitate molecular analysis of CyaA. In particular, in the presence of Mg^{2+}, detection of significant increases in FRET and direct fluorescence with MANT-nucleotides was impossible (data not shown).

3.5.4 CaM-Independent Interaction of CyaA with Nucleotides

The fact that fluorescence of TNP-nucleotides increased upon interaction with CyaA in the absence of the activator CaM (Fig. **5**) indicates that the nucleotide binding site of CyaA is already functional in the catalytically inactive toxin. However, our data suggest that CyaA does not bind MANT-nucleotides in the absence of CaM, because FRET and direct fluorescence with MANT-nucleotides was completely dependent on CaM (Figs. **1-4**). In contrast to CyaA, mammalian C1:C2 does bind MANT-nucleotides, to some extent, in the absence of the activator forskolin (Mou *et al.*, 2005, 2006), again supporting the concept of substantial structural differences between mammalian and bacterial AC. These data also imply that binding of CaM to CyaA induces a conformational change in the toxin that allows MANT-nucleotides to bind. The identification of the precise nature of this conformational change requires crystallization of CyaA complexes with TNP-nucleotides in the absence and presence of CaM as well as of CyaA with MANT-nucleotides in the presence of CaM. The opposite fluorescence responses of TNP-nucleotides and MANT-nucleotides to CaM are in agreement with the modeling studies showing that the TNP- and MANT-groups adopt similar but not identical positions in the catalytic site of CyaA (Fig. **6D**). The dramatic differences in fluorescence responses of TNP- and MANT-nucleotides in the absence and presence of CaM also demonstrate that these nucleotides are extremely sensitive probes for detecting small differences in nucleotide/CyaA interactions.

Another implication of the CaM-independent binding of TNP-nucleotides to CyaA is that the catalytic site of CyaA possesses different binding properties than the site in the presence of CaM, offering additional possibilities for inhibitor design and increasing inhibitor selectivity. Comparison of inhibition profiles of non-fluorescent nucleotides on TNP-nucleotide fluorescence bound to CyaA in the absence and presence of CaM is a feasible approach. With respect to catalysis, such comparison is impossible because enzymatic activity obligatorily depends on CaM (Ladant and Ullmann, 1999; Shen *et al.*, 2002).

3.5.5 Conclusions

In the present study, we have shown that the catalytic site of CyaA possesses unique pharmacological properties compared to other mammalian and bacterial ACs. The spacious catalytic site of CyaA accommodates a broad variety of 2´,3´-substituted nucleotides, even di-MANT-nucleotides. Some inhibitors can bind to CyaA even in the absence of CaM, and there is evidence for distinct interaction of CyaA with MANT-nucleotides and TNP-nucleotides. Finally, the fluorescence assays described in this study can be used for identification of novel CyaA inhibitors, ultimately resulting in the development of novel drugs for prophylaxis of whooping cough.

3.6   References

Ahuja N, Kumar P and Bhatnagar R (2004) The adenylate cyclase toxins. *Crit Rev Microbiol* **30**:187-196.

Boyd AP, Ross PJ, Conroy H, Mahon N, Lavelle EC and Mills KH (2005) *Bordetella pertussis* adenylate cyclase toxin modulates innate and adaptive immune responses: Distinct roles for acylation and enzymatic activity in immunomodulation and cell death. *J Immunol* **175**:730-738.

Carbonetti NH, Artamonova GV, Andreasen C and Bushar N (2005) *Pertussis* toxin and adenylate cyclase toxin provide a one-two punch for establishment of *Bordetella pertussis* infection of the respiratory tract. *Infect Immun* **73**:2698-2703.

Clark M, Cramer RDI and Van Opdenbosch N (1989) Validation of the general purpose tripos 5.2 force field. *J Comp Chem* **10**:982-1012.

Confer DL and Eaton JW (1982) Phagocyte impotence caused by an invasive bacterial adenylate cyclase. *Science* **217**:948-950.

Cornell WD, Cieplak P, Bayly CI, Gould IR, Merz KMJ, Ferguson DM, Spellmeyer DC, Fox T, Caldwell JW and Kollman PA (1995) A second generation force field for the simulation of proteins and nucleic acids. *J Am Chem* **117**:5179-5197.

Ghose AK, Viswanadhan VN and Wendoloski JJ (1998) Prediction of Hydrophobic (Lipophilic) Properties of Small Organic Molecules Using Fragmental Methods: An Analysis of ALOGP and CLOGP Methods. *J. Phys. Chem.* **102**:3762-3772.

Gille A, Lushington GH, Mou TC, Doughty MB, Johnson RA and Seifert R (2004) Differential inhibition of adenylyl cyclase isoforms and soluble guanylyl cyclase by purine and pyrimidine nucleotides. *J Biol Chem* **279**:19955-19969.

Gille A and Seifert R (2003) 2′(3′)-*O*-(*N*-methylanthraniloyl)-substituted GTP analogs: A novel class of potent competitive adenylyl cyclase inhibitors. *J Biol Chem* **278**:12672-12679.

Gilles AM, Munier H, Rose T, Glaser P, Krin E, Danchin A, Pellecuer C and Barzu O (1990) Intrinsic fluorescence of a truncated *Bordetella pertussis* adenylate cyclase expressed in *Escherichia coli*. *Biochemistry* **29**:8126-8130.

Guo Q, Shen Y, Lee YS, Gibbs CS, Mrksich M and Tang WJ (2005) Structural basis for the interaction of *Bordetella pertussis* adenylyl cyclase toxin with calmodulin. *EMBO J* **24**:3190-3201.

Heiden W, Moeckel G and Brickmann J (1993) A new approach to analysis and display of local lipophilicity/hydrophilicity mapped on molecular surfaces. *J Comput Aided Mol Des* **7**:503-514.

Hewlett EL, Donato GM and Gray MC (2006) Macrophage cytotoxicity produced by adenylate cyclase toxin from *Bordetella pertussis*: More than just making cyclic AMP! *Mol Microbiol* **59**:447-459.

Hewlett EL, Gordon VM, McCaffery JD, Sutherland WM and Gray MC (1989) Adenylate cyclase toxin from *Bordetella pertussis*. Identification and purification of the holotoxin molecule. *J Biol Chem* **264**:19379-19384.

Hiratsuka T (1983) New ribose-modified fluorescent analogs of adenine and guanine nucleotides available as substrates for various enzymes. *Biochim Biophys Acta* **742**:496-508.

Hiratsuka T (2003) Fluorescent and colored trinitrophenylated analogs of ATP and GTP. *Eur J Biochem* **270**:3479-3485.

Jameson DM and Eccleston JF (1997) Fluorescent nucleotide analogs: Synthesis and applications. *Methods Enzymol* **278**:363-390.

Johnson RA and Shoshani I (1990) Inhibition of *Bordetella pertussis* and *Bacillus anthracis* adenylyl cyclases by polyadenylate and "P"-site agonists. *J Biol Chem* **265**:19035-19039.

Ladant D and Ullmann A (1999) *Bordetella pertussis* adenylate cyclase: A toxin with multiple talents. *Trends Microbiol* **7**:172-176.

Lakowicz JR (1999) *Principles of fluorescence spectroscopy*. Kluwer Academic/Plenum, New York.

Mock M and Ullmann A (1993) Calmodulin-activated bacterial adenylate cyclases as virulence factors. *Trends Microbiol* **1**:187-192.

Moreland JL, Gramada A, Buzko OV, Zhang Q and Bourne PE (2005) The Molecular Biology Toolkit (MBT): A modular platform for developing molecular visualization applications. *BMC Bioinformatics* **6**:21.

Mou TC, Gille A, Fancy DA, Seifert R and Sprang SR (2005) Structural basis for the inhibition of mammalian membrane adenylyl cyclase by 2´(3´)-*O*-(*N*-methylanthraniloyl)-guanosine 5´-triphosphate. *J Biol Chem* **280**:7253-7261.

Mou TC, Gille A, Suryanarayana S, Richter M, Seifert R and Sprang SR (2006) Broad specificity of mammalian adenylyl cyclase for interaction with 2´,3´-substituted purine- and pyrimidine nucleotide inhibitors. *Mol Pharmacol* **70**:878-886.

Rottländer D, Matthes J, Vatner SF, Seifert R and Herzig S (2007) Functional adenylyl cyclase inhibition in murine cardiomyocytes by 2´(3´)-*O*-(*N*-methylanthraniloyl)-guanosine 5´-[γ-thio]triphosphate. *J Pharmacol Exp Ther* **321**:608-615.

Sarfati RS, Kansal VK, Munier H, Glaser P, Gilles AM, Labruyere E, Mock M, Danchin A and Barzu O (1990) Binding of 3´-anthraniloyl-2´-deoxy-ATP to calmodulin-activated adenylate cyclase from *Bordetella pertussis* and *Bacillus anthracis*. *J Biol Chem* **265**:18902-18906.

Shen Y, Lee YS, Soelaiman S, Bergson P, Lu D, Chen A, Beckingham K, Grabarek Z, Mrksich M and Tang WJ (2002) Physiological calcium concentrations regulate calmodulin binding and catalysis of adenylyl cyclase exotoxins. *EMBO J* **21**:6721-6732.

Shen Y, Zhukovskaya NL, Zimmer MI, Soelaiman S, Bergson P, Wang CR, Gibbs CS and Tang WJ (2004) Selective inhibition of anthrax edema factor by adefovir, a drug for chronic hepatitis B virus infection. *Proc Natl Acad Sci USA* **101**:3242-3247.

Soelaiman S, Wei BQ, Bergson P, Lee YS, Shen Y, Mrksich M, Shoichet BK and Tang WJ (2003) Structure-based inhibitor discovery against adenylyl cyclase toxins from pathogenic bacteria that cause anthrax and whooping cough. *J Biol Chem* **278**:25990-25997.

Chapter 4

Nucleotidyl Cyclase Activity
of *Bacillus anthracis* Exotoxin, Edema Factor,
and *Bordetella pertussis* Exotoxin, CyaA

4.1   Abstract

Cyclic adenosine 3′:5′-monophosphate (cAMP) and cyclic guanosine 3′:5′-monophosphate (cGMP) are key second messengers for a wide variety of mammalian cellular processes. The natural occurrence of a third cyclic nucleotide, cyclic cytidine 3′:5′-monophosphate (cCMP) had been discussed very controversially 30-35 years ago, but later, cCMP was identified unambiguously in various mammalian tissues indicating cCMP to be a novel second messenger with potential importance in regulation of cell growth, proliferation, tissue development and modulation of immune responses. However, the precise identity of the cCMP-forming enzyme in mammalian cells is still unclear. Here, for the first time, we provide evidence for cytidylyl cyclase (CC) activity of purified bacterial exotoxins. *Bacillus anthracis* and *Bordetella pertussis*, the causative bacteria of anthrax disease and whooping cough, respectively, secrete the adenylyl cyclase (AC) toxins edema factor (EF) and CyaA, weakening immune responses through massive cAMP production and, thereby, promoting the pathogenesis of the infections. We found that both toxins also possess CC activity, resulting in the conversion of CTP to cCMP. In our CC activity assay, the radioactively labeled substrate [α-^{32}P]CTP is converted to [^{32}P]cCMP which is quantified by liquid scintillation. Upon incubation of the toxins with [α-^{32}P]CTP, [^{32}P]cCMP is produced in a linear manner over time. As [^{32}P]cCMP production depends on the endogenous toxin activator protein calmodulin, as physiological pH promotes the reaction and as potent AC inhibitors show high potency on EF and CyaA, catalysis results from specific CC activity. Michaelis-Menten kinetics of EF CC activity yielded $K_m = 13 \pm 3$ μM and $V_{max} = 9 \pm 1$ s^{-1}. When CTP consumption and cCMP formation were monitored by HPLC, 100 μM CTP were converted to cCMP by 20 nM EF within 1 h. In the presence of heat-inactivated enzyme, no cCMP was formed. The identity of cCMP was confirmed by co-eluting standard cCMP in HPLC experiments and by mass spectrometry methods. Based on these findings and the fact that cCMP inhibits host immune responses, we propose that the bacterial exotoxins edema factor (EF) and CyaA generate cCMP, resulting in increased infection severity. The molecular targets of cCMP remain to be determined.

4.2   Introduction

Cyclic adenosine 3´:5´-monophosphate (cAMP) and cyclic guanosine 3´:5´-monophosphate (cGMP) are key second messengers for a wide variety of mammalian cellular processes. The natural occurrence of a third cyclic nucleotide, cyclic cytidine 3´:5´-monophosphate (cCMP) had been discussed very controversially 30-35 years ago. In 1974, Bloch *et al.* first observed that - in contrast to cAMP and cGMP - cCMP initiated the growth of leukemia L-1210 cells in a concentration-dependent manner suggesting that cCMP exerts a growth-regulatory function (Bloch *et al.*, 1974). In 1978, Cech *et al.* reported the identification of cCMP as product of the reaction between mouse liver homogenate, CTP and Mn^{2+} using chromatography on neutral alumina columns for the separation of potential cCMP from other nucleotide species (Cech and Ignarro, 1978). This finding was contradicted in 1979 by Gaion *et al.* who observed a different behaviour of the reaction product obtained according to the method of Cech *et al.* and authentic cCMP in various chromatographic systems, indicating that 5´-CMP and 5´-CDP are the major products, with no cCMP being formed (Gaion and Krishna, 1979).

The natural occurrence of cCMP in various mammalian organs was later confirmed unambiguously using mass spectrometry methods (Newton *et al.*, 1984), and besides cCMP, four novel cytidine cyclic phosphates were identified as biosynthetic products from CTP, providing a feasible explanation of the discrepancies in the reports of Cech *et al.* and Gaion *et al.* (Newton *et al.*, 1988). Further developments in the fields of column chromatography and mass spectrometry revealed the kinetic parameters of the CC reaction; similar CC activities were observed in nine organs of rat, and the CC activity was found to be inversely proportional to the age of the animals (Newton *et al.*, 1990, 1997). cCMP levels in urine obtained from leukemic patients were very much elevated in comparison to normal human samples as determined by radioimmunoassay methods (Newton *et al.*, 1994). The potential importance of cCMP as a regulator of cell function has been emphasized by the discovery of phosphodiesterase activity accounting for the selective degradation of cCMP (Newton *et al.*, 1986, 1999). Furthermore, protein kinase activity responsive to cCMP has been observed (Newton *et al.*, 1992) and ten proteins were identified in brain tissue undergoing phosphorylation due to challenge with cCMP (Bond *et al.*, 2007; Ding *et al.*, 2008).

cCMP may also modulate immune system functions. In macrophages, the cell-permeant cCMP-analog dibutyryl-cCMP inhibited thromboxane B_2 and leukotriene B_4 formation (Elliott *et al.*, 1991). In human neutrophils, dibutyryl-cCMP inhibited superoxide radical formation and the rise in cytosolic Ca^{2+} induced by a chemotactic peptide, resulting in neutrophil inactivation (Ervens and Seifert, 1991). Taken together, these findings point to cCMP being a potential novel second messenger with importance in regulation of cell growth, proliferation, tissue development and modulation of immune responses. However, so far the precise identity of the cCMP-forming cytidylyl cyclase enzyme in mammalian cells is still unclear.

The causative agents of anthrax disease and whooping cough, *Bacillus anthracis* and *Bordetella pertussis*, respectively, exert their deleterious effects by the release of exotoxins interfering with host signal transduction pathways resulting in inhibited immune response (Ahuja *et al.*, 2004; Basler *et al.*, 2006). After interacting with surface receptors of eukaryotic host immune cells and translocating into the cytosol (Ladant and Ullmann, 1999; Mogridge *et al.*, 2002), the AC toxins edema factor (EF) from *B. anthracis* and CyaA from *B. pertussis* bind to calmodulin (CaM), an endogenous calcium sensor, resulting in activation of the AC activity of the toxins (Drum *et al.*, 2000; Gallay *et al.*, 2004; Guo *et al.*, 2005). Both, EF and CyaA catalyze massive synthesis of cAMP leading to excessive intracellular cAMP accumulation and disruption of intracellular signaling pathways. Consequently, host phagocyte, macrophage and dendritic cell function is inhibited rendering the infection more severe (Paccani *et al.*, 2005; Tournier *et al.*, 2005; Hewlett *et al.*, 2006).

Substrate analogs may be used to inhibit the AC activity of EF and CyaA (Johnson and Shoshani, 1990; Soelaiman *et al.*, 2003; Gille *et al.*, 2004) in order to decrease weakening of the immune response and to mitigate the severity of infection. Mammals express nine membranous AC isoforms (mACs 1-9) and a soluble AC. We have used the cytosolic catalytic domains C1 of type 5 AC and C2 of type 2 AC for molecular AC analysis (Gille *et al.*, 2004; Mou *et al.*, 2005, 2006). Serendipitously, we had discovered 2′(3′)-*O*-(*N*-methylanthraniloyl)- (MANT)-substituted NTPs as competitive inhibitors of mammalian ACs and bacterial AC toxins (Gille *et al.*, 2003, 2004). Additionally, PMEApp, the active metabolite of adefovir, a drug for the treatment of chronic hepatitis B virus infection, was identified as a potent inhibitor of EF and CyaA (Shen *et al.*, 2004).

Using crystallographic and molecular modeling approaches, we developed a three-site pharmacophore model for mAC and bacterial AC toxins, with binding domains for the base, the MANT-group and the polyphosphate chain (Mou *et al.*, 2006; Göttle *et al.*, 2007). We resolved several EF and CyaA crystal structures and characterized the amino acids important for nucleotide binding and catalysis (Drum *et al.*, 2002; Guo *et al.*, 2005; Shen *et al.*, 2005). Furthermore, we systematically examined the interactions of natural purine and pyrimidine nucleotides and MANT-substituted analogs with EF and CyaA in terms of catalysis, fluorescence changes and molecular modeling (Göttle *et al.*, 2007; Taha *et al.*, 2009). MANT-CTP was the most potent competitive EF inhibitor among 16 compounds studied, showing unique preference of EF for the base cytosine. Taken together, those studies revealed the catalytic sites of EF and CyaA to exhibit conformational flexibility and to accommodate both purine and pyrimidine nucleotides. Those findings also raised the question whether in addition to ATP, other naturally occurring nucleotides, most importantly CTP, could be substrates for cyclization. Here, for the first time, we unequivocally demonstrate CC activity of the bacterial exotoxins EF and CyaA.

4.3   Materials and Methods

Chemicals and Biochemical Reagents. MANT-substituted nucleoside triphosphates of cytidine, inosine and uridine were synthesized as described (Taha *et al.*, 2009). MANT-ATP, MANT-GTP were from Jena Bioscience, Jena, Germany. [α-^{32}P]ATP (800 Ci/mmol), [α-^{32}P]CTP (800 Ci/mmol) and [α-^{32}P]UTP (800 Ci/mmol) were purchased from PerkinElmer, Wellesley, MA, USA. Aluminum oxide N Super 1 was purchased from MP Biomedicals, Eschwege, Germany. Acetonitrile (LC grade), ammonium acetate (p.A.), $CaCl_2$ dihydrate (p.A.), KCl (p.A.), methanol (LC grade), $MnCl_2$ tetrahydrate and $MgCl_2$ hexahydrate (highest quality), ortho-phosphoric acid (p.A.), sodium acetate (p.A.) and triethylamine were from Merck, Darmstadt, Germany. GTP·2 Na, ATP·2 Na and cAMP were purchased from Roche. cCMP·Na, cGMP·Na, cIMP·Na, cUMP·Na, cTMP·Na were from Biolog, Bremen, Germany. Bovine serum albumin (fraction V), 2´:3´-cCMP·Na, CMP·2 Na, CDP·3 Na, CTP·2 Na, 2´d-CTP·2 Na, EGTA, inosine, ITP·3 Na, TTP·Na, UDP·Na, UMP·Na and UTP·3 Na dihydrate were purchased from Sigma-Aldrich, Seelze, Germany. Tris (ultrapure) was from USB, Cleveland, OH, USA. PMEApp was supplied by Gilead Sciences, Foster City, CA, USA. The full-length AC toxin edema factor (EF) from *B. anthracis* and the catalytic domain of *B. pertussis* AC protein (CyaA, amino acids 1 to 373) were purified as described (Drum *et al.*, 2000, 2001). Lyophilized calmodulin from bovine brain was purchased from EMD Biosciences, Calbiochem, Darmstadt, Germany.

Isotopic Nucleotidyl Cyclase (NC) Assay. For the determination of the potency of AC/CC inhibitors, assay tubes contained 10 μL of inhibitor at final concentrations from 1 nM to 100 μM and 20 μL of EF or CyaA dissolved in 75 mM Hepes/NaOH, pH 7.4, supplemented with 0.1% (m/v) bovine serum albumin to prevent protein adsorption. Final protein concentrations were 10 pM EF or CyaA (AC) and 30 pM (CC). Tubes were preincubated for 2 min and reactions were initiated by the addition of 20 μL of reaction mixture consisting of the following components to yield the given final concentrations: 100 mM KCl, 5 mM free Mn^{2+}, 10 μM free Ca^{2+}, 100 μM EGTA, 100 μM cAMP and 100 nM CaM. In case of AC activity, ATP was added as non-labeled substrate at a final concentration of 40 μM and as radioactive tracer [α-^{32}P]ATP (0.2 μCi/tube). In case of CC activity, CTP was added as non-labeled substrate at a final concentration of 10 μM and as radioactive tracer [α-

^{32}P]CTP (0.4 µCi/tube). Reactions were carried out for 10 min at 25°C (AC) and 20 min at 37°C (CC).

For the determination of K_m and V_{max} values, assay tubes contained 10 µL of NTP/Mn^{2+} or NTP/Mg^{2+} and 20 µL of reaction mixture as described above. NTP/Mn^{2+} or NTP/Mg^{2+} (1 µM to 2 mM) plus 5 mM of free Mn^{2+} or Mg^{2+} were added. Reactions were initiated by the addition of 20 µL of EF or CyaA to yield the following final enzyme concentrations: 10 pM (EF and CyaA AC activities), 40 pM (EF and CyaA CC activities with Mn^{2+}), and 400 pM (EF CC activity with Mg^{2+} and UC activities). The amount of radioactive tracers was [α-^{32}P]ATP (0.2 µCi/tube), [α-^{32}P]CTP (0.8 µCi/tube) and [α-^{32}P]UTP 0.8 µCi/tube. Reactions were carried out for 10 min at 25°C (AC), 20 min at 37°C (CC) and 30 min at 37°C (UC). In saturation experiments using CTP/Mg^{2+} or UTP/Mn^{2+}, no extra non-labeled cyclic nucleotide was added to the reaction mixture. Saturation experiments using CTP/Mn^{2+} were performed in the presence of extra non-labeled cAMP or cCMP (100 µM each), and in the absence of cyclic nucleotide (without yielding significantly different results, data not shown). In saturation experiments using ATP/Mg^{2+} or CTP/Mg^{2+} on EF, 10 mM Tris/HCl were included in addition to the reaction mixture, and 1 mM EGTA and 400 nM free Ca^{2+} were used. In those experiments, the reaction mixture was incubated for 5 min at room temperature prior to the addition of CaM and again for 5 min after the addition of CaM.

Reactions were terminated by the addition of 20 µL of 2.2 N HCl, denaturated protein was sedimented by a 1-min centrifugation at 12,000 x g. [^{32}P]cNMP was separated from [α-^{32}P]NTP by transferring the samples to columns containing 1.4 g of neutral alumina. [^{32}P]cNMP was eluted by the addition of 4 mL 0.1 M ammonium acetate solution, pH 7.0 (Alvarez and Daniels, 1990). Blank values were about 0.02% of the total amount of [α-^{32}P]NTP added; substrate turnover was < 3% of the total added [α-^{32}P]NTP. Samples were filled up with 10 mL Millipore water and Čerenkov radiation was measured in a PerkinElmer Tricarb 2800TR liquid scintillation analyzer. Free concentrations of divalent cations were calculated with WinMaxC (http://www.stanford.edu/~cpatton/maxc.html). K_i values, K_m values and V_{max} values reported in Tab. **1** and **2** were calculated using the Prism 4.02 software (Graphpad, San Diego, CA, USA).

Non-Isotopic Nucleotidyl Cyclase (NC) Assay and HPLC Analysis. Reaction mixtures consisted of the following components to yield the given final concentrations in a total volume of 3 mL: 5 mM Mn^{2+}, 5 μM Ca^{2+}, 30 mM Hepes/NaOH, pH 7.4, 100 μM of the corresponding NTP and CaM at concentrations yielding 1:1 stoichiometry of CaM and bacterial cyclase toxin. Prior to the addition of enzyme, two sample aliquots (300 μL each) were taken as negative controls: One sample aliquot was taken and stored on ice; a second sample aliquot lacking enzyme was taken and incubated in parallel with the reaction batch containing enzyme for 60 min at 37°C. Both, negative controls and reaction samples, later underwent the sample preparation process described subsequently. Assay tubes were preincubated at 37°C for 4 min and reactions were initiated by the addition of 300 μL of EF or CyaA. Final protein concentrations ranged between 20 nM bacterial cyclase toxin and 20 nM CaM up to 1,500 nM bacterial cyclase toxin and 1,500 nM CaM as described in detail in "Results". Samples were taken at reaction times between 1 and 60 min. In order to achieve protein denaturation, sample aliquots (300 μL each) were added to 600 μL of acetonitrile and cooled to 4°C. Threehundred μL of 40 μM inosine were added as internal standard (IS). Denatured protein was sedimented by a 1-min centrifugation at 12,000 x g. In order to achieve separation of the aqueous phase from the organic phase, samples were transferred into 5-mL-vials and 2 mL of dichloromethane were added. Samples were agitated for 20 min at 4°C and centrifuged for 5 min at 1,000 x g. The aqueous phase was transferred into 1.5-mL-vials and stored at -80°C.

Nucleotides were quantified using a Shimadzu HPLC system consisting of a LC-10AT pump, SIL-10A auto-injector and SPD-10AV UV-VIS detector for monitoring nucleotide absorbance at 260 nm. A Phenomenex Synergi® Fusion-RP HPLC column (Phenomenex, Aschaffenburg, Germany), 150 x 4.6 mm, 4 μm particle size, Cat. No. 00F-4424-E0 was eluted with the mobile phase at 1 mL/min. The mobile phase consisted of 100 mM triethylamine with pH set to 6.6 using ortho-phosphoric acid. The mobile phase contained methanol at a concentration of 6% (v/v) in case of cCMP, cUMP and cIMP, 9% (v/v) in case of cGMP and cTMP as well as 12% (v/v) in case of cAMP. The mobile phase was run at 1 mL/min, the temperature of the column oven was 35°C and the injection volume was 5 μL. Standard substances of cCMP, cUMP, cIMP, cGMP, cTMP and cAMP were applied to HPLC analysis, and the resulting retention times were compared to those from the cyclic nucleotides

resulting from enzymatic reaction. Chromatograms were generated and evaluated using the Shimadzu LC solution 1.22 SP1 software.

Mass Spectrometry. LC-MS/MS was performed using an Agilent 1100 HPLC system and a TSQ-7000 Thermoquest Finnigan triple quadrupol mass spectrometer. A Phenomenex Luna C18 Aqua HPLC column (150 x 2 mm, 3 μm particle size) was eluted with the mobile phase at 0.3 mL/min using a gradient of 0.1% formic acid (A) and acetonitrile (B) with 0% B (v/v, min 0 to 2), 80% B (v/v, min 2 to 15), 80% B (v/v, min 15 to 20), 0% B (v/v, min 20 to 25) and 0% B (v/v, min 25 to 35). The autosampler system was cooled to 5°C, the temperature of the column oven was 40°C and the injection volume was 20 μL. Upon ESI (capillary temperature 250°C, ESI spray voltage 4 kV), argon was used for collision-induced dissociation with collision energies of 25 V (cCMP), 15 V (cUMP) and 20 V (cIMP). Selective reaction monitoring in positive mode was performed monitoring m/z transitions of 306.0 to 112.2 (cCMP), of 324.2 to 307.0 (cUMP) and of 330.9 to 137.2 (cIMP). Data were interpreted using the Xcalibur 3.1 software.

4.4 Results

4.4.1 Isotopic Nucleotidyl Cyclase Assay

Incubation of 20 pM EF with 0.4 μCi/tube [α-^{32}P]CTP and 10 μM unlabeled CTP in the presence of 5 mM Mn^{2+} followed by the alumina solid phase extraction procedure described in "Materials and Methods" and by liquid scintillation analysis resulted in a pronounced signal increasing linearly over time (Fig. **1A**). Blank values were generally < 0.02% of the total added amount of [α-^{32}P]CTP indicating full retention of [α-^{32}P]CTP on the column matrix during the solid phase extraction.

By successively increasing the enzyme concentration, the resulting signal increased proportionally (Fig. **1B**), pointing to dependence of the signal on the amount of purified enzyme added. As shown in Fig. **1C**, the signal intensity showed considerable dependence on pH with the highest intensity obtained at physiological pH values and poor intensities at low pH values (pH 6.0) or high pH values (pH 9.0). At pH 5.0, liquid scintillation did not show significantly higher signals as compared to blank values obtained from negative controls lacking enzyme, indicating that no conversion of [α-^{32}P]CTP occurred at this pH.

In order to investigate if the detected signal resulted from enzymatic conversion of [α-^{32}P]CTP by the ACs applied, the EF and CyaA activator CaM was added in increasing concentrations yielding concentration-response curves with EC$_{50}$ values of 670 ± 50 pM in case of EF (Fig. **1D**) and 80 ± 5 pM in case of CyaA (data not shown). In the absence of CaM, 40 pM EF increased the detected signal 3-fold compared with blank values obtained in the absence of enzyme. With 100 nM CaM and 40 pM EF, the detected signal was stimulated up to 200-fold compared with blank values obtained in the absence of enzyme. Thus, CaM considerably stimulated [α-^{32}P]CTP conversion by EF, but a clear turnover was also observed in the absence of CaM. Similar results were obtained with CyaA (data not shown). Our preliminary experiments indicated very poor enzymatic activity of EF on 2´d-CTP as compared to CTP, pointing to importance of the hydroxyl group at 2´-ribosyl position for catalysis (data not shown). Using UTP as substrate and [α-^{32}P]UTP as radioactive tracer, signals from liquid scintillation were also detected as shown below.
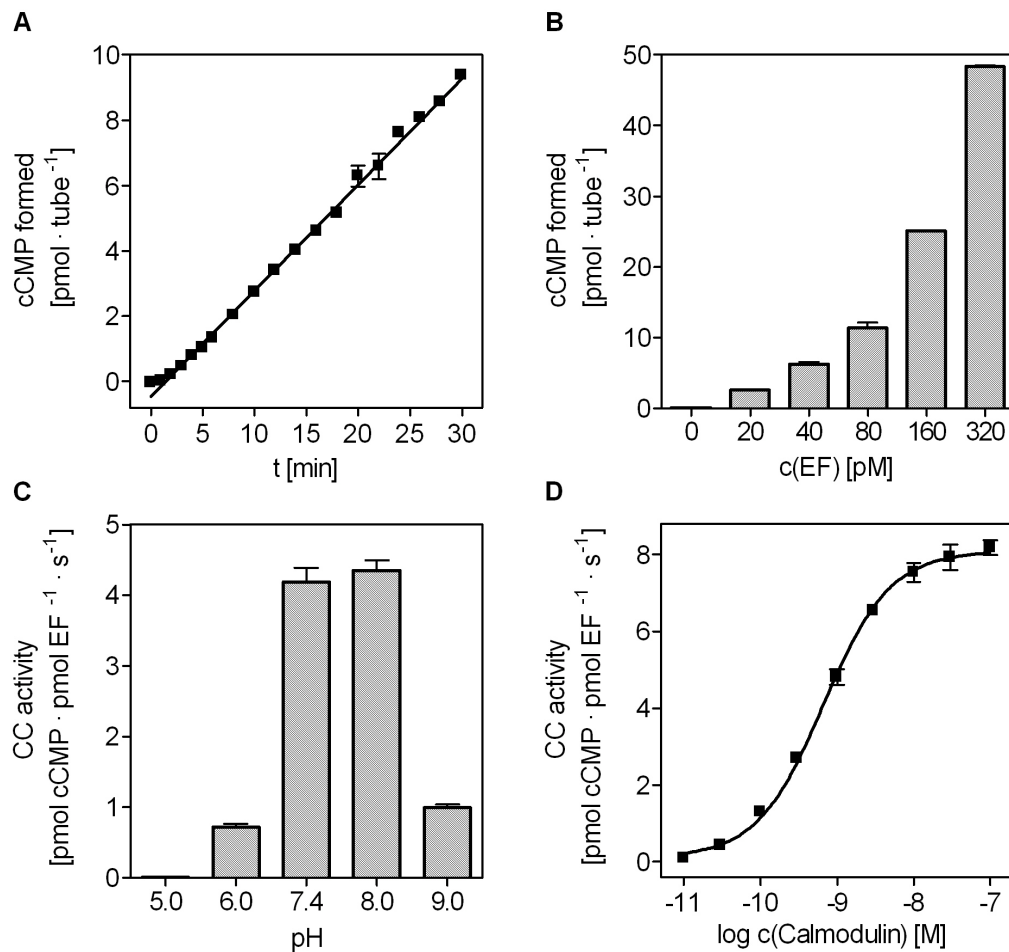
Fig. 1: Signals obtained using the isotopic EF cytidylyl cyclase assay. Reactions were carried out for 20 min at 37°C as described in "Materials and Methods". **A:** Time course experiment using 20 pM EF. Reaction mixtures contained the following components to yield the given final concentrations: 100 mM KCl, 5 mM Mn^{2+}, 10 μM free Ca^{2+}, 100 μM EGTA, 10 μM CTP, [α-^{32}P]CTP (0.4 μCi/tube), 100 nM CaM. **B:** Signal dependence on EF protein concentration. Reaction mixtures contained EF at various concentrations, the components listed under A and additionally 100 μM cAMP. **C:** Dependence of CC activity on pH. Reaction mixtures contained 80 pM EF and the components listed under B. Buffering systems were 30 mM sodium acetate·HCl (pH 5.0 and pH 6.0), 30 mM Hepes/NaOH (pH 7.4) and 30 mM Tris/HCl (pH 8.0 and pH 9.0). **D:** Activation of CC activity by CaM. Reaction mixtures contained 5 mM Mn^{2+}, 10 μM free Ca^{2+}, 100 μM EGTA, 10 μM CTP, [α-^{32}P]CTP (0.4 μCi/tube), 40 pM EF and CaM at various concentrations. Data shown are means ± SD of representative experiments performed in duplicates; similar results were obtained in at least 3 independent experiments.

4.4.2 Solid Phase Extraction of Cytosine and Uracil Nucleotides and HPLC Analysis

In order to ensure complete retention of the starting material $[\alpha\text{-}^{32}P]NTP$ on the alumina columns during solid phase extraction, and in order to determine recovery values for the product $[^{32}P]cNMP$, mixtures of non-labeled nucleotides were subjected to solid phase extraction (SPE) and HPLC analysis as described in "Materials and Methods". Prior to SPE, HPLC chromatograms from nucleotide mixtures show peaks from 15 μM CMP, CDP, CTP and 3´:5´-cCMP (Fig. **2A**, dashed line) as well as from 15 μM UMP, UDP, UTP and 3´:5´-cUMP (Fig. **2B**, dashed line). After SPE, 3´:5´-cCMP and 3´:5´-cUMP were eluted while the signals from acyclic nucleotides were missing. The recovery values were 70% in case of 3´:5´-cCMP and 50% in case of 3´:5´-cUMP. Therefore, the SPE procedure used in this work completely retained acyclic nucleotides on the alumina columns while cyclic pyrimidine nucleotides were eluted. Thus, the signals detected by liquid scintillation in the isotopic NC assay can only result from cyclic nucleotides; non-specific signals from acyclic nucleotides can be excluded.

In order to ensure that the cyclic nucleotides formed enzymatically were of 3´:5´-cNMP structure and not of the also naturally occurring 2´:3´-cNMP structure, we applied 15 μM 3´:5´-cCMP and 2´:3´-cCMP to SPE and HPLC analysis. As shown in Fig. **2C**, a peak from 2´:3´-cCMP at a retention time of 3.3 min was detected while the retention time of 3´:5´-cCMP was 8.2 min. Both nucleotides were eluted in SPE with recoveries of about 70%. Therefore, 3´:5´-cNMP and 2´:3´-cNMP isomers could easily be discriminated based on their retention times, and cyclic nucleotides with 2´:3´-cNMP structure were never detected in enzymatic reactions within this project. The term "cNMP" used in this work thus always refers to 3´:5´-cNMP, if not stated otherwise.
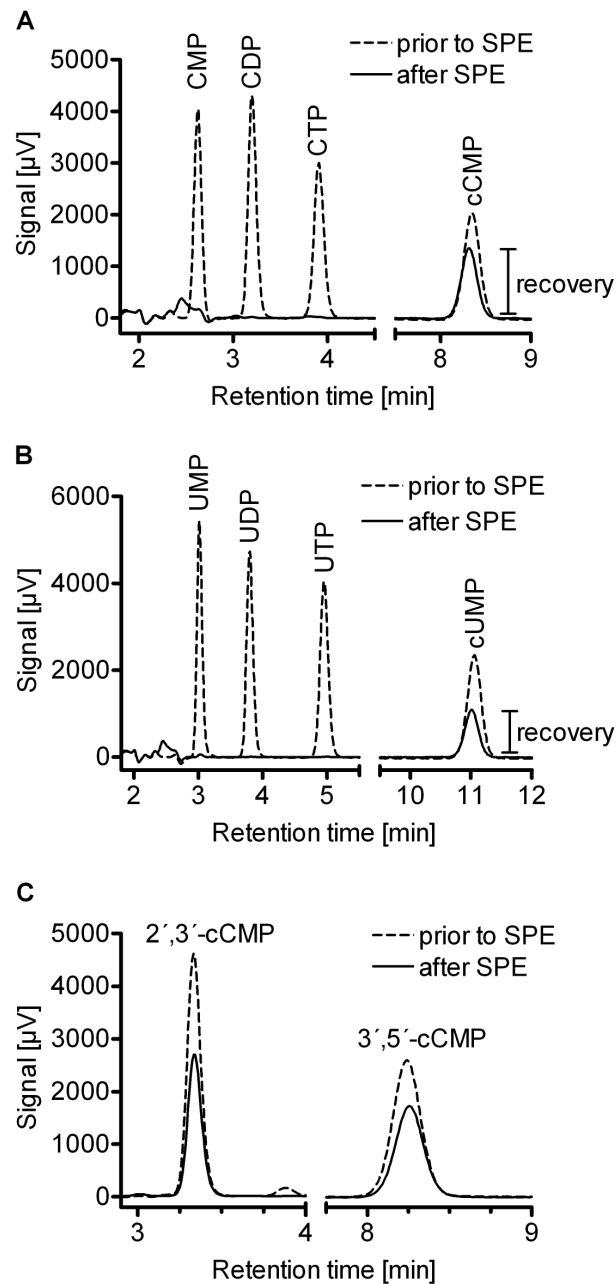
Fig. 2: HPLC chromatograms of nucleotide mixtures and eluates from solid phase extraction (SPE) using alumina. SPE and HPLC analytics were performed as described in "Materials and Methods". **A:** Chromatogram of a mixture of 15 μM CMP, CDP, CTP and 3′:5′-cCMP prior to SPE (dashed line) and chromatogram after SPE (solid line). **B:** Chromatogram of a mixture of 15 μM UMP, UDP, UTP and 3′:5′-cUMP prior to SPE (dashed line) and chromatogram after SPE (solid line). **C:** Chromatograms of 15 μM 2′:3′-cCMP and 3′:5′-cCMP prior to SPE (dashed line) and chromatogram after SPE (solid line). The same results were obtained in at least 3 independent experiments.

4.4.3 Michaelis-Menten Enzyme Kinetics

Fig. **3** shows the results of substrate saturation experiments using the isotopic NC assay with CTP/Mn^{2+} or UTP/Mn^{2+} on EF or CyaA; an overview of the kinetic properties of the AC activities, CC activities and UC activities of EF and CyaA is given in Tab. **1**.
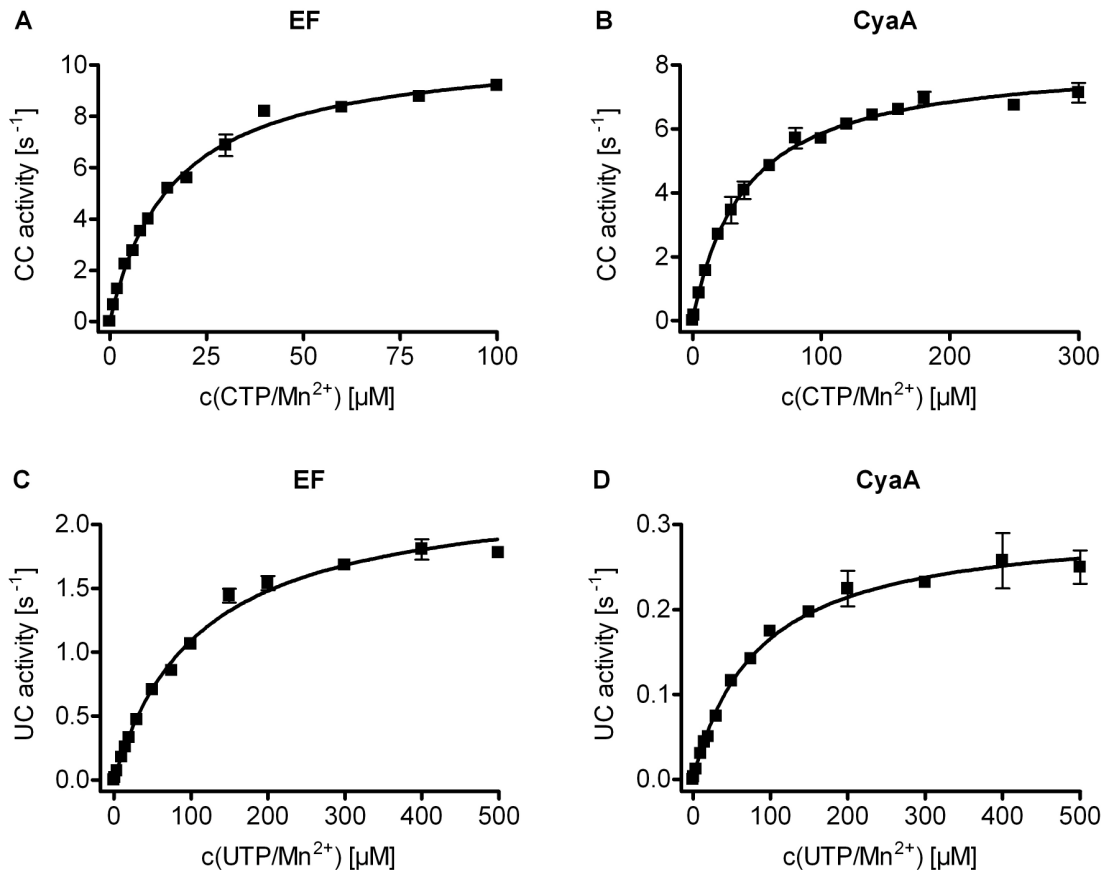
Fig. 3: Michaelis-Menten kinetics of CC and UC activities of EF and CyaA using the isotopic NC assay. Reactions were carried out as described in "Materials and Methods". Reaction mixtures contained the following components to yield the given final concentrations: 100 mM KCl, 10 μM free Ca^{2+}, 100 μM EGTA, [α-^{32}P]CTP (0.8 μCi/tube) or [α-^{32}P]UTP (0.8 μCi/tube), 100 nM CaM and non-labeled cyclic nucleotides as described in "Materials and Methods". CTP/Mn^{2+} or UTP/Mn^{2+} (1 μM to 1 mM) plus 5 mM of free Mn^{2+} were added. The final protein concentration was 40 pM EF or CyaA in case of CC activity (**A** and **B**) and 400 pM EF or CyaA in case of UC activity (**C** and **D**). Reactions were carried out at 37°C for 20 min in case of CC activity and for 30 min in case of UC activity. Data shown are means ± SD of representative experiments performed in duplicates; similar results were obtained in at least 5 independent experiments.

Tab. 1: Kinetic properties of AC activities, CC activities and UC activities from EF and CyaA.

Enzyme	NC activity	Divalent Cation	K_m [µM]	V_{max} [s^{-1}]
EF	AC	Mn^{2+}	35.3 ± 3.7	501.5 ± 55.9
		Mg^{2+}	175.8 ± 29.2	684.2 ± 272.5
	CC	Mn^{2+}	12.5 ± 3.4	8.8 ± 1.4
		Mg^{2+}	419.7 ± 115.1	7.2 ± 3.1
	UC	Mn^{2+}	134.5 ± 23.5	2.3 ± 0.2
CyaA	AC	Mn^{2+}	57.7 ± 4.6	332.0 ± 42.4
	CC	Mn^{2+}	46.6 ± 9.7	8.9 ± 2.0
	UC	Mn^{2+}	68.6 ± 9.8	0.3 ± 0.05

AC activities, CC activities and UC activities were determined as described under "Materials and Methods". 1 µM to 2 mM NTP/Mn^{2+} or NTP/Mg^{2+} were added, plus 5 mM of free Mn^{2+} or Mg^{2+}. As radioactive tracer, [α-^{32}P]ATP (0.2 µCi/tube), [α-^{32}P]CTP (0.8 µCi/tube) or [α-^{32}P]UTP (0.8 µCi/tube) were added. The final enzyme concentrations were: 10 pM (EF and CyaA AC activities), 40 pM (EF and CyaA CC activities with Mn^{2+}), and 400 pM (EF CC activity with Mg^{2+} and UC activities). Reactions were carried out for 10 min at 25°C (AC), 20 min at 37°C (CC) and 30 min at 37°C (UC). Apparent K_m and V_{max} values were obtained by non-linear regression analysis of substrate-saturation experiments and are the means ± SD of 3-4 independent experiments performed in duplicates. Saturation curves were analyzed by non-linear regression using the Prism 4.02 software (Graphpad, San Diego, CA).

Using Mn^{2+}, the K_m value of EF CC activity was 3-fold lower than the K_m value of EF AC activity. The K_m value of EF UC activity was 4-fold higher than the value of AC activity. Using Mg^{2+}, the K_m value of EF CC activity was 2-fold higher than the value of AC activity. Using CyaA and Mn^{2+} yielded similar K_m values in case of AC, CC and UC activity. Interestingly, enzyme activities decreased in the order AC > CC > UC as shown by the V_{max} values. Using Mn^{2+}, the V_{max} value of EF CC activity was 57-fold lower than the value of AC activity, and UC activity was even 4-fold lower than CC activity. Using CyaA and Mn^{2+}, the V_{max} value of CC activity was 37-fold lower than compared to the value of AC activity, and UC activity was even 30-fold lower than CC activity. However, the isotopic assay was sensitive enough to detect even those low enzyme activities.

4.4.4 Inhibition Data from the Isotopic Nucleotidyl Cyclase Assay

EF and CyaA CC activity was inhibited using standard AC inhibitors. Using Mn^{2+}, PMEApp (Shen *et al.*, 2004) inhibited EF AC activity with a K_i value of 2.0 ± 0.5 nM, while PMEApp inhibited CC activity with a K_i value of 4.5 ± 0.4 nM. The K_i values of PMEApp on CyaA were 1.0 ± 0.3 nM (AC activity) and 1.1 ± 0.02 nM (CC activity). The K_i values of five MANT-substituted nucleotides on EF and CyaA AC and CC activities are given in Tab. **2**. MANT-CTP was found to be the most potent MANT-nucleotide on EF AC and CC activity, yielding similar K_i values. MANT-ATP inhibited EF CC activity with about 7-fold lower potency than MANT-CTP, followed by MANT-GTP, MANT-UTP and MANT-ITP. The order of potency of MANT-nucleotides on CyaA CC activity was MANT-ITP > MANT-CTP > MANT-UTP > MANT-ATP > MANT-GTP.

Tab. 2: Inhibitor potencies at EF and CyaA AC and CC activities.

	K_i (μM)			
Nucleotide	**EF** **AC activity**	**EF** **CC activity**	**CyaA** **AC activity**	**CyaA** **CC activity**
MANT-ATP	0.43 ± 0.02	0.58 ± 0.03	4.3 ± 0.4***	4.4 ± 0.1
MANT-CTP	0.06 ± 0.01*	0.08 ± 0.01	1.1 ± 0.1***	1.3 ± 0.1
MANT-GTP	2.5 ± 0.1*	2.8 ± 0.4	5.9 ± 1.0***	6.1 ± 2.0
MANT-ITP	4.1 ± 0.1*	5.7 ± 0.03	0.6 ± 0.1***	1.0 ± 0.04
MANT-UTP	3.7 ± 0.1*	3.8 ± 0.6	2.6 ± 0.3***	1.8 ± 0.3

CC activities were determined as described under "Materials and Methods". Reaction mixtures contained the following components to yield the given final concentrations: 100 mM KCl, 5 mM free Mn^{2+}, 10 μM free Ca^{2+}, 100 μM EGTA, 10 μM CTP, [α-^{32}P]CTP (0.4 μCi/tube), 100 μM cAMP, 100 nM CaM. The final protein concentration was 30 pM EF or CyaA, reactions were carried out for 20 min at 37°C. Values labeled with (*) and (***) were taken from (Taha *et al.*, 2009) and (Göttle *et al.*, 2007), respectively. K_i values are given in μM and represent the means ± SD of at least three independent experiments performed in duplicates. Inhibition curves were analyzed by non-linear regression using the Prism 4.02 software (Graphpad, San Diego, CA).

As shown in Tab. **2**, similar K_i values were obtained inhibiting AC activity and CC activity by MANT-nucleotides. This result was found for both EF and CyaA activities. Linear regression analysis was performed for the quantification of the correlations (Fig. **4**). On EF and CyaA, the K_i values of AC and CC inhibition showed significant correlation.
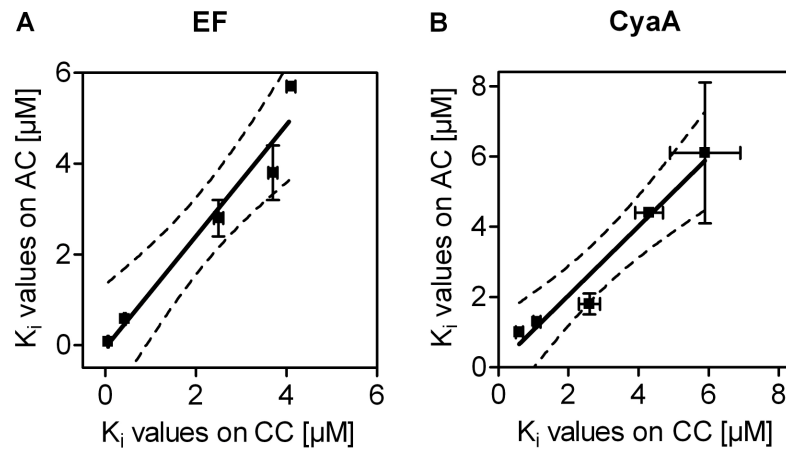
Fig. 4: Linear correlation of the K_i values of AC and CC inhibition by MANT-nucleotides. Data shown in Tab. **2** provide the basis for the correlations. Dashed lines represent 95% confidence intervals of the linear regression lines. **A:** Inhibition of EF; slope, 1.224 ± 0.1604; r^2, 0.9510; p, 0.0047; significant. **B:** Inhibition of CyaA; slope, 0.9847 ± 0.1226; r^2, 0.9555; p, 0.0040; significant. Linear regression analysis was performed using the Prism 4.02 software (Graphpad, San Diego, CA).

4.4.5 Non-Isotopic Nucleotidyl Cyclase Assay and HPLC Analysis

Within a screening for potential AC toxin substrates, EF and CyaA were incubated with several nucleoside 5´-triphosphates, and the formation of the corresponding cyclic nucleotides was analyzed. Fig. **5** shows HPLC chromatograms of reaction samples taken after reaction times between 0 min and 60 min. The chromatogram of the incubation of 20 nM EF with 100 μM CTP at a reaction time of 0 min (Fig. **5A**, purple line) showed a peak resulting from the starting material CTP at a retention time of 3.8 min while the internal standard (IS) inosine (40 μM) gave a peak at 5.7 min; no additional peaks were detected for 0 min reaction time at retention times of 6 min to 10 min.
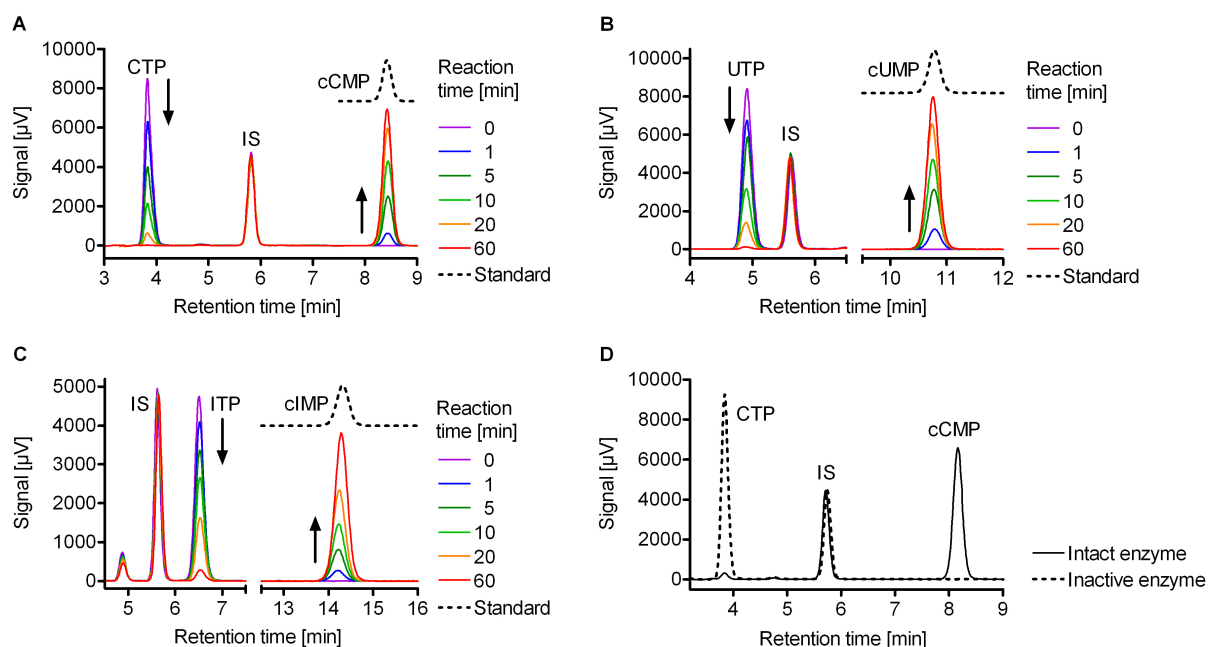

Fig. 5: HPLC chromatograms of reaction mixtures from the non-isotopic NC assay. The non-isotopic NC assay, sample preparation and HPLC analytics were carried out as described in "Materials and Methods". Reaction mixtures contained 5 mM Mn^{2+}, 10 μM Ca^{2+} and 100 μM CTP (**A**), UTP (**B**) or ITP (**C**). Protein concentrations were 20 nM EF and 20 nM CaM (A), 120 nM EF and 120 nM CaM (B) and 300 nM EF and 300 nM CaM (C). Samples were withdrawn at the indicated reaction times (colored solid lines). 20 μM inosine were added as internal standard (IS); cCMP, cUMP and cIMP were also added as standard substances (black, dotted lines). In order to prevent overlapping of the lines, the chromatograms of the standard substances were moved vertically. **D:** Chromatograms of reaction samples containing 20 nM EF, 20 nM CaM and 100 μM CTP after 60 min reaction time. Results for active enzyme (solid line) and heat-inactivated enzyme (dotted line). Similar results were obtained in at least 3 independent experiments.

With increasing reaction time, the CTP peak at a retention time of 3.8 min decreased, while at a retention time of 8.3 min, a new peak was detected. This peak increased proportionally to the decrease of the CTP peak. This newly detected signal at a retention time of 8.3 min exhibited an identical retention time as 20 μM 3´:5´-cCMP applied as external standard (Fig. **5A**, dashed line). At different reaction times, the internal standard (inosine, 40 μM) yielded constant signals at a retention time of 5.7 min ensuring reproducible nucleotide recoveries.

In order to answer the question which NTP is converted preferentially by EF, ATP or CTP, both NTPs (100 μM each) were incubated simultaneously with 1 nM EF and 1 nM CaM in one reaction vial, allowing competition of ATP and CTP for the catalytic site. ATP turned out to be converted preferentially, e.g. after 2 h of incubation at 37°C, the turnover was about 90% for ATP and about 10% for CTP (data not shown).

When 120 nM EF were incubated with 100 μM UTP, chromatograms showed the UTP signal at a retention time of 4.9 min (Fig. **5B**, purple line). With increasing reaction time, a decrease of the UTP signal was observed, and at a retention time of 10.8 min, a new signal was detected exhibiting the identical retention time as 20 μM 3´:5´-cUMP applied as external standard (Fig. **5B**, dashed line).

Similarly, upon incubation of 100 μM ITP with 500 nM EF (Fig. **5C**), a decrease of the ITP peak at a retention time of 6.2 min was observed while a new peak increased at a retention time of 14.2 min, exhibiting the identical retention time as 20 μM 3´:5´-cIMP applied as external standard (Fig. **5C**, dashed line).

In order to ensure that the observed NTP conversions resulted from specific enzymatic activity, 20 nM EF and 100 μM CTP were incubated similarly to the experiment shown in Fig. **5A**, and for comparison, 20 nM of heat-inactivated EF were incubated with 100 μM CTP. After 60 min of incubation using EF, the CTP peak at a retention time of 3.8 min had been converted to a signal at 8.3 min exhibiting the retention time of cCMP external standard (Fig. **5D**, solid line). The chromatogram resulting from an incubation of 60 min using heat-inactivated EF showed no new peak from cCMP at a retention time of 8.3 min, but the peak from the starting material CTP persisted at a retention time of 3.8 min (Fig. **5D**, dashed line). Thus, no conversion of CTP was detected using heat-inactivated enzyme.

HPLC chromatograms shown in Fig. **5** were used to calculate nucleotide concentrations and to depict NTP conversion to cNMP by EF with increasing reaction

time (Fig. **6**). EF concentrations were adjusted according to the efficiency of conversion of the individual NTPs. With 20 nM EF, 120 nM EF and 500 nM EF, respectively, complete conversion of 100 μM CTP, UTP and ITP occurred within 60 min. When 500 nM EF were incubated with 100 μM GTP, chromatograms showed a decrease of the signal from GTP and a new signal exhibiting the retention time of standard cGMP (data not shown). However, although the EF concentration was high (500 nM), the turnover of GTP within a reaction time of 60 min was 13% only, showing inferior enzymatic activity of EF on GTP as compared to CTP, UTP and ITP. When 500 nM EF were incubated with 100 μM TTP, chromatograms showed a decrease of the signal from TTP and the appearance of a new signal displaying the retention time of standard cTMP. The turnover of TTP after 60 min was only 5%, pointing to minimal enzymatic activity of EF on TTP.

When CyaA was used instead of EF, similar chromatographic results were obtained (data not shown). Chromatograms also showed complete conversion of CTP, UTP and ITP within 60 min yielding peaks at retention times of the corresponding cyclic nucleotide standards. CyaA concentrations needed for complete turnover of 100 μM NTP within 60 min were 30 nM (CTP), 600 nM (UTP) and 1,500 nM (ITP). When 1,500 nM CyaA were applied to 100 μM GTP or 100 μM TTP, the turnover within 60 min was 90% or 30%, respectively.
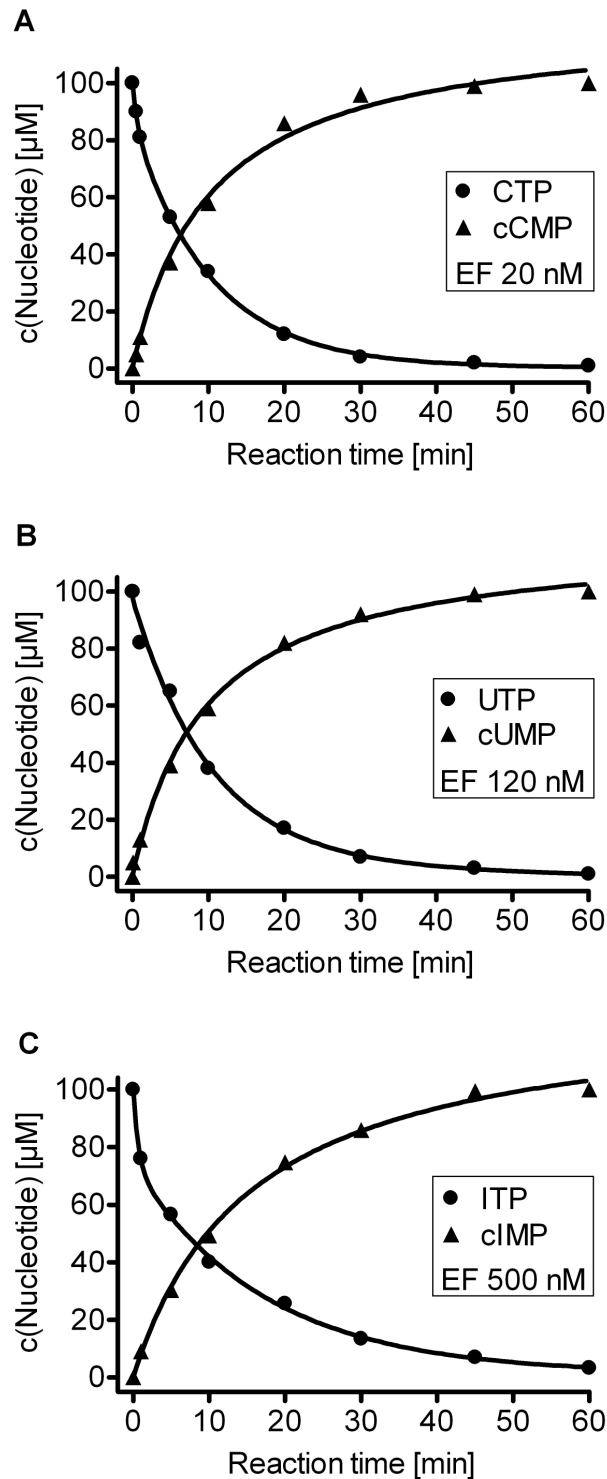
Fig. 6: Turnover of NTPs to cNMPs by EF using the non-isotopic NC assay. Nucleotide concentrations were calculated by evaluating the chromatograms shown in Fig. **5**. CTP (**A**), UTP (**B**) or ITP (**C**), 100 µM each, were converted to the corresponding cyclic nucleotides by the indicated concentrations of EF and equivalent concentrations of CaM ensuring 1:1 stoichiometry of EF and CaM. Experiments were performed as described in "Materials and Methods". Similar results were obtained in at least 3 independent experiments.

4.4.6 Mass Spectrometry

In order to ensure the exact identities of the cyclic nucleotide products from enzymatic reactions, samples were applied to LC-MS/MS and the resulting data were compared to results from cNMP standards. Fig. **7** shows mass spectra and chromatograms from selective reaction monitoring (SRM) in case of cCMP (A-C), cUMP (D-F) and cIMP (G-I).
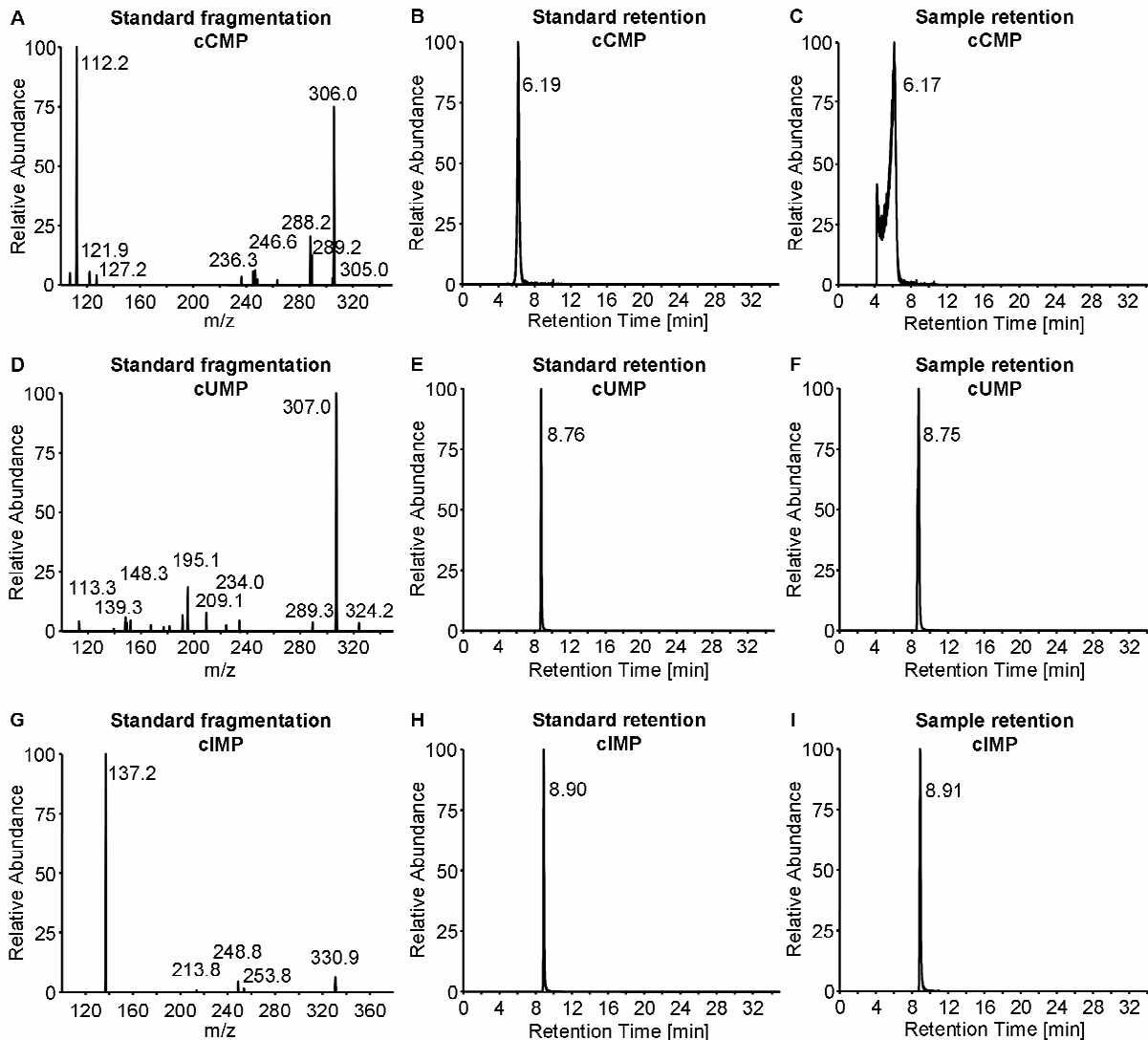
Fig. 7: Verification of the identities of the cyclic nucleotides formed in the non-isotopic NC assay by mass spectrometry. HPLC-MS analytics were performed as described in "Materials and Methods". Shown are fragmentation patterns of the standard cyclic nucleotides, chromatograms from standard cyclic nucleotides and chromatograms from reaction samples for cCMP (**A-C**), cUMP (**D-F**) and cIMP (**G-I**). Similar results were obtained in at least 3 independent experiments.

The mass spectrum of cCMP (Fig. **7A**) shows signals from protonated cCMP (m/z = 306.0) and from the protonated cytosine base (m/z = 112.2). Selective reaction monitoring of the m/z transition of 306.0 to 112.2 proofed the existence of cCMP in the nucleotide standard (Fig. **7B**) as well as in samples from the enzymatic reaction of EF with CTP (Fig. **7C**). In case of cUMP, mass signals resulted from the protonated cUMP molecule (m/z = 307.0), the cUMP-ammonia adduct (m/z = 324.2) and the protonated uracil base (m/z = 113.3) (Fig. **7D**). SRM of the m/z transition of 324.2 to 307.0 proofed the existence of cUMP in the nucleotide standard (Fig. **7E**) and in reaction samples (Fig. **7F**). The mass spectrum of cIMP (Fig. **7G**) shows signals from protonated cIMP (m/z = 330.9) and from the protonated hypoxanthine base (m/z = 137.2). As determined by SRM of the m/z transition of 330.9 to 137.2, cIMP was found in nucleotide standard and reaction sample (Fig. **7H-I**).

4.5   Discussion

4.5.1   Multiple cNMPs Formed by EF and CyaA

The signals obtained in the isotopic NC assay using $[\alpha\text{-}^{32}P]NTP$ as substrate were dependent on the amount of "AC" toxin (Fig. **1B**), on pH (Fig. **1C**) and on the cyclase toxin activator CaM (Fig. **1D**). HPLC analytics confirmed that only cyclic nucleotides were eluted in the SPE procedure applied in this work (Fig. **2A** and **B**), and no cyclic nucleotide was formed when heat-inactivated enzyme was used (Fig. **2C**). The turnover of $[\alpha\text{-}^{32}P]NTP$ was inhibited by PMEApp, a standard AC toxin inhibitor and by five MANT-nucleotides. Thereby, similar K_i values were obtained in both cases, i.e. when AC was inhibited (use of $[\alpha\text{-}^{32}P]ATP$ as substrate) and when CC was inhibited (use of $[\alpha\text{-}^{32}P]CTP$ as substrate, Tab. **2**). Linear correlation analysis showed significant correlation between the K_i values obtained from AC and CC inhibition (Fig. **4**). Mass spectrometry confirmed the existence of the corresponding cyclic nucleotides in the reaction samples. Taken together, these data corroborate that the signals detected in the isotopic NC assay and in the non-isotopic assay only originated from specific enzymatic catalysis by EF or CyaA. 3´:5´-cNMP and 2´:3´-cNMP isomers could easily be discriminated based on their different retention times, allowing us to exclude the formation of cyclic nucleotides possessing 2´:3´-cNMP structure. The EC_{50} values for CaM obtained from the isotopic CC assay are in good agreement with values from literature. While CaM stimulated CC activity with EC_{50} values of 670 ± 50 pM (EF) and 80 ± 5 pM (CyaA), AC activity was stimulated with EC_{50} values of 1,600 pM in case of EF (Gupta *et al.*, 2006) and 200 pM in case of CyaA (Glaser *et al.*, 1991; Bouhss *et al.*, 1996). On the basis of the V_{max} values given in Tab. **1** and as a result from the non-isotopic NC assay, the rank order of substrate preference was ATP > CTP > UTP > ITP > GTP > TTP, for both EF and CyaA. The decreasing efficiencies of substrate cyclization to yield rare cyclic nucleotides required the use of higher enzyme concentrations, higher temperature and lower concentrations of non-labeled NTP (in the isotopic NC assay) as compared to the more efficient conversion of ATP. When substrate saturation experiments using the isotopic NC assay were performed with CTP/Mg^{2+} instead of CTP/Mn^{2+}, similar V_{max} values were obtained under both conditions (Tab. **1**), showing that CC activity is not restricted to the use of Mn^{2+}; the physiological divalent cation Mg^{2+} enables EF to convert CTP, too.

4.5.2 Accommodation of Various Purine and Pyrimidine Nucleotides at the Catalytic Sites of EF and CyaA

In our previous work, we characterized the interactions of the catalytic sites of EF and CyaA with non-substituted NTPs and various MANT-nucleotides possessing various purine and pyrimidine bases (Göttle *et al.*, 2007; Taha *et al.*, 2009). We developed a three-site pharmacophore model for mAC, EF and CyaA attributing major importance to the ribose substituent for nucleotide affinity, followed by the phosphate tail (Gille *et al.*, 2005; Mou *et al.*, 2006). The higher affinity of MANT-substituted nucleotides is a result from additional hydrophobic interactions of the MANT-group with F586 in EF and F306 in CyaA (Göttle *et al.*, 2007; Taha *et al.*, 2009). The base turned out to play a minor role as the catalytic site of AC is spacious and conformationally flexible and accommodates various purine and pyrimidine nucleotides (Göttle *et al.*, 2007; Taha *et al.*, 2009). Using kinetic FRET competition experiments, we have shown that both MANT-ATP and MANT-CTP reversibly bind to the catalytic site of EF, further corroborating a single nucleotide binding site in EF (Taha *et al.*, 2009). Modeling the binding modes of MANT-ATP and MANT-CTP to the catalytic site of EF, we found that in 3′-MANT-CTP, the oxygen in the 2′-position of the base may align with the positive pole of the amide dipole of N583. The cytosine oxygen may be close to the guanidine group of R329. Additionally, a water molecule may mediate H-bonding between the cytosine oxygen with the side chains of R329 and E580. Taken together, these results confirm that various bases, in particular cytosine, can be accommodated by the EF catalytic site. Modeling of the binding modes of MANT-nucleotides to the catalytic site of CyaA suggested that all of the nucleobases may be aligned in similar position (Göttle *et al.*, 2007). In case of GTP, ITP and UTP, backbone NH functions of G299 and V271 could serve as hydrogen donors for the carbonyl oxygens in the 6 and 4 positions, respectively. Therefore, the catalytic site of CyaA forms a large cavity with considerable conformational freedom to accommodate various nucleotides. Collectively, our previous studies show that other NTPs than ATP can bind to both EF and CyaA opening up the formation of rare cyclic nucleotides.

4.5.3 Multiple cNMPs: A Strategy to Blunt Host Immune Responses?

The natural occurrence of cCMP resulting from specific CC activity was confirmed unambiguously in various mammalian organs (Newton *et al.*, 1984, 1990, 1997). Additionally, phosphodiesterase activity mediating degradation of cCMP was found (Newton *et al.*, 1986, 1999). Moreover, protein kinase activity responsive to cCMP has been observed (Newton *et al.*, 1992; Bond *et al.*, 2007; Ding *et al.*, 2008). Accordingly, cCMP may be a novel cyclic nucleotide with second messenger function, regulating cell functions such as cell growth and differentiation. To the best of our knowledge, we have shown for the first time that an enzyme purified to apparent homogeneity possesses cytidylyl cyclase activity. Additionally, we observed broad NTP specificity of both adenylyl cyclase toxins, EF and CyaA, forming cCMP, cUMP, cIMP, cGMP and cTMP. As the cell-permeant cCMP-analog dibutyryl-cCMP blunts host immune responses, e.g. formation of cytokines in macrophages (Elliott *et al.*, 1991) and oxygen radical formation in neutrophils (Ervens and Seifert, 1991), we hypothesize that the formation of multiple cyclic nucleotide species by EF and CyaA synergizes with adenylyl cyclase activity to accomplish effective disruption of immune responses during infection. The discovery of these multiple nucleotidyl cyclase activities contributes to our understanding of the mechanisms of action of bacterial exotoxins, providing the basis for the rational development of potent and selective EF and CyaA inhibitors for the treatment of toxinemia and antibiotic-resistant bacteria strains.

4.6 References

Ahuja N, Kumar P and Bhatnagar R (2004) The adenylate cyclase toxins. *Crit Rev Microbiol* **30**:187-196.

Alvarez R and Daniels DV (1990) A single column method for the assay of adenylate cyclase. *Anal Biochem* **187**:98-103.

Basler M, Masin J, Osicka R and Sebo P (2006) Pore-forming and enzymatic activities of *Bordetella pertussis* adenylate cyclase toxin synergize in promoting lysis of monocytes. *Infect Immun* **74**:2207-2214.

Bloch A, Dutschman G and Maue R (1974) Cytidine 3′,5′-monophosphate (cyclic CMP). II. Initiation of leukemia L-1210 cell growth *in vitro*. *Biochem Biophys Res Commun* **59**:955-959.

Bond AE, Dudley E, Tuytten R, Lemiere F, Smith CJ, Esmans EL and Newton RP (2007) Mass spectrometric identification of Rab23 phosphorylation as a response to challenge by cytidine 3′,5′-cyclic monophosphate in mouse brain. *Rapid Commun Mass Spectrom* **21**:2685-2692.

Bouhss A, Vincent M, Munier H, Gilles AM, Takahashi M, Barzu O, Danchin A and Gallay J (1996) Conformational transitions within the calmodulin-binding site of *Bordetella pertussis* adenylate cyclase studied by time-resolved fluorescence of W242 and circular dichroism. *Eur J Biochem* **237**:619-628.

Cech SY and Ignarro LJ (1978) Cytidine 3′,5′-monophosphate (cyclic CMP) formation by homogenates of mouse liver. *Biochem Biophys Res Commun* **80**:119-125.

Ding S, Bond AE, Lemiere F, Tuytten R, Esmans EL, Brenton AG, Dudley E and Newton RP (2008) Online immobilized metal affinity chromatography/mass spectrometric analysis of changes elicited by cCMP in the murine brain phosphoproteome. *Rapid Commun Mass Spectrom* **22**:4129-4138.

Drum CL, Shen Y, Rice PA, Bohm A and Tang WJ (2001) Crystallization and preliminary X-ray study of the edema factor exotoxin adenylyl cyclase domain from *Bacillus anthracis* in the presence of its activator, calmodulin. *Acta Crystallogr D Biol Crystallogr* **57**:1881-1884.

Drum CL, Yan SZ, Bard J, Shen YQ, Lu D, Soelaiman S, Grabarek Z, Bohm A and Tang WJ (2002) Structural basis for the activation of anthrax adenylyl cyclase exotoxin by calmodulin. *Nature* **415**:396-402.

Drum CL, Yan SZ, Sarac R, Mabuchi Y, Beckingham K, Bohm A, Grabarek Z and Tang WJ (2000) An extended conformation of calmodulin induces interactions between the structural domains of adenylyl cyclase from *Bacillus anthracis* to promote catalysis. *J Biol Chem* **275**:36334-36340.

Elliott GR, Lauwen AP and Bonta IL (1991) Dibutyryl cytidine 3´:5´-cyclic monophosphate; an inhibitor of A23187-stimulated macrophage leukotriene B_4 synthesis. *Agents Actions* **32**:90-91.

Ervens J and Seifert R (1991) Differential modulation by N^4, 2´-*O*-dibutyryl cytidine 3´:5´-cyclic monophosphate of neutrophil activation. *Biochem Biophys Res Commun* **174**:258-267.

Gaion RM and Krishna G (1979) Cytidylate cyclase: The product isolated by the method of Cech and Ignarro is not cytidine 3´,5´-monophosphate. *Biochem Biophys Res Commun* **86**:105-111.

Gallay J, Vincent M, Li de la Sierra IM, Munier-Lehmann H, Renouard M, Sakamoto H, Barzu O and Gilles AM (2004) Insight into the activation mechanism of *Bordetella pertussis* adenylate cyclase by calmodulin using fluorescence spectroscopy. *Eur J Biochem* **271**:821-833.

Gille A, Guo J, Mou TC, Doughty MB, Lushington GH and Seifert R (2005) Differential interactions of G proteins and adenylyl cyclase with nucleoside 5´-triphosphates, nucleoside 5´-[γ-thio]triphosphates and nucleoside 5´-[β,γ-imido]triphosphates. *Biochem Pharmacol* **71**:89-97.

Gille A, Lushington GH, Mou TC, Doughty MB, Johnson RA and Seifert R (2004) Differential inhibition of adenylyl cyclase isoforms and soluble guanylyl cyclase by purine and pyrimidine nucleotides. *J Biol Chem* **279**:19955-19969.

Gille A and Seifert R (2003) 2´(3´)-*O*-(*N*-methylanthraniloyl)-substituted GTP analogs: A novel class of potent competitive adenylyl cyclase inhibitors. *J Biol Chem* **278**:12672-12679.

Glaser P, Munier H, Gilles AM, Krin E, Porumb T, Barzu O, Sarfati R, Pellecuer C and Danchin A (1991) Functional consequences of single amino acid substitutions in calmodulin-activated adenylate cyclase of *Bordetella pertussis*. *EMBO J* **10**:1683-1688.

Göttle M, Dove S, Steindel P, Shen Y, Tang WJ, Geduhn J, König B and Seifert R (2007) Molecular analysis of the interaction of *Bordetella pertussis* adenylyl cyclase with fluorescent nucleotides. *Mol Pharmacol* **72**:526-535.

Guo Q, Shen Y, Lee YS, Gibbs CS, Mrksich M and Tang WJ (2005) Structural basis for the interaction of *Bordetella pertussis* adenylyl cyclase toxin with calmodulin. *EMBO J* **24**:3190-3201.

Gupta M, Alam S and Bhatnagar R (2006) Kinetic characterization and ligand binding studies of H351 mutants of *Bacillus anthracis* adenylate cyclase. *Arch Biochem Biophys* **446**:28-34.

Hewlett EL, Donato GM and Gray MC (2006) Macrophage cytotoxicity produced by adenylate cyclase toxin from *Bordetella pertussis*: More than just making cyclic AMP! *Mol Microbiol* **59**:447-459.

Johnson RA and Shoshani I (1990) Inhibition of *Bordetella pertussis* and *Bacillus anthracis* adenylyl cyclases by polyadenylate and "P"-site agonists. *J Biol Chem* **265**:19035-19039.

Ladant D and Ullmann A (1999) *Bordetella pertussis* adenylate cyclase: A toxin with multiple talents. *Trends Microbiol* **7**:172-176.

Mogridge J, Cunningham K, Lacy DB, Mourez M and Collier RJ (2002) The lethal and edema factors of anthrax toxin bind only to oligomeric forms of the protective antigen. *Proc Natl Acad Sci USA* **99**:7045-7048.

Mou TC, Gille A, Fancy DA, Seifert R and Sprang SR (2005) Structural basis for the inhibition of mammalian membrane adenylyl cyclase by 2´(3´)-O-(N-Methylanthraniloyl)-guanosine 5´-triphosphate. *J Biol Chem* **280**:7253-7261.

Mou TC, Gille A, Suryanarayana S, Richter M, Seifert R and Sprang SR (2006) Broad specificity of mammalian adenylyl cyclase for interaction with 2´,3´-substituted purine- and pyrimidine nucleotide inhibitors. *Mol Pharmacol* **70**:878-886.

Newton RP, Bayliss MA, Khan JA, Bastani A, Wilkins AC, Games DE, Walton TJ, Brenton AG and Harris FM (1999) Kinetic analysis of cyclic CMP-specific and multifunctional phosphodiesterases by quantitative positive-ion fast-atom bombardment mass spectrometry. *Rapid Commun Mass Spectrom* **13**:574-584.

Newton RP, Evans AM, van Geyschem J, Diffley PJ, Hassam HG, Hakeem NA, Moyse CD, Cooke R and Salvage BJ (1994) Radioimmunoassay of cytidine 3´,5´-cyclic monophosphate: Unambiguous assay by means of an optimized protocol incorporating a trilayer column separation to obviate cross-reactivity problems. *J Immunoassay* **15**:317-337.

Newton RP, Groot N, van Geyschem J, Diffley PE, Walton TJ, Bayliss MA, Harris FM, Games DE and Brenton AG (1997) Estimation of cytidylyl cyclase activity and monitoring of side-product formation by fast-atom bombardment mass spectrometry. *Rapid Commun Mass Spectrom* **11**:189-194.

Newton RP, Hakeem NA, Salvage BJ, Wassenaar G and Kingston EE (1988) Cytidylate cyclase activity: Identification of cytidine 3´,5´-cyclic monophosphate and four novel cytidine cyclic phosphates as biosynthetic products from cytidine triphosphate. *Rapid Commun Mass Spectrom* **2**:118-126.

Newton RP, Khan JA, Brenton AG, Langridge JI, Harris FM and Walton TJ (1992) Quantitation by fast-atom bombardment mass spectrometry: Assay of cytidine 3´,5´-cyclic monophosphate-responsive protein kinase. *Rapid Commun Mass Spectrom* **6**:601-607.

Newton RP and Salih SG (1986) Cyclic CMP phosphodiesterase: Isolation, specificity and kinetic properties. *Int J Biochem* **18**:743-752.

Newton RP, Salih SG, Salvage BJ and Kingston EE (1984) Extraction, purification and identification of cytidine 3´,5´-cyclic monophosphate from rat tissues. *Biochem J* **221**:665-673.

Newton RP, Salvage BJ and Hakeem NA (1990) Cytidylate cyclase: Development of assay and determination of kinetic properties of a cytidine 3´,5´-cyclic monophosphate-synthesizing enzyme. *Biochem J* **265**:581-586.

Paccani SR, Tonello F, Ghittoni R, Natale M, Muraro L, D´Elios MM, Tang WJ, Montecucco C and Baldari CT (2005) Anthrax toxins suppress T lymphocyte activation by disrupting antigen receptor signaling. *J Exp Med* **201**:325-331.

Shen Y, Zhukovskaya NL, Guo Q, Florian J and Tang WJ (2005) Calcium-independent calmodulin binding and two-metal-ion catalytic mechanism of anthrax edema factor. *EMBO J* **24**:929-941.

Shen Y, Zhukovskaya NL, Zimmer MI, Soelaiman S, Bergson P, Wang CR, Gibbs CS and Tang WJ (2004) Selective inhibition of anthrax edema factor by adefovir, a drug for chronic hepatitis B virus infection. *Proc Natl Acad Sci USA* **101**:3242-3247.

Soelaiman S, Wei BQ, Bergson P, Lee YS, Shen Y, Mrksich M, Shoichet BK and Tang WJ (2003) Structure-based inhibitor discovery against adenylyl cyclase

toxins from pathogenic bacteria that cause anthrax and whooping cough. *J Biol Chem* **278**:25990-25997.

Taha HM, Schmidt J, Göttle M, Suryanarayana S, Shen Y, Tang WJ, Gille A, Geduhn J, König B, Dove S and Seifert R (2009) Molecular analysis of the interaction of anthrax adenylyl cyclase toxin, edema factor, with 2´(3´)-*O*-(*N*-(methyl)anthraniloyl)-substituted purine and pyrimidine nucleotides. *Mol Pharmacol* **75**:693-703.

Tournier JN, Quesnel-Hellmann A, Mathieu J, Montecucco C, Tang WJ, Mock M, Vidal DR and Goossens PL (2005) Anthrax edema toxin cooperates with lethal toxin to impair cytokine secretion during infection of dendritic cells. *J Immunol* **174**:4934-4941.

Chapter 5

Summary

The specific aims of this thesis were to provide the basis for exploring AC as target for the treatment of heart failure and several bacterial infections and to explore the enzymatic activities of AC toxins.

1. As one major achievement of this thesis, a biochemical method was developed to prepare membranous AC from cardiac tissue, yielding the components of the cAMP signaling cascade, i.e. GPCRs, G proteins and AC in intact form. A radiochemical approach was used to determine the parameters required for AC activity, producing robust signals from cardiac AC activity by both direct stimulation of AC and by stimulation *via* GPCRs. With these prerequisites fulfilled, we applied pharmacological approaches to characterize AC enzyme activity in mouse heart membranes. Using forskolin analogs for stimulating AC activity and MANT-substituted nucleotides as inhibitors, and by investigating Michaelis-Menten enzyme kinetics, we found AC from heart tissue to correlate to some extent with recombinant AC5, compatible with the notion that AC5 is the major AC isoform in the heart. However, AC isoforms other than AC5 appear to contribute to total AC activity in mouse heart membranes, too. These findings were corroborated by results obtained by applying further techniques, i.e. real-time PCR and immunoblot analysis. In the course of this work, MANT-substituted hypoxanthine nucleotides were found to inhibit cardiac AC with very high potencies. In summary, by the use of several techniques, we provide a pharmacological profile of cardiac AC and an excellent starting point for the design of potent and selective inhibitors. When conventional treatment of heart failure is limited, e.g. due to ineffective β-adrenoceptor antagonist therapy, as a promising novel therapeutic strategy, future clinical treatment strategies may be complemented by nucleotide prodrugs accomplishing beneficial effects on the heart and increased survival of the patient.

2. The bacterial AC toxins CyaA and EF are key virulence factors impairing host immune responses and worsening the infections by *Bordetella pertussis*, the causative agent of whooping cough, and *Bacillus anthracis*, causing anthrax disease. The second aim of this doctoral thesis was to investigate the detailed modes of action of EF and CyaA and to provide the basis for the development of AC toxin inhibitors.

Using radiochemical methods, we investigated the structure/activity relationships of substituted NTPs as CyaA inhibitors, revealing hypoxanthine nucleotides to be superior to other purine and pyrimidine nucleotides. Molecular modeling revealed hydrophobic interactions of the ribosyl substituent and lipophilic amino acid residues in CyaA to account for the increased potency of MANT-substituted nucleotides compared with non-substituted NTPs. One major achievement of this thesis is the development of fluorescence-based approaches allowing monitoring the binding of potential inhibitor molecules to CyaA. Actually, two approaches were considered: First, a method basing upon fluorescence resonance energy transfer (FRET) from enzyme tryptophan residues to fluorescent inhibitor molecules, and second, a technique basing upon direct inhibitor fluorescence. These powerful techniques were applied to investigate the interactions of fluorescent MANT-, ANT- and TNP-substituted nucleotides with CyaA and to determine inhibitor potencies. Even the binding of non-labeled inhibitors to CyaA was monitored with this approach. Selective CyaA inhibitors may be used to prevent dampening of the immune response upon *Bordetella pertussis* infection and to reduce mortality in severe courses of disease. The fluorescence-based approaches developed in this thesis are available for future high-throughput screening to support the development of highly potent and selective CyaA inhibitors.

3. Cyclic cytidine 3´:5´-monophosphate (cCMP) was identified unambiguously in various mammalian tissues, protein kinase activity responsive to cCMP was observed and phosphodiesterase activity accounting for the selective degradation of cCMP was discovered. Therefore, cCMP may be a novel second messenger with potential importance in many physiological processes, including regulation of immune responses. However, so far, the precise identity of the cCMP-forming enzyme is unknown. As the aim of this doctoral thesis was to investigate the detailed modes of action of bacterial AC toxins, we investigated the interactions of various NTPs with EF and CyaA. Thereby, we found hitherto unknown enzymatic activities: For the first time, we provide evidence for cytidylyl cyclase (CC) activity of purified bacterial exotoxins, resulting in the conversion of CTP to cCMP.

As a major achievement of this thesis, various nucleotidyl cyclase activities of bacterial AC toxins were investigated and monitored by the use of several techniques. First, the isotopic nucleotidyl cyclase assay based upon detection of

radioactively labeled cNMPs showed that EF and CyaA possess CC activity, and additionally, we also observed the conversion of UTP to cUMP. We performed substrate saturation experiments to determine the kinetic properties of CC and UC activities. Moreover, we determined the potencies of AC inhibitors at CC activity and obtained similar K_i values when inhibiting AC activity and CC activity.

Second, the non-isotopic nucleotidyl cyclase assay basing upon an advanced sample preparation process and detection of cNMPs by HPLC was developed and used to monitor NTP consumption and cNMP formation by both AC toxins. Using this approach, in addition to the formation of cAMP, cCMP and cUMP, we also observed the formation of cIMP, cGMP and cTMP. The rank order of substrate preference was ATP > CTP > UTP > ITP > GTP > TTP, for both EF and CyaA. Third, mass spectrometry was used to unambiguously identify the corresponding cNMPs obtained from enzymatic reactions.

Based on the fact that cCMP-analogs inhibit immune responses, we hypothesize that cCMP may be a novel endogenous second messenger and that the multiple nucleotidyl cyclase activities of bacterial AC toxins described in this thesis for the first time contribute to weakening of the immune defense by bacterial exotoxins, resulting in increased infection severity. Regarding future research, the endogenous CC enzyme remains to be discovered. The physiological role and the molecular targets of cCMP remain to be determined. What is the impact of multiple nucleotidyl cyclase activities of bacterial AC toxins on cyclic nucleotide metabolism in host cells? And finally, - regarding the occurrence of bacterial strains resistant to antibiotic treatment - can our findings lead to advancements in the prevention and therapy of bacterial infections?

Appendix

A.1   Curriculum Vitae

Personal Details

Name	Martin Göttle
Date of birth	March, 10th, 1979
Place of birth	Albstadt-Ebingen, Germany
Martial status	bachelor

Tertiary Education

08.2005 - 06.2009	PhD in Pharmacology and Toxicology Institute of Chemistry and Pharmacy University of Regensburg, Germany <u>Thesis advisor:</u> Prof. Dr. R. Seifert
08.2004 - 06.2005	Master Thesis "Development of Methods for the Determination of Affinity, Selectivity and Activity of New Ligands for G Protein-Coupled Receptors" Department of Pharmaceutical/Medicinal Chemistry II University of Regensburg, Germany <u>Thesis advisor:</u> Prof. Dr. A. Buschauer
03.2003 - 07.2004	Master of Science in Medicinal Chemistry Department of Pharmaceutical/Medicinal Chemistry II University of Regensburg, Germany Final examination July, 1st, 2004
08.1999 - 02.2003	Bachelor in Chemistry Major in Biotechnology University of Applied Sciences, Reutlingen, Germany Final examination: February, 14th, 2003

School Education

1989 - 1998   High School

Majors in Chemistry and French

Hechingen, Germany

Graduation in July 1998

1985 - 1989   Elementary School, Bisingen, Germany

Internships

07.2002 - 09.2002   Naturwissenschaftliches und Medizinisches Institut (NMI)

University of Tübingen, Germany

08.2001 - 01.2002   BASF, Ludwigshafen, Germany

07.2000 - 09.2000   Akzo Nobel N.V., Reutlingen, Germany

A.2   Professional Training

<u>2009</u>

Advanced Courses in Pharmacology

"Tiermodelle in der Pharmakologischen Forschung"

Mainz (Germany), March 2009

Advanced Courses in Pharmacology

"Arzneimittelinteraktionen, -metabolismus und –transport"

Mainz (Germany), March 2009

<u>2008</u>

4th International Summer School „Medicinal Chemistry"

Regensburg (Germany), September 2008

<u>2007</u>

Advanced training "Versuchstierkunde und Tierschutz"

FELASA Recommendations for the Education and Training of Persons Carrying out Animal Experiments (Category B)

Dr. T. Spruss

Regensburg (Germany), April 2007

<u>2006</u>

Advanced training in FPLC

„GE Healthcare training course, ÄKTA^{TM} design systems and UNICORN^{TM} Control Software"

Dr. L. Briese, Dr. D. Johänning

Munich (Germany), March 2006

Advanced training "Umgang mit offenen radioaktiven Stoffen"

Dr. R. Schupfner

Regensburg (Germany), March 2006

Advanced training „Gentechnik-Fortbildungsveranstaltung nach §§ 15 und 17 der Gentechniksicherheitsverordnung"

Prof. Dr. S. Modrow

Regensburg (Germany), April 2006

<u>2005</u>

Since August 2005 associate member of the Research Training Group (Graduiertenkolleg 760) *"Medicinal Chemistry: Molecular Recognition – Ligand Receptor Interactions"*

A.3   Participation in Exchange Programs

<u>2007</u>

RISE Research Internships in Science and Engineering

Deutscher Akademischer Austauschdienst

June-August 2007

<u>2006</u>

RISE Research Internships in Science and Engineering

Deutscher Akademischer Austauschdienst

June-August 2006

Eidesstattliche Erklärung

Ich erkläre hiermit an Eides statt, dass ich die vorliegende Arbeit ohne unzulässige Hilfe Dritter und ohne Benutzung anderer als der angegebenen Hilfsmittel angefertigt habe. Die aus anderen Quellen direkt oder indirekt übernommenen Daten und Konzepte sind unter Angabe des Literaturzitats gekennzeichnet. Weitere Personen waren an der inhaltlich-materiellen Herstellung der vorliegenden Arbeit nicht beteiligt. Insbesondere habe ich hierfür nicht die entgeltliche Hilfe eines Promotionsberaters oder anderer Personen in Anspruch genommen. Niemand hat von mir weder unmittelbar noch mittelbar geldwerte Leistungen für Arbeiten erhalten, die im Zusammenhang mit dem Inhalt der vorgelegten Dissertation stehen. Die Arbeit wurde bisher weder im In- noch im Ausland in gleicher oder ähnlicher Form einer anderen Prüfungsbehörde vorgelegt.

Regensburg, den   _____

                                                            Martin Göttle